

NASA-CR-169284
19820023761

NASA-CR-169,284

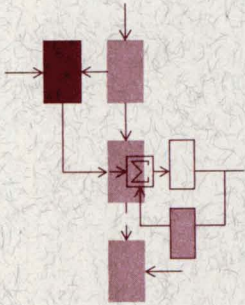
July, 1982

LIDS-R-1220

Research Supported By:

*NASA Ames and Langley
Research Centers*

*Grant NGL-22-009-124
OSP No. 76265*



**REAL TIME ESTIMATION AND PREDICTION OF SHIP
MOTIONS USING KALMAN FILTERING TECHNIQUES**

Michael A. Triantafyllou
Marc Bodson
Michael Athans

LIBRARY COPY

OCT 26 1982

LANGLEY RESEARCH CENTER
LIBRARY, NASA
HAMPTON, VIRGINIA

**Laboratory for Information and Decision Systems
MASSACHUSETTS INSTITUTE OF TECHNOLOGY, CAMBRIDGE, MASSACHUSETTS 02139**

ENTER:

13 DISPLAY DX111: PREVIOUS OUTPUT COMPLETED
13 95 95 AU/VAUGHAN, R. W.
14 6 6 LIMIT 13/82-83
15 DISPLAY DX111: PREVIOUS OUTPUT COMPLETED
15 1 1 AU/VORLICEK, P. L.
16 177 177 AU/ATHANS, M.
16 LIMIT 16/1981-1983 LM119: INVALID YEAR ARGUMENT
17 16 16 LIMIT 16/81-83
18 DISPLAY DX111: PREVIOUS OUTPUT COMPLETED
18 1 1 RN/LIDS-R-1220

DISPLAY 18/2/1

82N31637**# ISSUE 22 PAGE 3130 CATEGORY 34 RPT#: NASA-CR-169284 MAS
1.26:169284 LIDS-R-1220 CNT#: NGL-22-009-124 82/07/00 142 PAGES
UNCLASSIFIED DOCUMENT

UTTL: Real time estimation and prediction of ship motions using Kalman filtering techniques

AUTH: A/TRIANTAFYLLOU, M. A.; B/BODSON, M.; C/ATHANS, M.

CORP: Massachusetts Inst. of Tech., Cambridge. CSS: (Lab. for Information and Decision Systems.) AVAIL.NTIS SAP: HC A07/MF A01

MAJS: /*COMPUTERIZED SIMULATION/*ESTIMATES/*KALMAN FILTERS/*LANDING SIMULATION/*
REAL TIME OPERATION/*ROLL/*SEA ROUGHNESS/*SHIPS/*V/STOL AIRCRAFT

MINS: / AIRCRAFT LANDING/ COMPUTER PROGRAMS/ DIFFERENTIAL EQUATIONS/ EQUATIONS
OF MOTION/ HYDRODYNAMICS/ LINEAR EQUATIONS/ VERTICAL LANDING

ABA: R. J. F.

ABS: A landing scheme for landing V/STOL aircraft on rolling ships was sought using computerized simulations. The equations of motion as derived from hydrodynamics, their form and the physical mechanisms involved and the general form of the approximation are discussed. The modeling of the sea

July 1982

LIDS-R- 1220

REAL TIME ESTIMATION AND PREDICTION
OF SHIP MOTIONS USING KALMAN FILTERING TECHNIQUES

by

Michael S. Triantafyllou

Marc Bodson

Michael Athans

The research was conducted at the M.I.T. Laboratory for Information and Decision Systems with support by the U.S. National Aeronautics and Space Administration Ames and Langley Research Centers, under Grant NGL-22-009-124.

Laboratory for Information and Decision Systems
Massachusetts Institute of Technology
Cambridge, MA, 02139

N 82 - 31637 #

REAL TIME ESTIMATION AND PREDICTION
OF SHIP MOTIONS USING KALMAN FILTER TECHNIQUES

ABSTRACT

A study of the real time estimation and prediction of ship motions, velocities and accelerations is presented. The ship motion estimations are of particular interest for operations in rough seas such as aircraft or helicopter landing, transfer of equipment or cargo at sea and off-shore installations.

In the present study the estimation and prediction of heave, pitch, roll, sway, yaw motions of a DD-963 destroyer is considered, using Kalman filter techniques, for application in VTOL landing.

The governing equations are obtained from hydrodynamic considerations in the form of linear differential equations with frequency dependent coefficients. In addition non-minimum phase characteristics are obtained due to the spatial integration of the water wave forces.

The resulting transfer matrix function is irrational and non-minimum phase. The conditions for a finite-dimensional approximation are considered and the impact of the various parameters is assessed.

A detailed numerical application for a DD-963 destroyer is presented and simulation results of the estimations obtained from Kalman filters are discussed. The effect of

the various modeling parameters on the rms error is assessed and simplifying conclusions are drawn.

The models developed are used to predict the motions a few seconds ahead. An upper bound for prediction time of about five seconds is established, with the exception of roll which can be predicted up to ten seconds ahead. The effect of noise and modeling errors on the rms prediction error is investigated in detail.

TABLE OF CONTENTS

Table of Figures	4
Tables	8
Introduction	9
Overview	11
<u>Chapter 1: EQUATIONS OF MOTION</u>	13
Definitions	13
Simple Derivation	14
Strip Theory	18
Relation between Added Mass and Damping	19
Speed Effects	19
Frequency of Encounter	20
Equations of Motion	22
Heave - Pitch Approximation	24
Sway - Roll - Yaw Approximation	28
<u>Chapter 2: SEA MODELING</u>	51
<u>Chapter 3: DERIVATION OF THE STATE-SPACE EQUATION</u>	60
Heave Pitch Model	60
Sway - Roll - Yaw Model	64
<u>Chapter 4: KALMAN FILTER AND SIMULATION</u>	69
Heave - Pitch Motions	69
Sway - Roll - Yaw Motions	71
<u>Chapter 5: SHIP MOTION PREDICTION</u>	90
Theoretical Background	90
Reduced Number of States	96
CONCLUSIONS	115
ACKNOWLEDGEMENTS	117
REFERENCES	118
<u>Appendix 1: Hydrodynamic Theory</u>	121
<u>Appendix 2: Hydrodynamic Data</u>	127
<u>Appendix 3: Simulations</u>	129
<u>Appendix 4: Computer Program Listing</u>	132

TABLE OF FIGURES

- 1.1 Ship Reference Systems
- 1.2 Wave Profile
- 1.3 Hydrodynamic Problem
- 1.4a Radiation Problem
- 1.4b Diffraction Problem
- 1.5 Strip Subdivision of Ship Hull
- 1.6 Effects of Ship Speed
- 1.7 Angle of Incoming Waves
- 1.8 Heave Exciting Force on a Rectangular Barge
of Length L, Beam B
- 1.9 Effect of Ship Speed on Heave Force and Pitch
Moment at Head Seas
- 1.10 The Equivalent Wavelength for Heave and Pitch
is $\lambda/\cos\phi$
- 1.11 Phase Difference Between Heave and Pitch
- 1.12 Wave Force and Moments in Sway, Roll, and Yaw
at 60° Angle and Zero Forward Speed
- 1.13 Sway Force Versus Frequency for the DD963 Destroyer
and Its Finite Dimensional Approximation (dotted line)
for Zero Speed and 90° Angle of Incidence
- 1.14 Roll Moment for DD963. Same conditions as in 1.13.
- 1.15 Yaw Moment for DD963. Same conditions as in 1.13.
- 1.16 Sway Force Versus Frequency for the DD963 Destroyer
and Its Finite Dimensional Approximation (dotted line)
for Speed U=15.5 ft/sec and 45° Angle of Incidence
- 1.17 Roll Moment for DD963. Same conditions as in 1.16
- 1.18 Yaw Moment for DD963. Same conditions as in 1.16.
- 1.19 Sway Transfer Function for the DD963 Destroyer and
Its Finite Dimensional Approximation (dotted line), for
Speed U = 15.5 ft/sec and 45° Angle of Incidence
- 1.20 Roll Transfer Function for DD963. Same conditions as
in 1.19.
- 1.21 Yaw Transfer Function for DD963. Same conditions as
in 1.19.

TABLE OF FIGURES

(continued)

- 2.1 Typical Wave Spectrum with Two Peaks
- 2.2 Frequency Content of a Wave Spectrum According to Storm Duration
- 2.3 Bretschneider Spectrum at Various Wind Speeds (Fully developed seas)
- 2.4 Bretschneider Spectrum for $H^{1/3} = 10$ ft and Modal Frequency 0.72 rad/sec (sea state 3) and Its Finite Dimensional Approximation (dotted line)
- 4.1 Results of Heave Simulation and Its Kalman Filter Estimate (dotted line), Using Accurate Model at $U=21$ ft/sec and 0° Angle of Incidence and in sea state 5.
- 4.2 Results of Pitch Simulation and Its Kalman Filter Estimate. Same conditions as in 4.1
- 4.3 Results of Sway Simulation and Its Kalman Filter Estimate (dotted line), Using Accurate Model at $U=15.5$ ft/sec and 45° Angle of Incidence, and in sea state 5.
- 4.4 Results of Roll Simulation and Its Kalman Filter Estimate. Same conditions as in 4.3
- 4.5 Results of Yaw Simulation and Its Kalman Filter Estimate. Same conditions as in 4.3
- 4.6 Results of Heave Simulation and Its Kalman Filter Estimate (dotted line). The actual wave spectrum model frequency is 0.52 rad/sec, while the value used in the Kalman Filter is 0.72 rad/sec. All other parameters as in 4.1.
- 4.7 Results of Pitch Simulation and Its Kalman Filter Estimate. Same conditions as in 4.6.
- 4.8 Results of Sway Simulation and Its Kalman Filter Estimate (dotted line). Actual $W_m=0.52$ rad/sec, while in Kalman Filter $W_m=0.72$ rad/sec.^m All other parameters as in 4.3.
- 4.9 Results of Roll Simulation and Its Kalman Filter Estimate. Same conditions as in 4.8.

TABLE OF FIGURES

(continued)

- 4.10 Results of Yaw Simulation and Its Kalman Filter Estimate. Same conditions as in 4.8.
- 4.11 Results of Sway Simulation and Its Kalman Filter Estimate (dotted line), using noisy measurements (light line) when the roll measurement is disconnected. Same other conditions as in 4.3.
- 4.12 Results of Sway Simulation and Its Kalman Filter Estimate (dotted line), using noisy measurements (light line) when the actual angle of incidence is 60° and the value used in the Kalman Filter is 45° . Same other conditions as in 4.3.
- 5.1 Heave Simulation Results and Its Prediction (dotted line starting at $t=40$ sec) for $U=21$ ft/sec and $\phi=0^\circ$, and in sea state 5. Perfect state knowledge is assumed.
- 5.2 Pitch Simulation Results and Its Prediction. Same conditions as in 5.1.
- 5.3 Sway Simulation Results and Its Prediction (dotted line starting at $t=40$ sec) for $U=15.5$ ft/sec and $\phi=45^\circ$, and in sea state 5. Perfect state knowledge is assumed.
- 5.4 Roll Simulation Results and Its Prediction. Same conditions as in 5.3.
- 5.5 Yaw Simulation Results and Its Prediction. Same conditions as in 5.3.
- 5.6 RMS Prediction Error Over RMS Motion Versus Prediction Time for Heave and Pitch, $U=21$ ft/sec, $W_m=0.72$ rad/sec, sea state 5.
- 5.7 RMS Prediction Error Over RMS Motion Versus Prediction Time for Sway, Roll, Yaw. $U=15.5$ ft/sec, $\phi=45^\circ$, sea state 5.
- 5.8 Heave Simulation Results, Its Kalman Filter Estimate (up to 40 sec) and Its Prediction Using the Kalman Filter Estimate (after $t=40$ sec). Same conditions as in 5.1.
- 5.9 Sway Simulation Results, Its Kalman Filter Estimate (up to 40 sec) and Its Prediction Using the Kalman Filter Estimate (after $t=40$ sec). Same conditions as in 5.3.

TABLE OF FIGURES

(continued)

- 5.10 Roll Simulation and Prediction. Same conditions as in 5.9.
- 5.11 Yaw Simulation and Prediction. Same conditions as in 5.9.
- 5.12 RMS Prediction Error Versus RMS Motion Versus Prediction Time for Sway. Actual $W_m=0.52$ rad/sec, used $W_m=0.72$ rad/sec. All other conditions as in 5.3.
- 5.13 RMS Error Versus Prediction Time for Roll. Same condition as in 5.12.
- 5.14 RMS Error Versus Prediction Time for Yaw. Same conditions as in 5.12.
- 5.15 RMS Prediction Error Over RMS Motion for Heave and Pitch. $U=21$ ft/sec, $\phi=0^\circ$, sea state 5. In the prediction model the nonminimum phase zero have been omitted.

TABLES

- 2.1 Sea spectrum coefficients
- 3.1 Matrices used in the numerical applications
- 4.1 Poles of the heave, pitch model
- 4.2 Poles of the heave, pitch Kalman filter
- 4.3 Sensitivity of the rms error for sway, roll, yaw to changes in the model parameters
- 4.4 Poles of the sway, roll, yaw model
- 4.5 Poles of the sway, roll, yaw Kalman filter

INTRODUCTION

The present study started as part of the effort directed toward designing an efficient scheme for landing VTOL aircraft on destroyers in rough seas. A first study [14] showed a significant effect of the ship model used on the thrust level required for safe landing.

In a landing scheme therefore it would be desirable to have accurate ship models capable of providing a good real time estimation of the motions, velocities and accelerations of the landing area, resulting in safer operations and with reduced thrust requirements.

The modeling is quite complex and a substantial effort is required to reduce the governing equations to a finite dimensional system of reasonable order.

The study contains a first chapter on the equations of motion as derived from hydrodynamics, their form and the physical mechanisms involved and the general form of the approximation.

The second chapter describes the modeling of the sea, which proved to be a crucial part of the overall problem.

The third chapter describes the derivation of the state-space equations for the DD-963 destroyer.

In the fourth chapter the Kalman filter studies are presented and the influence of the various parameters is assessed.

In the fifth chapter the feasibility of predicting the ship motions a few seconds ahead in time is studied within the present formulation.

Finally the appendices provide the characteristics of the destroyer, hydrodynamic information and some computer programs used.

OVERVIEW

The real time estimation of the rigid body motions, velocities and accelerations of a vessel in rough seas requires accurate modeling of the wave exciting forces and the hydrodynamic coefficients of the ship.

The wave forces are obtained after an integration over the ship hull of the pressure forces, so that their evaluation requires a seakeeping program, while their magnitude and phase represent clearly an infinitely dimensional system with non-minimum phase characteristics.

The complexity of the resulting equations is due primarily to the wave formation as the vessel moves, which is a mechanism of energy dissipation and additionally it introduces memory effects.

The wave spectrum contains a rather narrow band of frequencies so that an efficient approximation of the ship characteristics can be achieved within this frequency band.

A DD-963 destroyer was used as the basis for the present study. First the geometric and mass properties of the vessel were analysed by the M.I.T. Ocean Engineering Department Seakeeping program and its hydrodynamic forces and coefficients were obtained.

Subsequently a finite dimensional approximation was fitted in this data within the wave frequency range. Two groups of ship motions were distinguished, the heave-pitch and the roll-sway-yaw sets of motion, which up to the first order are uncoupled to each other.

The parameters of the approximations are four:

The speed of the vessel, the direction of the waves, the significant wave height and the modal frequency of the wave spectrum.

These models were used to estimate the ship motions, velocities, accelerations using noisy measurements of the motions. The Kalman filter designed for this purpose gives very good results when a relatively accurate estimate of the modal frequency of the spectrum is available. The modal frequency was found to be the most significant parameter in the overall scheme since it influences the estimation error significantly and is the most difficult to estimate.

The ship speed and the wave heading are important parameters also, but can be estimated easily and accurately.

The double peak spectrum, i.e. seas containing swell also, require separate treatment, because the low frequency peak is hard to estimate, while its influence is quite important.

The predictability of ship motions has been investigated within the frame of the present study. First perfect state information is assumed and by propagating the prediction error covariance from zero initial value it has been established that within 25% rms error over rms motion, the prediction time is about five seconds for all motions with the exception of roll which can be predicted up to ten seconds ahead. Simulations confirmed these results.

The effect of noise and modeling errors is to reduce the prediction time. Omission of the non-minimum phase zeros has a particularly pronounced effect.

In summary, the approximations described in the sequel provide a good model of the quite complex ship equations of motion within the wave frequency range. The derived models can be used for a real time estimation and prediction of the ship motions and other responses using Kalman filter techniques.

Computer programs have been prepared that provide the required model matrices once the parameter of the problem has been specified.

Chapter 1: EQUATIONS OF MOTION

Definitions

The rigid body motions of a ship in six degrees of freedom are shown in Figure 1.1: We define the $x_1 z_1$ plane to coincide with the symmetry plane of the ship, with the z_1 axis pointing vertically upwards when the vessel is at rest, and the y_1 axis so as to obtain an orthogonal right-hand system, while the origin need not coincide with the center of gravity. The $x_0 y_0 z_0$ system is an inertial system with $x_0 y_0$ fixed on the undisturbed sea surface, while the $x y z$ system is moving with the steady speed of the vessel (i.e. it follows the vessel but it does not participate in its unsteady motion). Then the linear motions along the x_1 , y_1 , z_1 axes are surge, sway and heave respectively. In order to define the angular motions, we normally require Euler angles, in the present case, though, we consider small motions so that the tensor of angular displacements can be replaced by a vector of small angular displacements, which are roll, pitch, yaw around the x_1 , y_1 , z_1 axes respectively.

The characteristics of a ship are its slender form, i.e. $L/B \gg 1$, $L/T \gg 1$, where L is the length, B the beam and T the draft. Also, the ship is symmetric about the xz plane and near symmetric about the yz plane. For this reason

$$I_{yz} = I_{zy} = 0$$

$$I_{xy} = I_{yx} = 0$$

The value of I_{xz} is typically small compared with I_{xx} , I_{yy} . The justification of using the linearity assumption is as follows: The excitation consists of wave induced forces, which include fluid inertia forces and hydrostatic forces. It is well established that the wave height to wave length ratio is small, since at a typical upper value of 1/7 the wave breaks and loses all its energy [15] (Figure 1.2). As a result, the major part of the wave force is a linear function of the wave elevation and can be obtained by a first order perturbation expansion of the nonlinear fluid equation, using the wave height to length ratio as the perturbation parameter [15].

The wave spectrum, as will be shown later, has a frequency range between typically 0.2 and 2 rad/sec. Given the large mass of the vessel, the resulting motions, within this frequency range, are of the order of a few feet, or a few degrees, so that the equations of motion can be linearized.

The only motion that requires attention is roll, because due to the slender form of the ship, the rolling motion may become large, in which case nonlinear damping becomes important.

Simple Derivation

We derive the equation of motion for a simple two dimensional object to demonstrate the overall procedure.

Let us assume that we wish to derive the motion of a two dimensional cylinder subject to wave excitation, allowed to move in heave only (Figure 1.3).

The incoming wave of amplitude a_0 and frequency ω_0 will cause a force on the cylinder, and, therefore, heave motion. Due to the linearity of the problem, the following decomposition can be used, which simplifies the problem considerably.

(a) Consider the sea calm and the ship forced to move sinusoidally with unit heave amplitude, and frequency ω_0 , and find the resulting force.

(b) Consider the ship motionless and find the force on the cylinder due to the incoming waves and the diffraction effects (diffraction problem).

(c) In order to find the heave amplitude, within linear theory, we equate the force found in (a) times the (yet unknown) heave amplitude, with the force found in (b). (Figure 1.4)

The force in (b) can be decomposed further for modeling purposes, again due to linearity: One part is due to the undisturbed incoming waves and the other part due to the diffracted waves. The first is called the Froude-Krylov force and the second the diffraction force. The total force is called the excitation force [15].

The force in (a) due to linearity can be also decomposed: The first part is simply the hydrostatic force. The second part is the dissipative force, caused by the fact that the refraction waves carry energy from the ship to infinity. For this reason, we define a damping coefficient B so that the dissipative force will be $-B\dot{x}$ where \dot{x} is the heave velocity. The third part is

is an inertia force, caused by the fact that the heaving ship causes the fluid particles to move in an unsteady motion so that we define an "added" mass A and the inertia force becomes $-Ax''$ with x'' the heave acceleration. If we denote the undisturbed incoming wave elevation amidships as $\eta(t)$:

$$\eta(t) = a_0 e^{i\omega_0 t} \quad (1)$$

Where the real part of all complex quantities is meant, here and in the sequel. Then the excitation force will be

$$F = F_0 e^{i\omega_0 t} a_0 \quad (2)$$

Where F_0 is complex (to take into account the phase difference with respect to the wave elevation), and the equation of motion becomes:

$$Mx'' = F - Ax'' - Bx' - Cx \quad (3)$$

Where M the mass of the cylinder; the motion is also sinusoidal so with x_0 complex:

$$x(t) = x_0 e^{i\omega_0 t} \quad (4)$$

A very important remark is that F_0, A, B depend on the frequency of the incoming wave ω_0 . This can be easily understood by the fact that at various frequencies the heaving cylinder will produce waves with different wavelength. We rewrite, therefore, equation (3) as:

$$-Mx_0 \omega_0^2 e^{i\omega_0 t} = \{F_0(\omega_0) a_0 + [A(\omega_0) \omega_0^2 - i\omega_0 B(\omega_0) - C] x_0\} e^{i\omega_0 t} \quad (3a)$$

By dropping $e^{i\omega_0 t}$, we can rewrite equation (3a) as:

$$\{-[M + A(\omega_0)] \omega_0^2 + i\omega_0 B(\omega_0) + C\} x_0 = F_0(\omega_0) a_0 \quad (3b)$$

The motion of a cylinder in water, therefore, results in an increase in the mass and damping term. Equation (3b) is used because of its similarity to a second order system, it is strictly valid, though, only for a monochromatic wave.

Ultimately, we wish to obtain the response in a random sea, so equation (3b) must be extended for a random sea. This can be done by obtaining the inverse Fourier transform of (3a), i.e.

$$\int_{-\infty}^{\infty} K_a(t - \tau) \ddot{x}(\tau) d\tau + \int_{-\infty}^{\infty} K_u(t - \tau) \dot{x}(\tau) d\tau + C x(t) = \int_{-\infty}^{\infty} K_f(t - \tau) \eta(\tau) d\tau \quad (5)$$

Where K_a, K_u, K_f the inverse Fourier transform of $-\omega^2 [M + A(\omega)]$, $i\omega B(\omega)$ and $F_o(\omega)$ respectively. The random undisturbed wave elevation is denoted by $\eta(t)$. Equation (5) is not popular with hydrodynamicists, because the effort required to evaluate the kernels K_a, K_u, K_f is by far greater than that required to find the added mass, damping and excitation force. For this reason, equation (5) is rewritten in a hybrid form as follows:

$$- [M + A(\omega)] \ddot{x}(t) + B(\omega) \dot{x}(t) + C x(t) = F(\omega) \eta(t) \quad (6)$$

This is an integro-differential equation (or differential equation with frequency dependent coefficients), whose meaning is in the sense of equation (5).

Strip Theory

The evaluation of $A(\omega)$, $B(\omega)$, $F(\omega)$ is not an easy task for complex geometries, such as the hull of a ship. The hydrodynamic particulars can be found in a later section, but we can give a simple description here of a technique used to simplify the derivations: [15],[17]

The ship can be divided in many transverse strips as shown in Figure (1.5). Due to its elongated form and for high frequencies, each strip has small interactions with the other strips, except near the ends. Usually these end effects are small, so that instead of solving the overall three dimensional problem, we can solve many two dimensional problems (one for each strip) and sum up all the partial results. For the case of heave, for example, if $A(\omega, x)$ $B(\omega, x)$ are the added mass and damping in heave of a strip at location x , then

$$A(\omega) = \int_{-L/2}^{L/2} A(\omega, x) dx \quad (7)$$

$$B(\omega) = \int_{-L/2}^{L/2} B(\omega, x) dx \quad (8)$$

The strip theory has larger errors at smaller frequencies. It so happens, though, that at small frequencies the hydrostatic forces are predominant, so that the motion error is quite small. Comparison with experiments has shown that for slender ship

configurations, the strip theory provides very good predictions [15],[17].

Relation Between Added Mass And Damping

The added mass and damping coefficients are not independent of each other, because their frequency dependence is caused by the same refraction waves. If we define

$$T(\omega) = \omega^2 \left[A(\omega) - \frac{B(\omega)}{\omega} \right] \quad (9)$$

Then $T(\omega)$ is an analytic function [16]. As a result, $A(\omega)$, $B(\omega)$, which are real, are related by the Kramers-Kronig relations, in order to describe a causal system. This fact will be used later to obtain a single approximation for $T(\omega)$ instead of two separate approximations for $A(\omega)$, $B(\omega)$.

Speed Effects

As it can be seen in Figure 1.6 when the ship is heaving with a small angle θ and at the same time is moving forward with speed U , then a heave velocity results, which is $\dot{x} = U\theta$. The effect of the forward speed, therefore, is to couple the various motions by speed dependent coefficients. As it can be found in Appendix 1, there are simplified expressions for the added mass, damping and exciting force with a parametric dependence on the speed U . Then

expressions greatly facilitate the evaluation of the ship motions.

Frequency Of Encounter

An additional effect of the ship speed is the change in the frequency of encounter. If the incident wave has a frequency ω and a wave number k , then the frequency of encounter ω_e is

$$\omega_e = \omega + k U \cos \phi \quad (10)$$

Where ϕ is the angle between the x axis of the ship and the direction of wave propagation (Figure 1.7). In deep water, the dispersion relation for water waves is

$$\omega^2 = kg \quad (11)$$

so that we can rewrite (10) as

$$\omega_e = \omega + \frac{\omega^2}{g} U \cos \phi \quad (12)$$

A very important consideration in the difference between frequency of encounter and wave frequency is the following: The ship motions due to linearity will be of frequency ω_e so that the refraction waves are of frequency ω_e and the added mass and damping can be written as $A(\omega_e)$, $B(\omega_e)$.

The amplitude of the exciting force though, consists of the Froude Krylov part which depends on ω and the diffraction and speed dependent parts which depend on ω_e . The time dependence is again $\omega_e \cdot t$, i.e.

$$F(t) = a_0 F(\omega, \omega_e, \nu) e^{i\omega_0 t} \quad (13)$$

with a_0 the incident wave amplitude.

This is a very crucial observation and can cause significant errors if not taken into account.

Equation of Motion

Following the notation of Appendix 1, we write the equations of motion. It should be noted that, due to the slenderness of the ship, the surge motion is left out as a second order motion. This is in agreement with experiments [17]. Within linear theory and using the ship symmetry, the heave and pitch motions are not coupled with the group of sway, roll, yaw motions. This is not to imply that the motions are independent, because they are excited by the same wave, so there is a definite relation both in amplitude and phase.

(1) Heave - Pitch Motions

$$\left\{ \begin{bmatrix} M & 0 \\ 0 & I_Y \end{bmatrix} + \begin{bmatrix} A_{33} & A_{35} \\ A_{53} & A_{55} \end{bmatrix} \right\} \ddot{\underline{x}}_V + \begin{bmatrix} B_{33} & B_{35} \\ B_{53} & B_{55} \end{bmatrix} \dot{\underline{x}}_V + \begin{bmatrix} C_{33} & C_{35} \\ C_{53} & C_{55} \end{bmatrix} \underline{x}_V = \begin{bmatrix} F_3 \\ F_5 \end{bmatrix} \eta \quad (14)$$

(2) Sway - Roll - Yaw Motion

$$\left\{ \begin{bmatrix} M & M_{24} & M_{26} \\ M_{42} & I_X & I_{XZ} \\ M_{62} & I_{XZ} & I_Z \end{bmatrix} + \begin{bmatrix} A_{22} & A_{24} & A_{26} \\ A_{42} & A_{44} & A_{46} \\ A_{62} & A_{64} & A_{66} \end{bmatrix} \right\} \ddot{\underline{x}}_u + \begin{bmatrix} B_{22} & B_{24} & B_{26} \\ B_{42} & B_{44} & B_{46} \\ B_{62} & B_{64} & B_{66} \end{bmatrix} \dot{\underline{x}}_u + \begin{bmatrix} 0 & 0 & 0 \\ 0 & C_{44} & 0 \\ 0 & 0 & 0 \end{bmatrix} \underline{x}_u = \begin{bmatrix} F_2 \\ F_4 \\ F_6 \end{bmatrix} \eta \quad (15)$$

Where A_{ij} , B_{ij} , C_{ij} the added mass, damping, hydrostatic coefficient matrices; F_j the exciting forces; η the wave elevation;

$$\underline{x}_v = \{x_3, x_5\}^T \quad (16)$$

$$\underline{x}_u = \{x_2, x_4, x_6\}^T \quad (17)$$

The frequency and velocity dependence is not written explicitly, but is understood, as described in the previous sections.

Heave - Pitch Approximation

We start with the heave and pitch motions approximation.

As it is obvious from equation (14), it involves two stages:

- (a) Approximation of the exciting force
- (b) Approximation of the added mass and damping coefficients

Data are provided by the hydrodynamic theory for both components and within the wave frequency range.

A. Exciting Force Approximation

Figure 1.8 shows the exciting heave force on a box-like ship [25]. This information is important to demonstrate several zeros of the amplitude of the heaving force. Figure 1.9 shows the amplitude and phase of the exciting force on a destroyer, where, again, the same zeros appear, accompanied in the phase plot by jumps in the phase.

The transfer function between the wave elevation and the heave force cannot be represented as a ratio of polynomials of finite degree as evidenced by Figure 1.9. Similar plots can be obtained for the pitch moment. Within the wave frequency range, though, only the first zero is important, while the remaining peaks are of minor significance. This is not true for other types of vehicles such as the semi-submersible, but for ships it is valid for both heave force and pitch moment, so it will be used to simplify considerably the modeling procedure.

As it was mentioned before, the exciting force changes with frequency ω_e , but its amplitude is determined on the basis of the frequency ω . The following variables must be included in an

appropriate modeling of the exciting forces

- (1) frequency ω
- (2) speed V
- (3) wave angle ϕ

$$F_3(t, \alpha_0, \phi, U) = F_3(\omega, \phi) \alpha_0 e^{i\omega_e t} \quad (18)$$

$$F_5(t, \alpha_0, \phi, U) = \left\{ F_5(\omega, \phi) + \frac{U}{i\omega} f_3(\omega_e, \phi) \right\} e^{i\omega_e t} \quad (19)$$

where a_0 the wave amplitude, f_3 the heave diffraction force. Equations (18), (19) show that the heave force does not depend on the ship speed, whereas the pitch moment does, in a linear fashion.

In order to approximate $F_3(\omega, \phi)$, $F_5(\omega, \phi)$, $f_3(\omega_e, \phi)$ we use the plots in Figure 1.9 as well as Figure 1.10, which show the approximate influence of the wave angle on the excitation force.

In order to model the DD963 destroyer, the M.I.T. five degrees of freedom seakeeping program [27] was used to derive hydrodynamic results. The following model was derived to model shape of the heave force at $V = 0$ and $\phi = 0$ (no speed, head seas)

$$F_3(s) = \frac{\alpha_1 \eta}{\left[1 + 2J \frac{s}{\omega_a} + \frac{s^2}{\omega_a^2} \right]^2} \quad (20)$$

Where $J = 0.707$, α_1 a constant to be determined from hydrodynamic data, η the wave elevation and ω_a the corner frequency. Remembering the analysis above concerning the dependence of the force on ω and Figure 1.10, we can derive.

$$\omega_a = \sqrt{\frac{2 \pi g}{L \cos \phi + B}} + \frac{2 \pi}{L \cos \phi + B} U \cos \phi \quad (21)$$

where L is the ship length, B the beam.

Before we establish a relation similar to (20) above, we have to discuss Figure 11, where it is shown that for long waves, the heave force and the pitching movement are 90° out of phase. This means that the transfer function between heave and pitch is a non-minimum phase one, because the amplitude is constant, while the phase is 90°. We choose to attribute the non-minimum phase to pitch. Also, the pitch angle tends to the wave slope for large wavelengths, so the pitching moment can be written as

$$F_5 = \alpha_2 \frac{1 - s/\omega_o}{1 + s/\omega_o} \frac{s^2 \cos \phi}{[1 + 2J \frac{s}{\omega_a} + \frac{s^2}{\omega_a^2}]} \eta \quad (22)$$

Where α_2 a constant to be determined, ω_a is the same (for simplicity) as in equation (21) and ω_o is an artificial frequency to model the non-minimum phase. It will be chosen to be equal to the wave spectrum modal frequency, so we defer the discussion until the corresponding section.

B. Added Mass and Damping

By using equation (9), we can rewrite the equations of motion as

$$\begin{bmatrix} T_{33} s^2 + Ms^2 + C_{33} & T_{35} + UsT_{33} + C_{35} \\ T_{53} s^2 - UsT_{33} + C_{35} & Is^2 + T_{55} s^2 - U^2 T_{33} + C_{55} \end{bmatrix} \begin{bmatrix} X_3 \\ X_5 \end{bmatrix} = \begin{bmatrix} F_3 \\ F_5 \end{bmatrix} \eta \quad (23)$$

Here we construct a simplified model where

$$T_{ij} = A_{ij} - \frac{B_{ij}}{i\omega} \quad (24)$$

with A_{ij}, B_{ij} to be evaluated from the hydrodynamic data. Then equation (23) can be written, after we define

$$\begin{aligned} Y_1 &= x_3 & Y_2 &= \dot{x}_3 \\ Y_3 &= x_5 & Y_4 &= \dot{x}_5 \end{aligned} \quad (25)$$

$$\underline{Y} = \{Y_1, Y_2, Y_3, Y_4\}^T$$

in the form:

$$\begin{bmatrix} \dot{Y}_2 \\ Y_4 \end{bmatrix} = \begin{bmatrix} A_{33} & A_{35} \\ A_{53} & A_{55} \end{bmatrix}^{-1} \left\{ - \begin{bmatrix} C_{33} & B_{33} & C'_{35} & B_{35} \\ C'_{53} & B_{53} & C'_{55} & B_{55} \end{bmatrix} \underline{Y} + \begin{bmatrix} F_3 \\ F_5 \end{bmatrix} \eta \right\} \quad (23a)$$

where

$$\begin{aligned} C'_{35} &= C_{35} + U A_{33} \\ C'_{53} &= C_{35} - U A_{33} \\ C'_{55} &= C_{55} - U^2 \times A_{33} \end{aligned} \quad (26)$$

Sway-Roll-Yaw Approximation

Next we approximate the sway-roll-yaw group of motions, which is uncoupled to first order from the heave-pitch group of motions. Again a two stage approximation is required, i.e.:

- (a) Approximation of the exciting force
- (b) Approximation of the added mass and damping coefficients

Data are obtained by using the sea-keeping program.

A. Exciting force approximation

The same infinite-dimensional form is obtained for the exciting force as seen in Figure 1.12 (17abc) for all three motions, as in the case of pitch and heave. Again, within the wave frequency range, a finite dimensional approximation can be achieved, and of reasonably small order.

The important fact that the exciting force depends on the wave frequency rather than the frequency of encounter, is used, while the following three quantities define the exciting force amplitude and phase

- (1) Wave frequency
- (2) Speed V
- (3) Wave angle ϕ

In Appendix 1 the strip theory approximation of the sway, roll, yaw forces can be found. Using the M.I.T. five degrees of freedom seakeeping program the following finite dimensional approximation was found in case of $V = 0$, $\phi = 90^\circ$ for sway, roll and yaw

$$F_2 (S) = \frac{A_2 S^2}{\left(\frac{S}{\omega_2}\right)^2 + 2J_2 \frac{S}{\omega_2} + 1} \quad (27)$$

$$F_4 (S) = \frac{A_4 S^2}{\left(\frac{S}{\omega_4}\right)^2 + 2J_4 \frac{S}{\omega_4} + 1} \quad (28)$$

$$F_6 (S) = \frac{A_6 S^2}{\left(\frac{S}{\omega_6}\right)^2 + 2J_6 \frac{S}{\omega_6} + 1} \quad (29)$$

$$\begin{aligned} \text{where } \omega_2 &= 0.65 & J_2 &= .5 \\ \omega_4 &= 0.85 & J_4 &= .3 \\ \omega_6 &= 0.85 & J_6 &= .3 \end{aligned} \quad (30)$$

and A_2, A_4, A_6 are obtained from hydrodynamic data.

We redefine the value of $\omega_2, \omega_4, \omega_6$ such that it will be valid for angles ϕ other than 90° , and speed other than 0:

$$\omega'_j = (\omega_j + \omega_j^2 \frac{V}{g} \cos\phi) \sin\phi \quad (31)$$

where $j = 2, 4, 6$ and ω_j is given above.

It should be noted that the sway, roll and yaw forces are proportional to the wave slope, i.e. 90° out of phase with respect to the wave amplitude. This means that they belong to the same group with pitch, and the same non-minimum phase transfer function:

$$\frac{s - \omega_0}{s + \omega_0}$$

must be used for all three of them, when the total system (all 5 degrees of motion) is considered.

B. Added Mass and Damping

The amplitude of the transfer function between the wave elevation and the rolling motion has a very narrow peak so that the coefficients can be approximated as constant [17]. Using Appendix 1:

$$\begin{aligned}
 A_{44} &= A_{44}^0 & B_{44} &= B_{44}^0 \\
 A_{42} &= A_{24}^0 & B_{42} &= B_{24}^0 \\
 A_{46} &= A_{46}^0 + \frac{V}{\omega^2} B_{24}^0 \\
 B_{46} &= B_{46}^0 - V A_{24}^0
 \end{aligned} \tag{32}$$

using the value of ω at the roll peak. It should be noted that roll involves a significant nonlinear (viscous) damping, which is approximated by introducing an additional "equivalent" damping coefficient B_{44}^* [3]

Similarly, we calculate the sway, yaw coefficients at the same frequency:

$$\begin{aligned}
 A_{22} &= A_{22}^0 & B_{22} &= B_{22}^0 \\
 A_{26} &= A_{26}^0 + \frac{V}{\omega^2} B_{22}^0 \\
 B_{26} &= B_{26}^0 - V A_{22}^0 \\
 A_{62} &= A_{26}^0 - \frac{V}{\omega^2} B_{22}^0 \\
 B_{62} &= B_{26}^0 + V A_{22}^0 \\
 A_{66} &= A_{66}^0 + \frac{V^2}{\omega^2} A_{22}^0 \\
 B_{66} &= B_{66}^0 + \frac{V}{\omega^2} B_{22}^0
 \end{aligned} \tag{33}$$

$$\left[s^2 \{A_{ij} + M_{ij}\} + s \{B_{ij}\} + \{C_{ij}\} \right] \begin{pmatrix} X_2 \\ X_4 \\ X_6 \end{pmatrix} = \begin{pmatrix} F_2 \\ F_4 \\ F_6 \end{pmatrix} \quad \begin{matrix} i = 2, 4, 6 \\ j = 2, 4, 6 \end{matrix} \tag{34}$$

where $C_{ij} = 0$ except for C_{44} , which is the roll hydrostatic constant, i.e. $C_{44} = \Delta \cdot (GM)$ with Δ the ship displacement and (GM) the metacentric height.

Due to the special form of the matrix C , a zero-pole cancellation results from a direct state space representation of the equation above. After some manipulations, the following representation can be obtained which avoids zero-pole cancellation problems:

$$\dot{\underline{X}} = T \underline{X} + U \underline{F}$$

$$\text{where } \underline{X} = \{X_2, \dot{X}_4, X_4, X_6\}^T$$

$$\underline{F} = \{\int F_2, F_2, F_4, \int F_6, F_6\} \quad (35)$$

where $\int F$ indicates the time integral of F and $T = \{t_{ij}\}$ and $U = \{u_{ij}\}$, with:

$$t_{11} = \frac{r}{r_{22}} P_{21} - P_{11}, \quad t_{12} = \frac{r}{r_{22}} P_{12}, \quad t_{13} = \frac{r}{r_{22}} P_{22} - P_{12}, \quad t_{14} = \frac{r}{r_{22}} P_{23} - P_{13}$$

$$t_{41} = \frac{r}{r_{22}} P_{21} - P_{31}, \quad t_{42} = \frac{r_{32}}{r_{22}}, \quad t_{43} = \frac{r}{r_{22}} P_{22} - P_{32}, \quad t_{44} = \frac{r}{r_{22}} P_{23} - P_{33}$$

$$t_{21} = -P_{21} t_{11} - P_{23} t_{41}, \quad t_{22} = -P_{21} t_{12} - P_{23} t_{42} - P_{22}$$

$$t_{23} = -P_{21} t_{13} - P_{23} t_{43} - r_{22} C_{44}$$

$$t_{24} = -P_{21} t_{14} - P_{23} t_{44}$$

$$t_{3i} = 0 \quad \text{except for } t_{32} = 1$$

(36)

$$U_{ij} = 0 \quad \text{except for } U_{11} = r_{11} - \frac{r_{12} r_{21}}{r_{22}}$$

$$U_{14} = r_{13} - \frac{r_{12} r_{23}}{r_{22}}, \quad U_{41} = r_{31} - \frac{r_{32} r_{21}}{r_{22}}$$

$$U_{44} = r_{33} - \frac{r_{32} r_{23}}{r_{22}}, \quad U_{21} = -P_{21} U_{11} - P_{23} U_{41}$$

$$U_{22} = r_{21}, \quad U_{23} = r_{22}, \quad U_{24} = -P_{21} U_{14} - P_{23} U_{44}$$

$$U_{25} = r_{23}$$

(37)

$$\text{where } R = \{r_{ij}\} = [A+M]^{-1}, \quad P = \{P_{ij}\} = R B \quad (38)$$

Figures 1.13 through 1.15 show the actual force and moments versus frequency and the achieved finite dimensional approximation for zero speed and beam seas ($\phi=90^\circ$). It should be noted again that the approximation is not as good outside the wave frequency range.

Figures 1.16 through 1.18 show the same quantities for speed $U=15.5$ ft/sec and 45° angle of incidence. From these figures it can be seen that above 1 rad/sec the approximation is poor, nonetheless no significant wave energy is contained in that range, so the approximation is acceptable.

Figures 1.19 through 1.21 show the overall transfer function between the corresponding motion and the sea elevation.

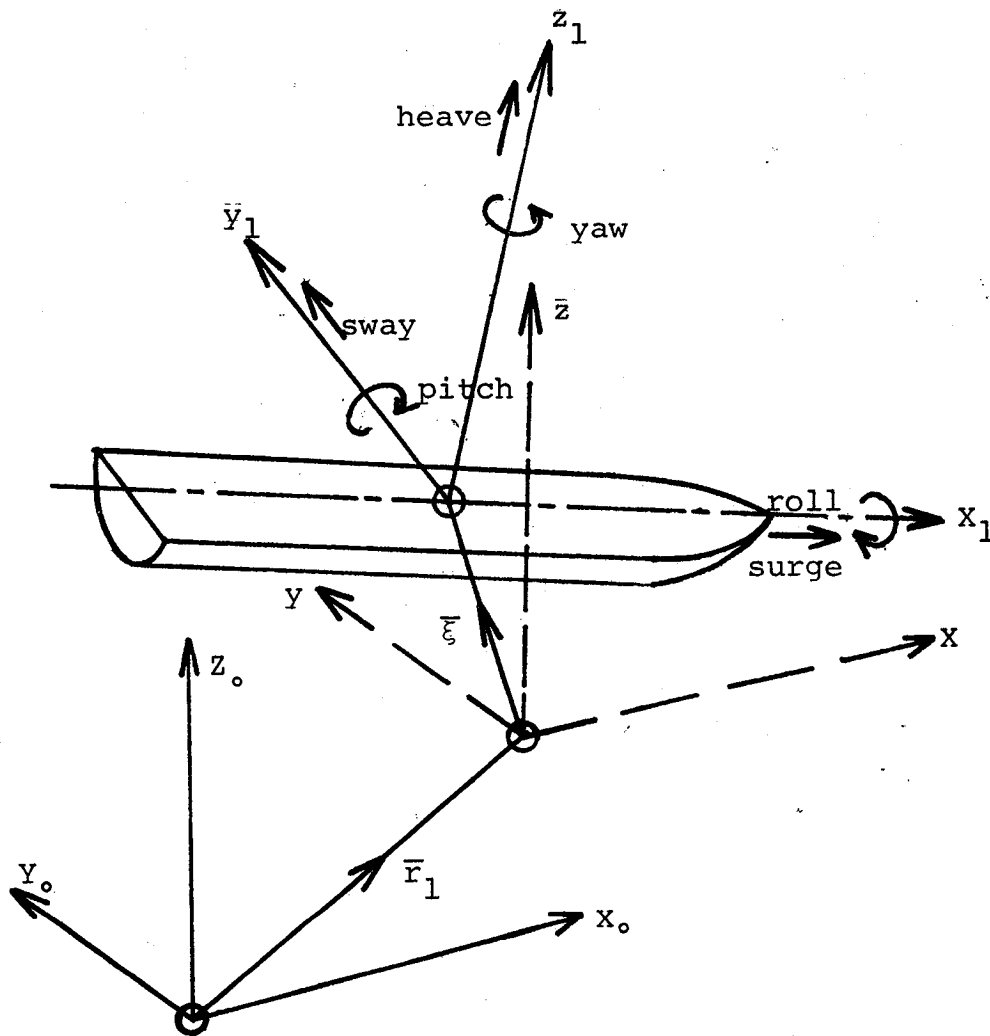


Figure 1.1

Ship Reference Systems

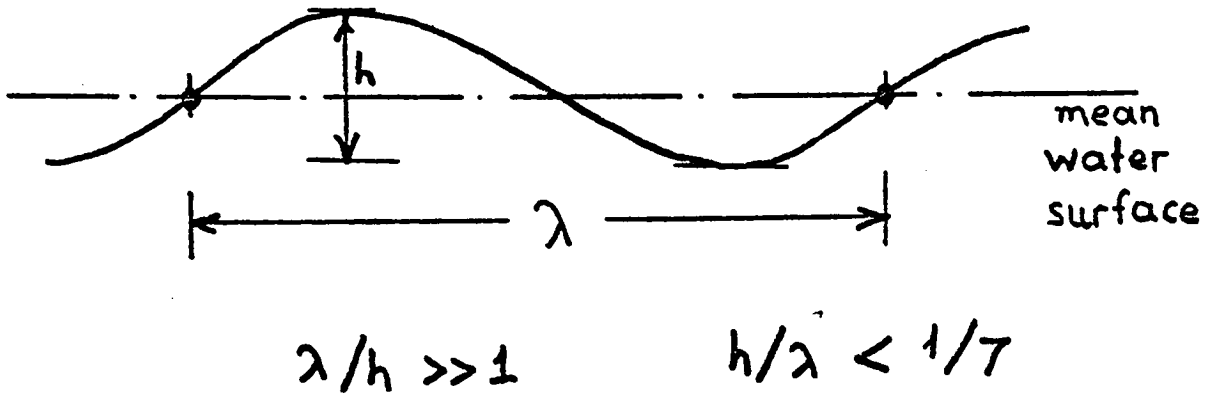


Figure 1.2

Wave Profile

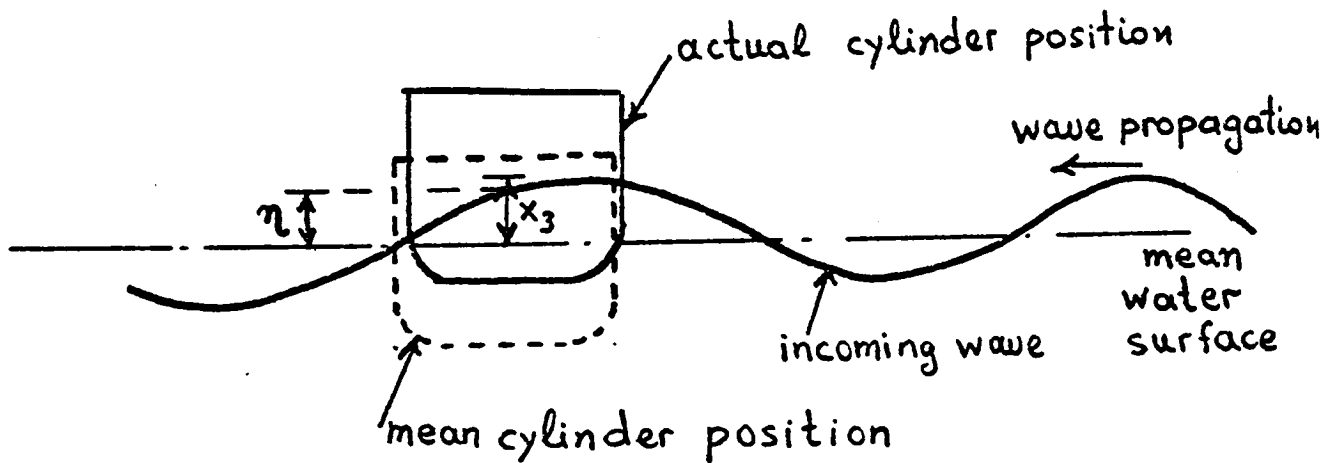


Figure 1.3

Hydrodynamic Problem

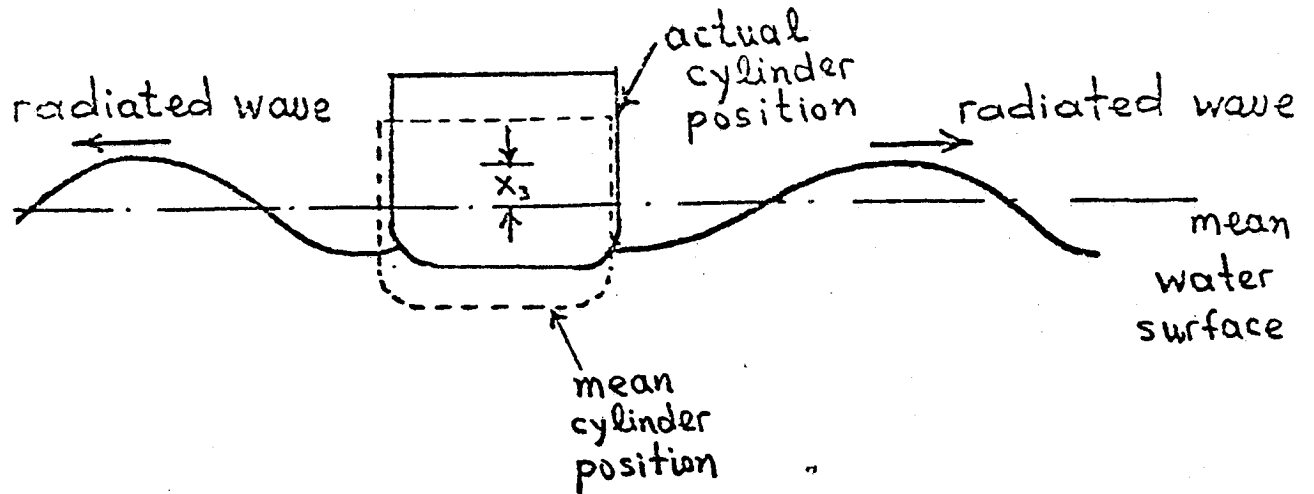


Figure 1.4a
Radiation Problem

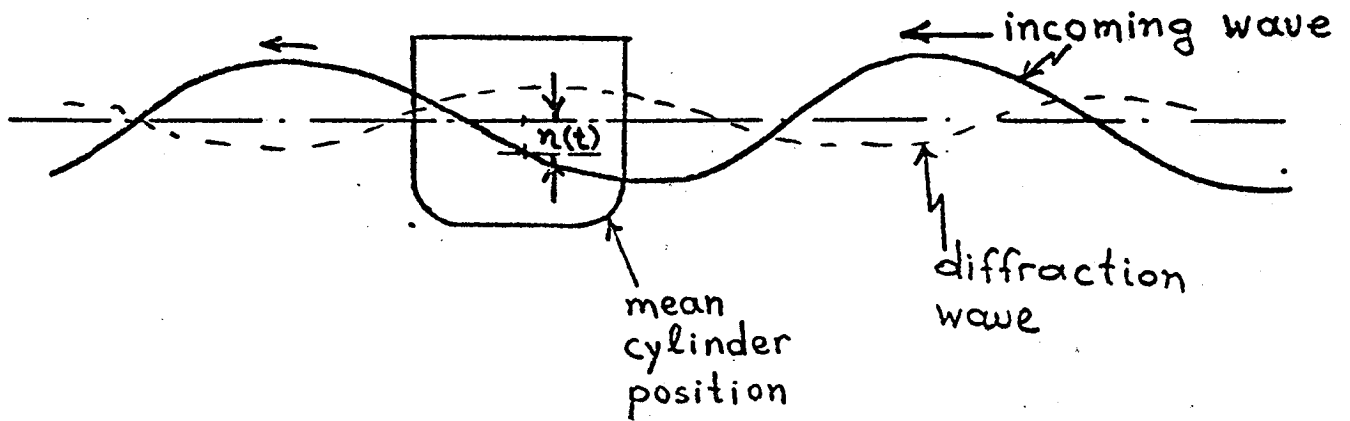


Figure 1.4b
Diffraction Problem

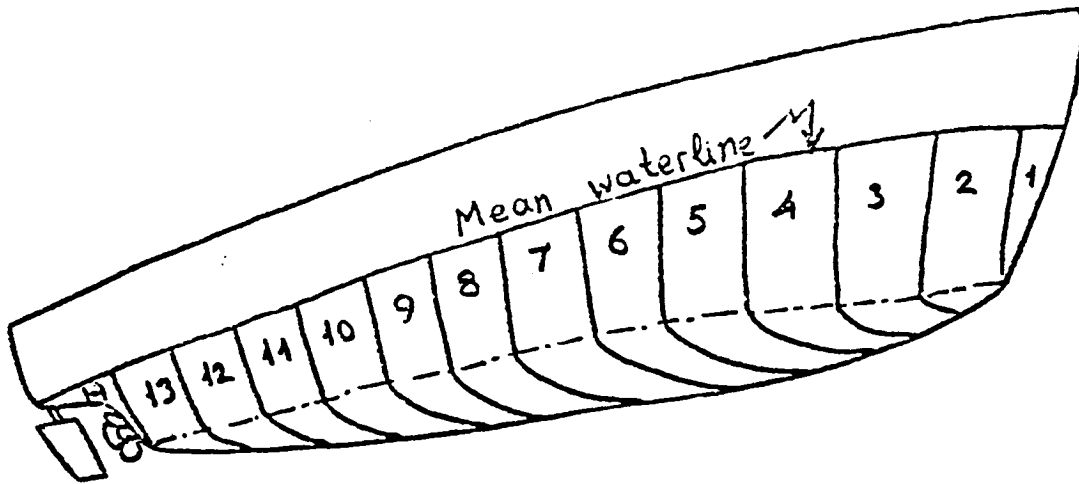


Figure 1.5
Strip Subdivision of Ship Hull

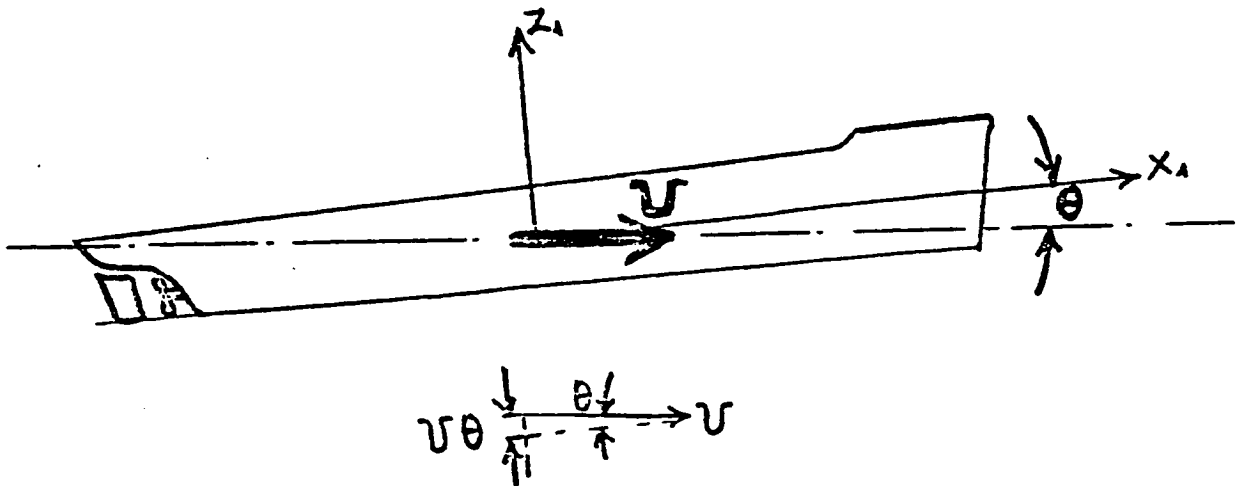


Figure 1.6
Effects of Ship Speed

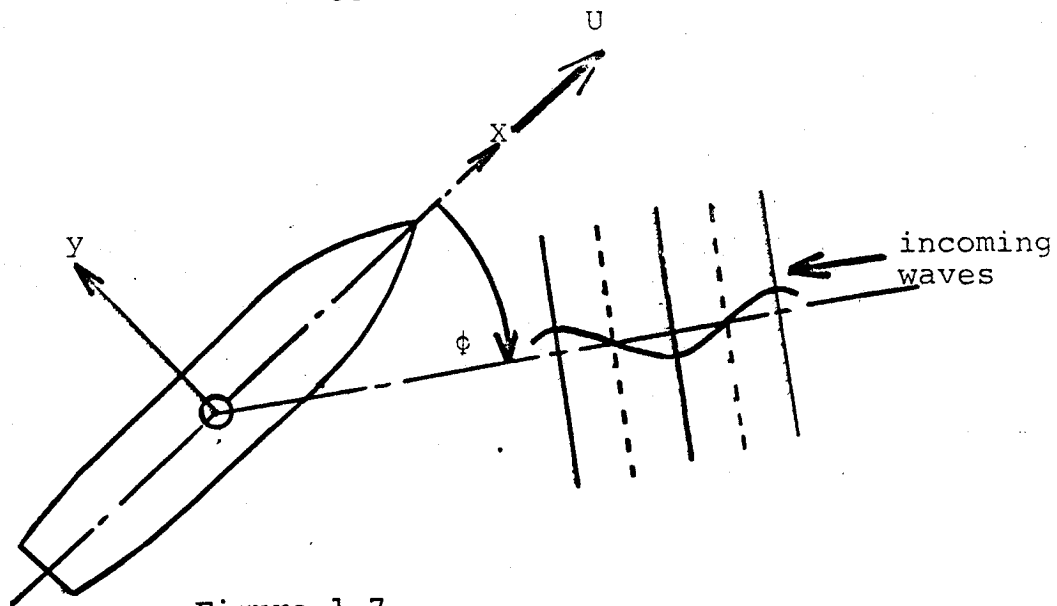


Figure 1.7
Angle of Incoming Waves

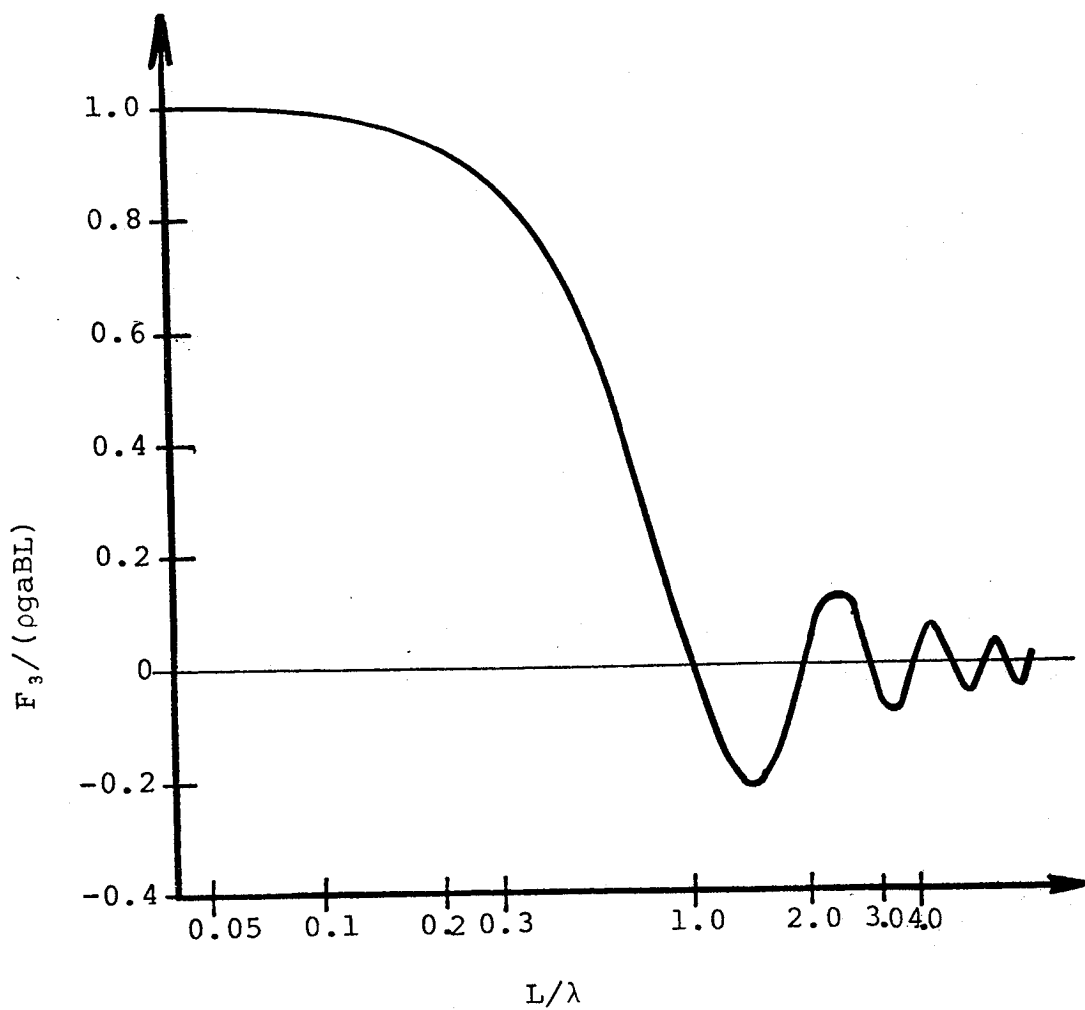


Figure 1.8
Heave Exciting Force on a Rectangular Barge
of Length L , Beam B

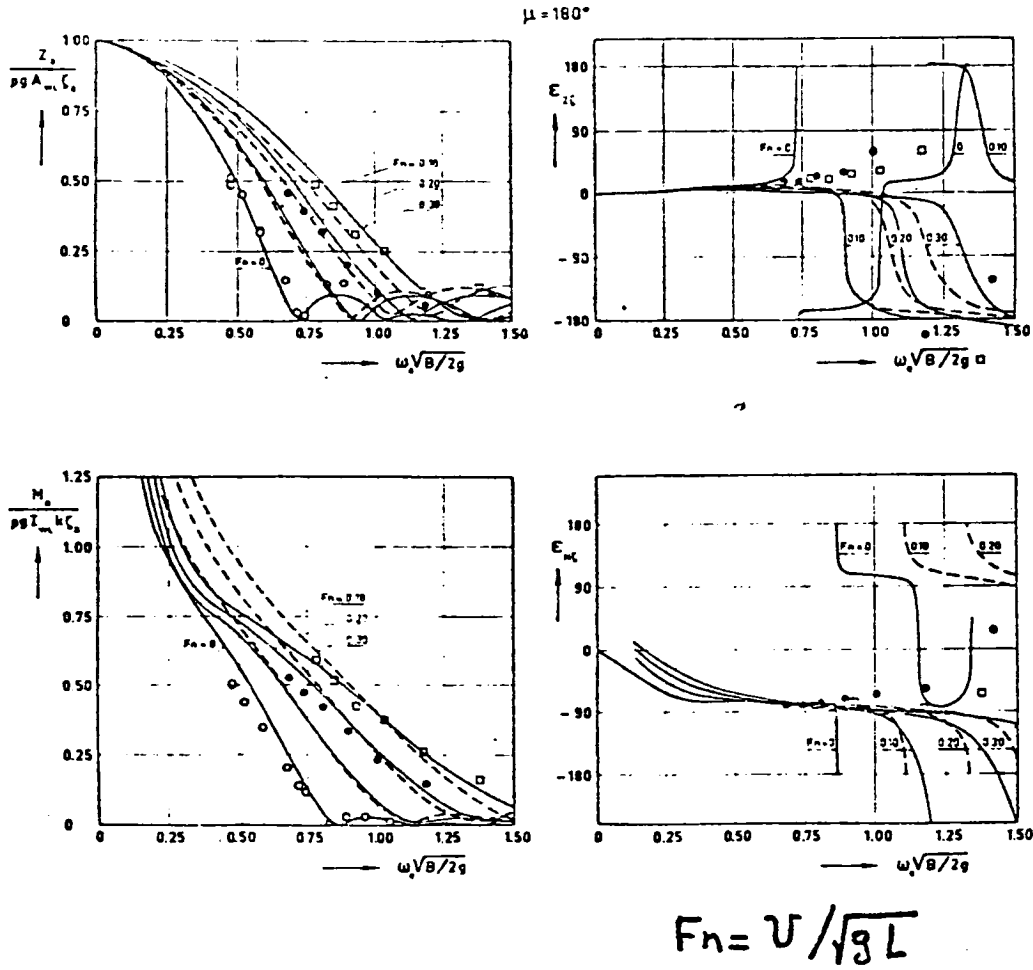


Figure 1.9

Effect of Ship Speed on Heave Force and Pitch Moment at Head Seas

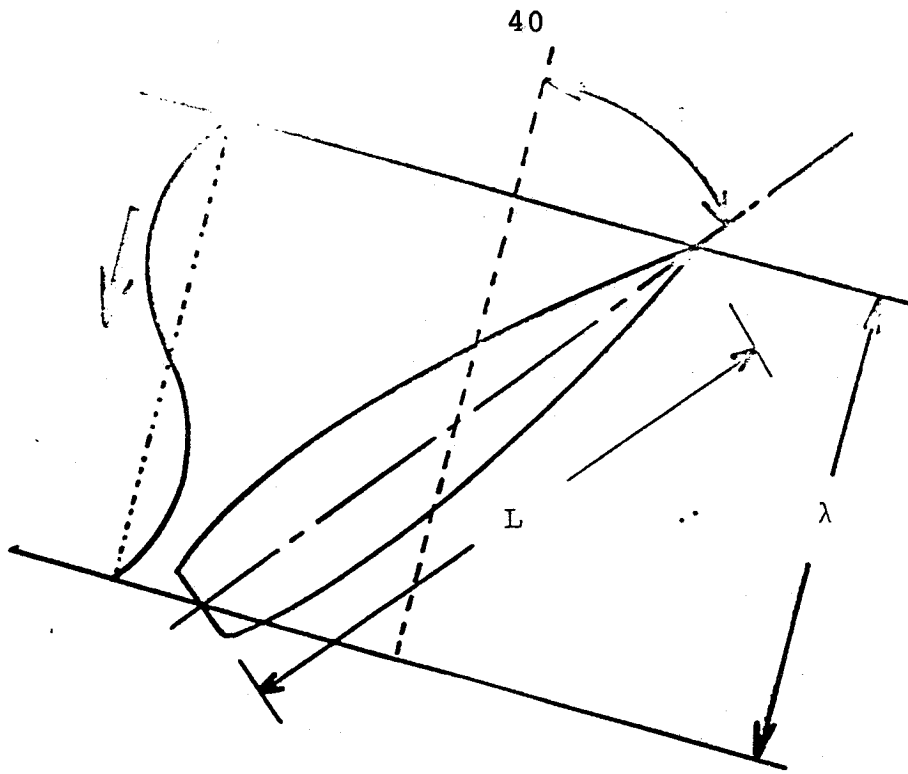


Figure 1.10

The Equivalent Wavelength for Heave and Pitch is $\lambda / \cos \phi$

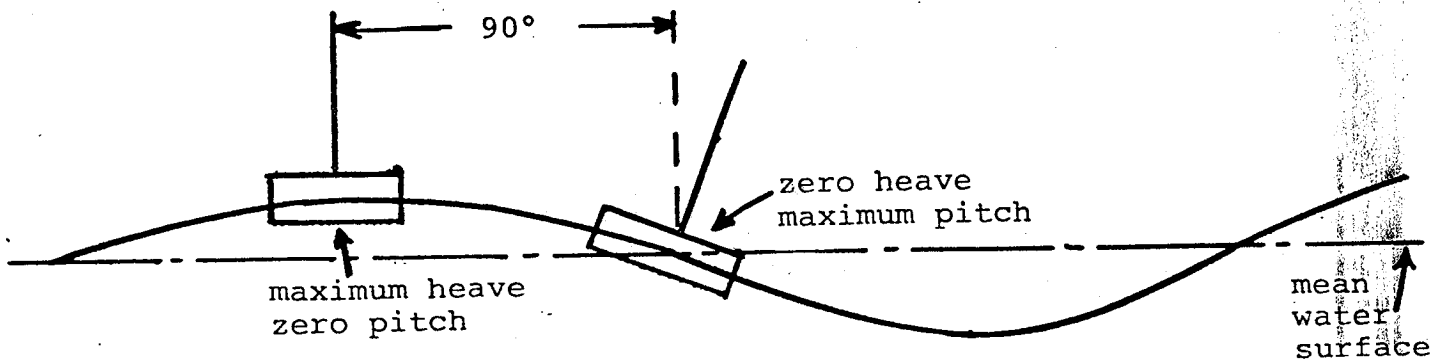


Figure 1.11

Phase Difference Between Heave and Pitch

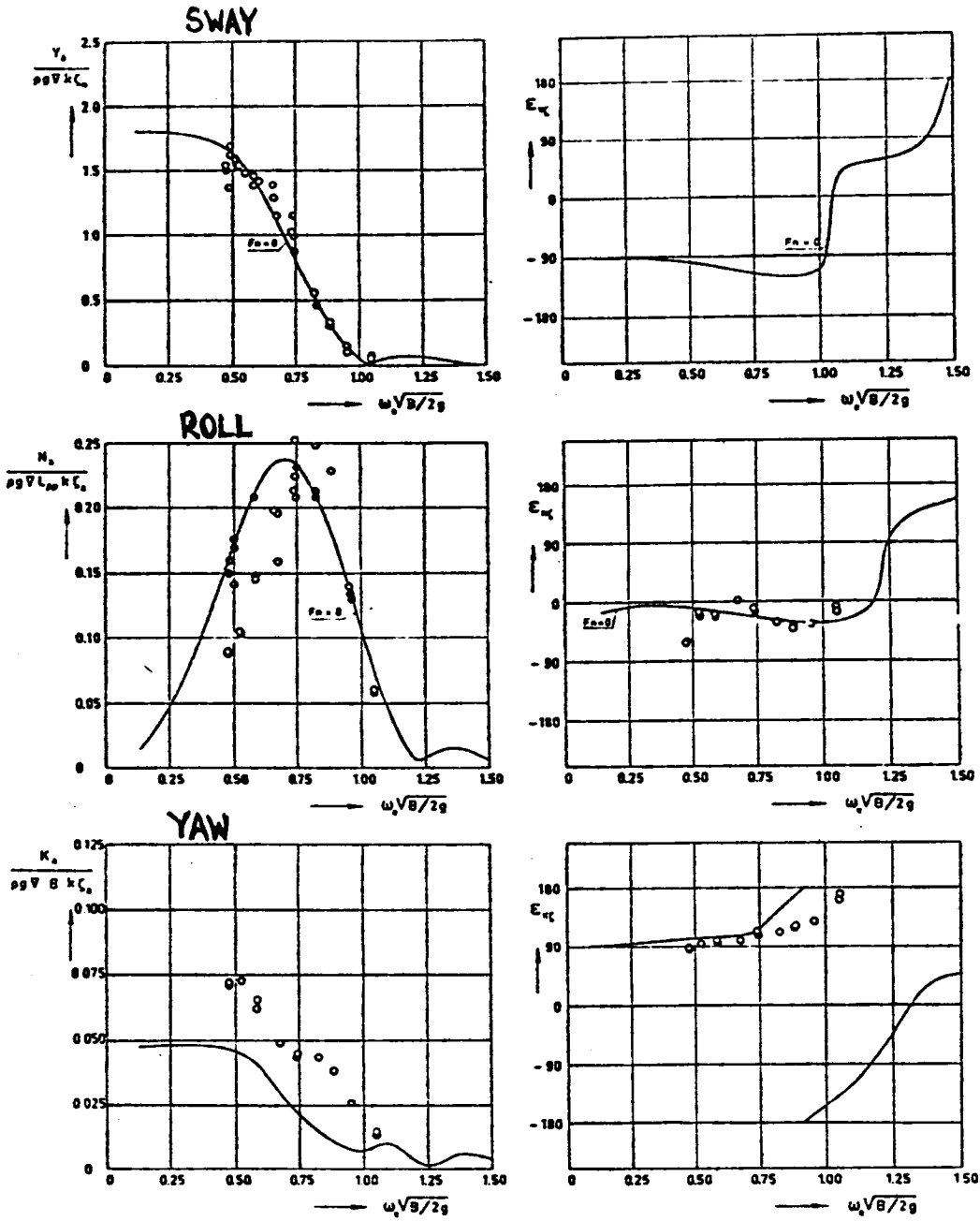


Figure 1.12

Wave Force and Moments in Sway, Roll, and Yaw at 60° Angle and Zero Forward Speed

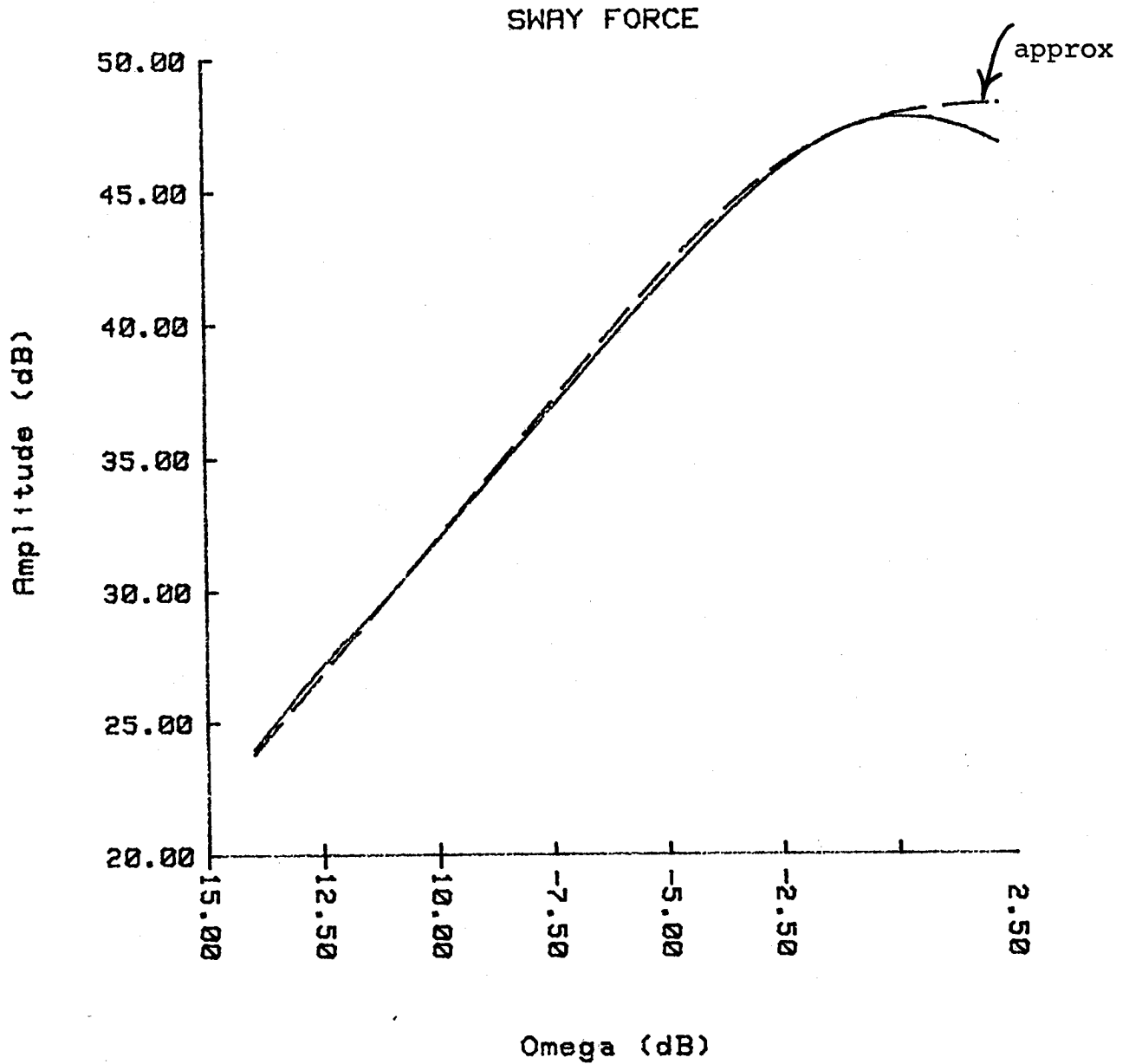


Figure 1.13

Sway Force Versus Frequency for the DD963 Destroyer and Its Finite Dimensional Approximation (dotted line) for Speed $U = 15.5$ ft/sec and 45° Angle of Incidence

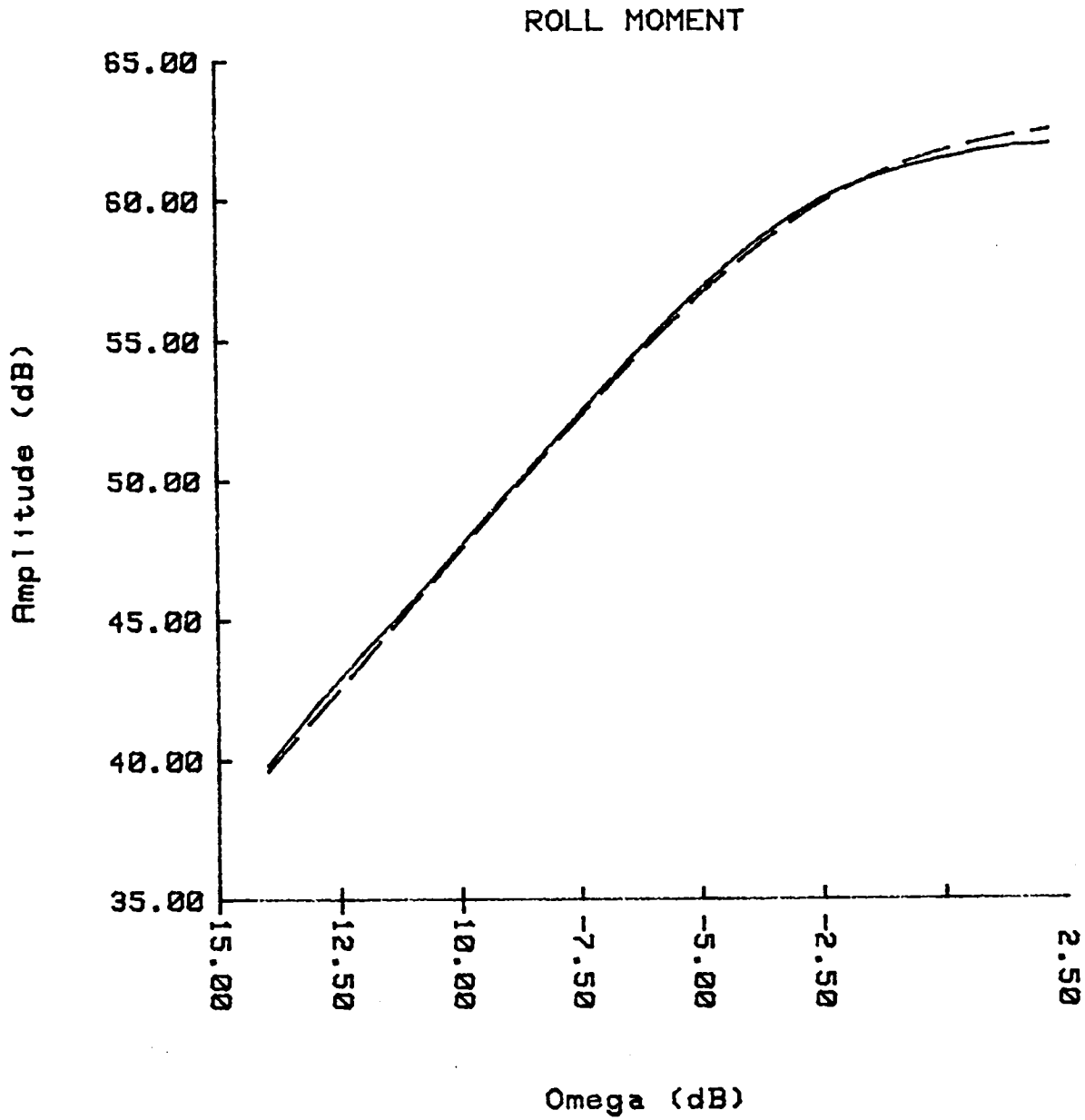
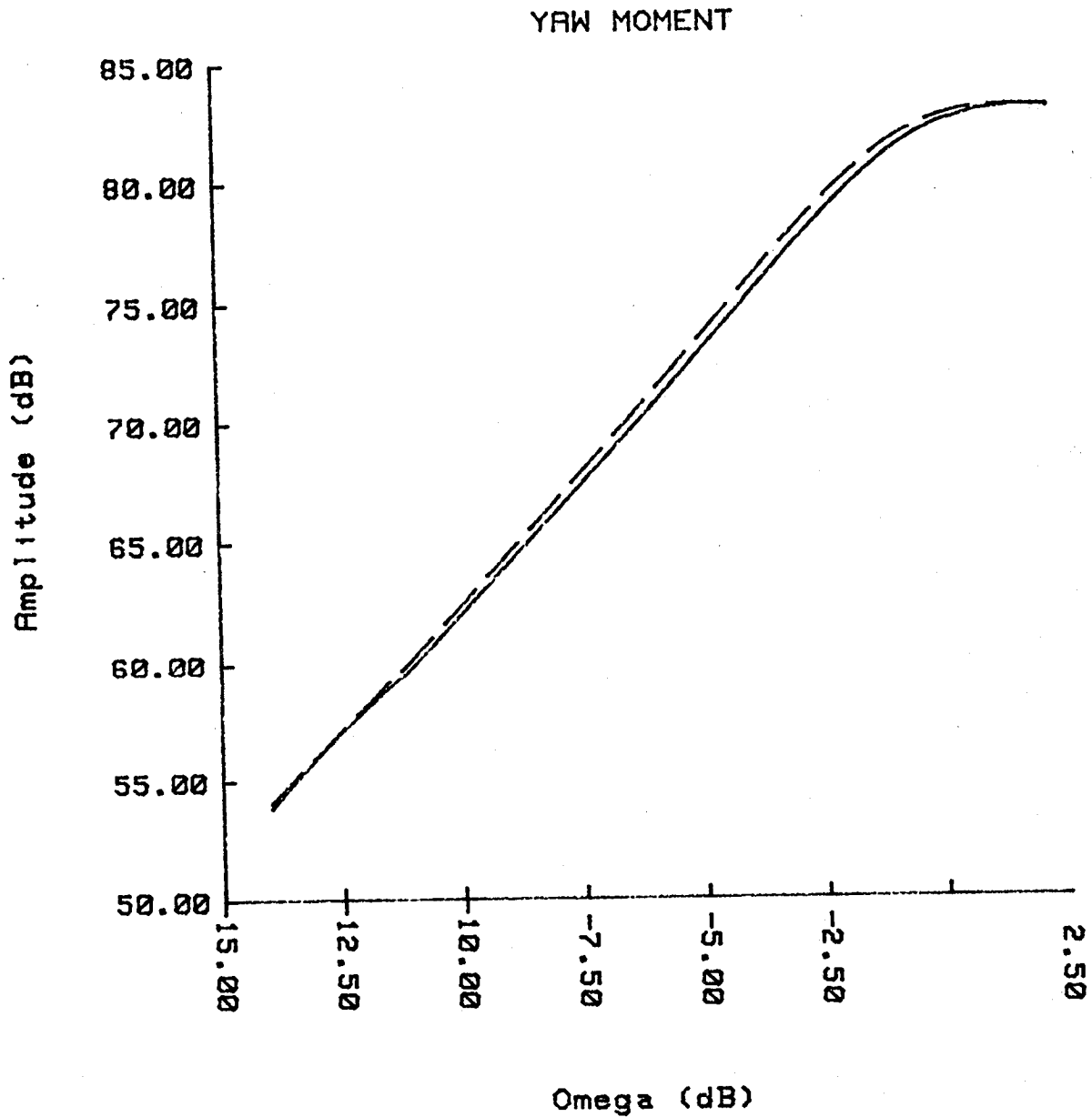


Figure 1.14

Roll Moment for DD963. Same conditions as in 1.13.



Omega (dB)

Figure 1.15

Yaw Moment for DD963. Same conditions as in 1.13.

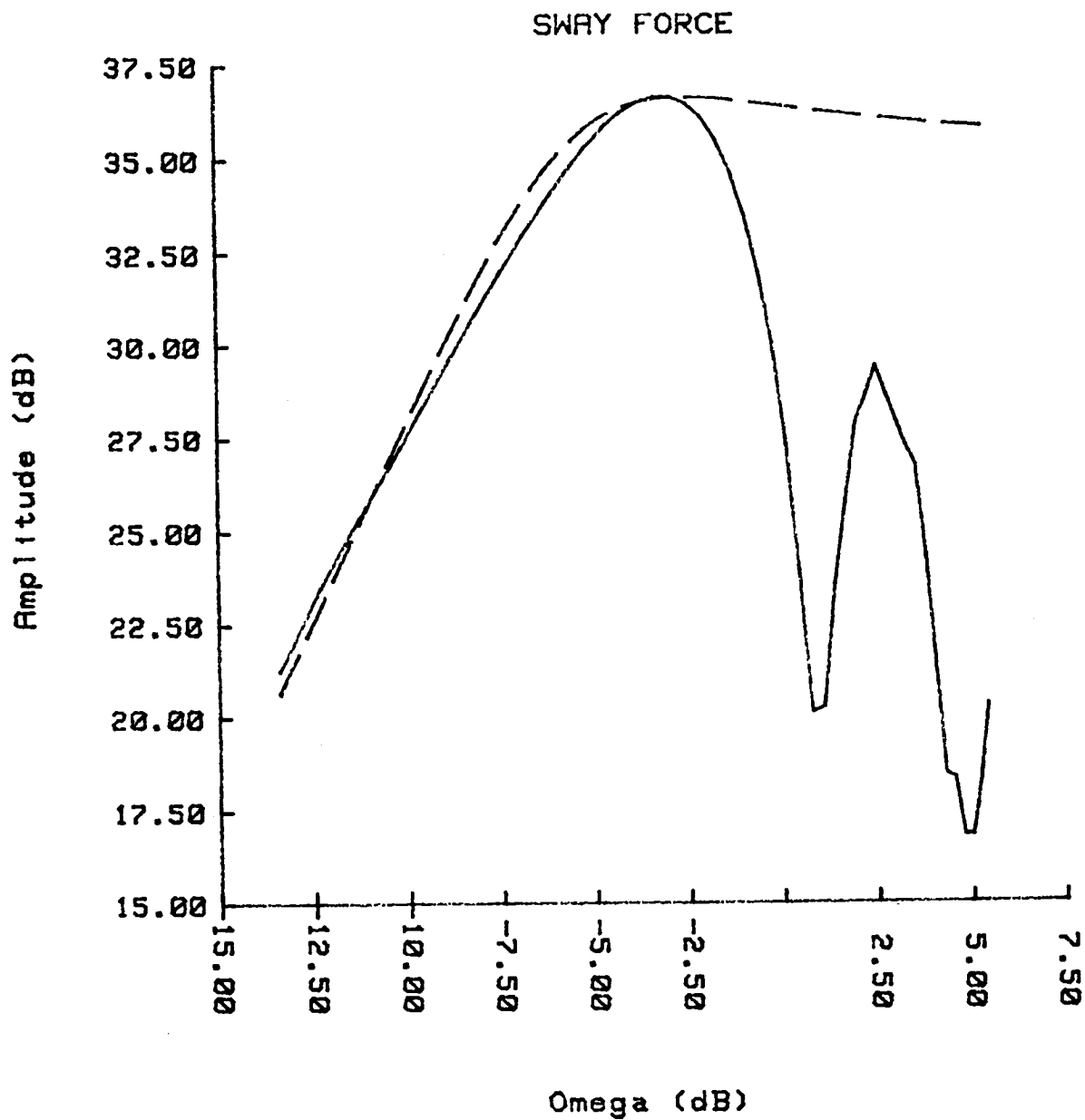


Figure 1.16

Sway Force Versus Frequency for the DD963 Destroyer and Its Finite Dimensional Approximation (dotted line), for Speed $U = 15.5$ ft/sec and 45° Angle of Incidence

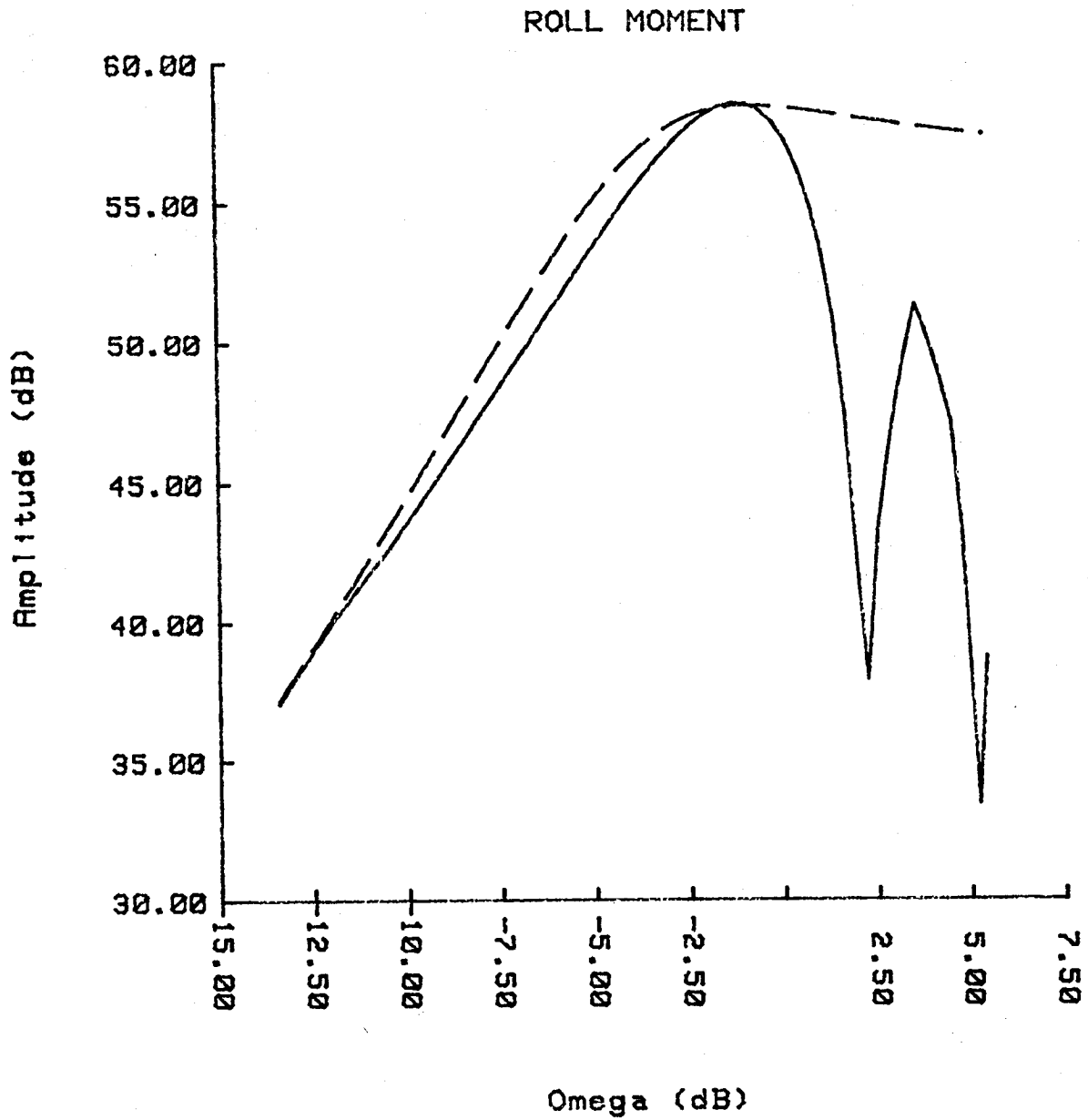


Figure 1.17

Roll Moment for DD963. Same conditions as in 1.16.

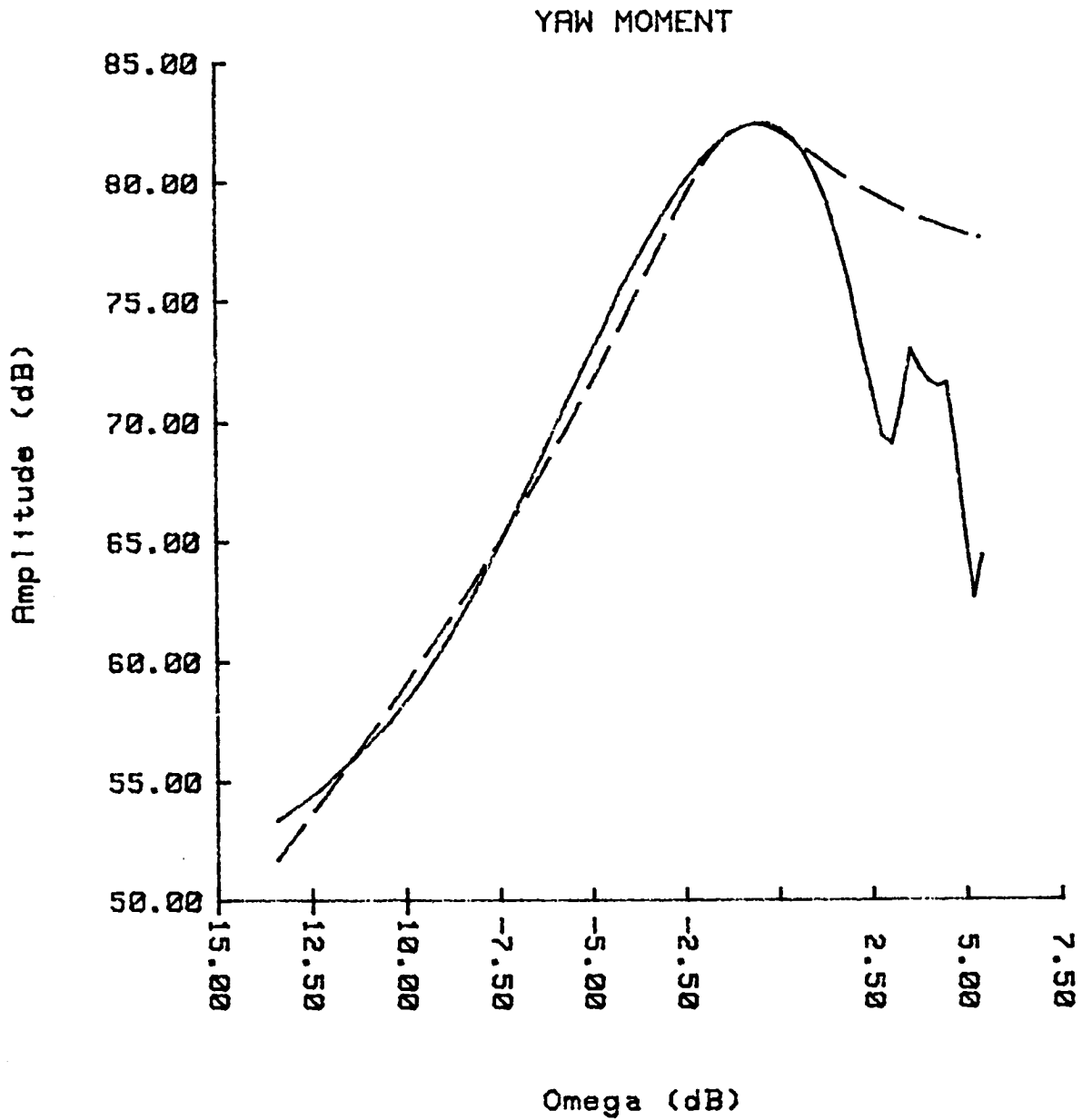


Figure 1.18

Yaw Moment for DD963. Same conditions as in 1.16.

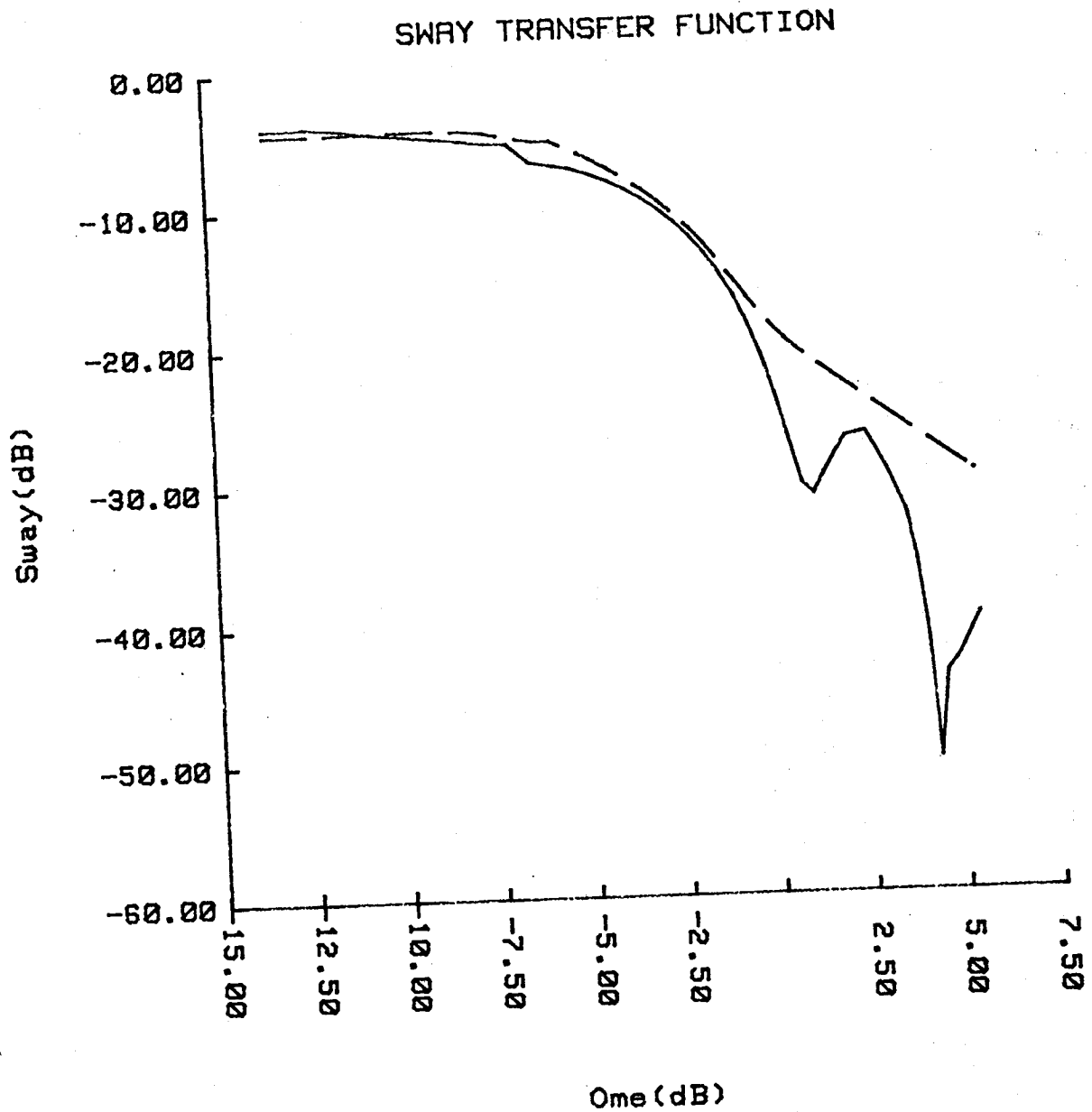


Figure 1.19

Sway Transfer Function for the DD963 Destroyer and Its Finite Dimensional Approximation (dotted line), for Speed $U = 15.5$ ft/sec and 45° Angle of Incidence

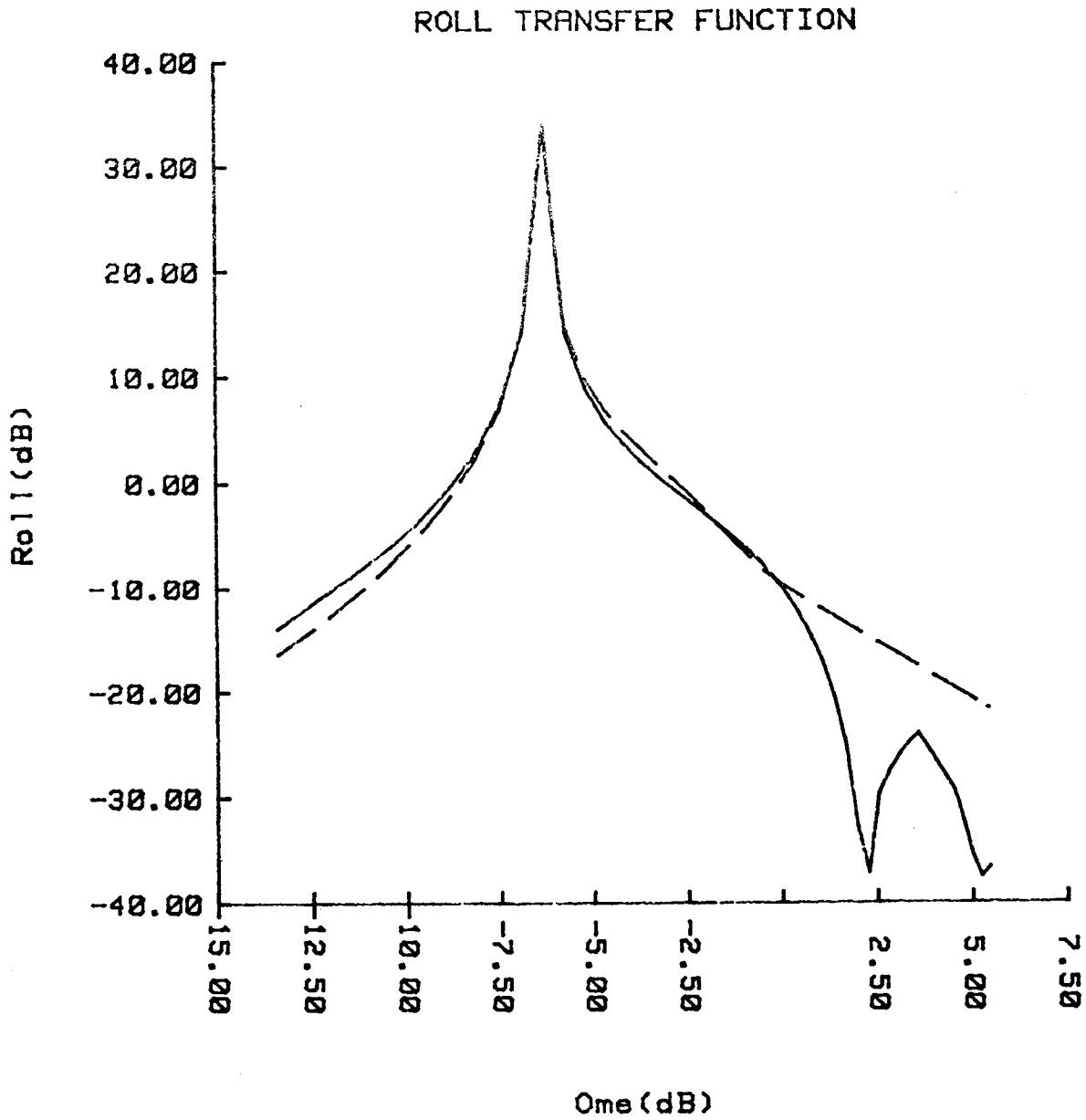


Figure 1.20

Roll Transfer Function for DD963. Same conditions as in 1.19.

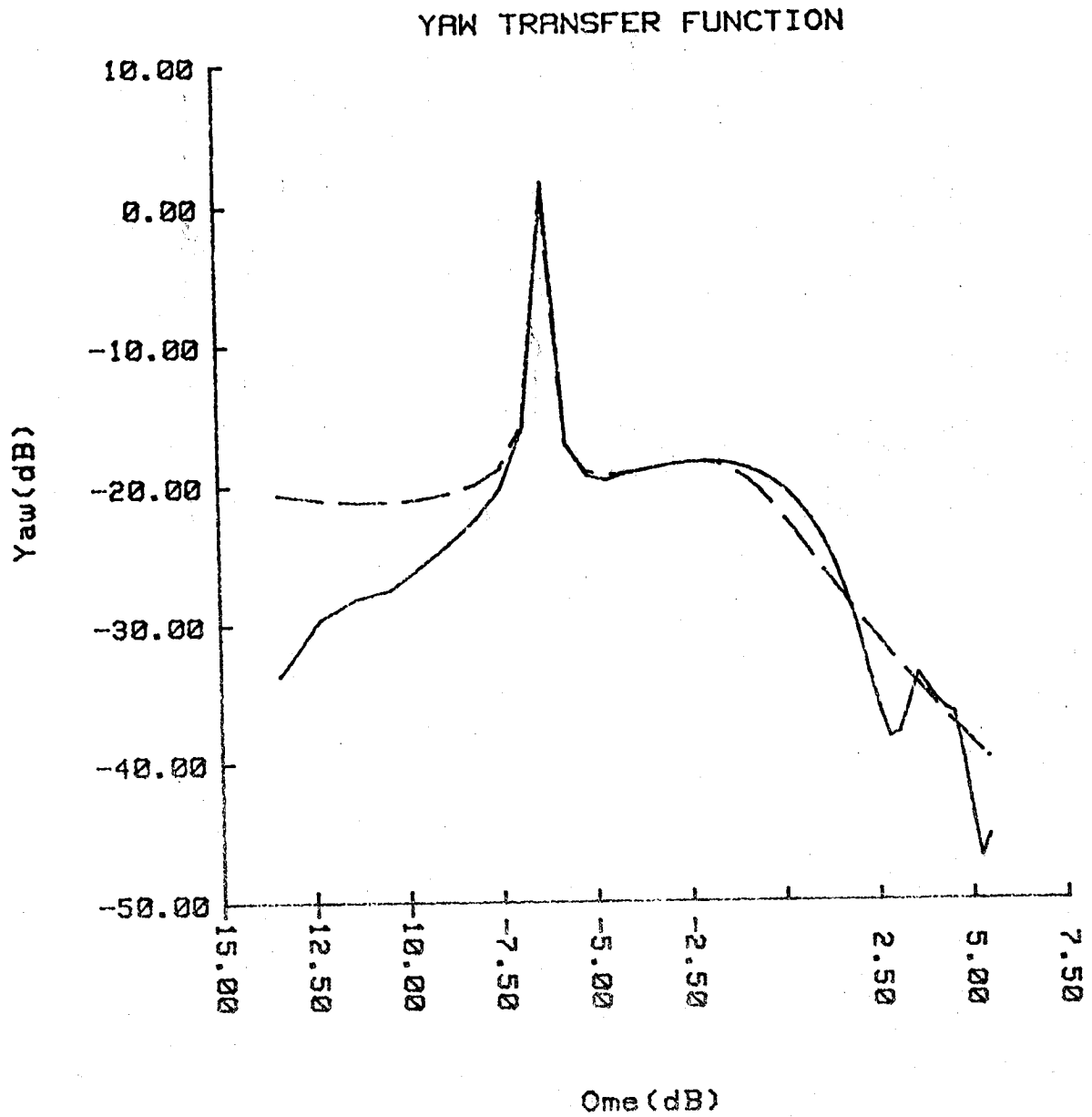


Figure 1.21

Yaw Transfer Function for DD963. Same conditions as in 1.19.

Chapter 2: SEA MODELING

The sea waves are generated by the wind, except for very few cases. The process of wave generation is of importance in modeling, so we will outline, briefly, a simple theoretical model:

When the wind starts blowing over a calm water surface, it contains gust components of high frequency, which cause wavelets on the surface. This is due to the inherent instability of the wave air interface. As soon as the surface becomes rough, a significant drag force develops between air and water, which becomes zero only if the average wind speed (which causes the major part of the drag) equals the phase wave velocity. As a result, the steady-state condition of the sea develops slowly by creating waves whose phase velocity is close to the wind speed. Since the process starts with high frequencies, we conclude that a young storm will contain a peak at high frequency. We usually distinguish between a developing storm and a fully developed storm.

As soon as the wind stops blowing, then the water viscosity dissipates the high frequency waves so that the so called swell (decaying seas) forms, which consists of long waves (low frequency content), which travel away from the storm that originates them. For this reason, swell can be found together with another local storm (Figure 2.1).

A storm usually contains one peak (except if swell is present when it contains two peaks) and the peak frequency ω_m is called the modal frequency (Figure 2.2). Also, the intensity of the storm is required, which can be described in a number of ways: Beaufort Scale, Sea State, Wind Average Velocity, Significant Wave Height. The best is the significant wave height H defined as the statistical average of the 1/3 highest waveheight. For a narrow band spectrum of area M_0 .

$$H \approx 4 \sqrt{M_0} \quad (39)$$

From our discussion on sea storm generation, we conclude that it is important to model a storm by both H (intensity) and ω_m (duration of storm). For this reason, the Bretschneider Spectrum will be used defined as:

$$S(\omega) = \frac{1.25}{4} H^2 \frac{\omega_m^4}{\omega^5} \exp \left\{ -1.25 \left(\frac{\omega_m}{\omega} \right)^4 \right\} \quad (40)$$

The spectrum was developed by Bretschneider for the North Atlantic, for unidirectional seas, with unlimited fetch, infinite depth and no swell. It was developed to satisfy asymptotic theoretical predictions and to fit North Atlantic data. It was found to fit reasonably well in any sea location. Also, by combining two such spectra, we can model the swell as well. Its main limitations are unidirectionality and unlimited fetch.

It was felt, however, that it could provide an adequate description for the present application for open sea.

As it has already been mentioned, the forward speed of the vessel causes a shift in the wave frequency to the frequency of encounter. The spectrum, now, can be defined for ship coordinates as follows

$$S(\omega_e) = \left[\frac{S(\omega)}{d\omega_e/d\omega} \right]_{\omega = f(\omega_e)} \quad (41)$$

where

$$\omega = f(\omega_e) = \frac{-1 + \sqrt{1 + 4\omega_e \frac{U \cos \phi}{g}}}{2 \frac{U}{g} \cos \phi} \quad (42)$$

A rational approximation was found to (29) subject to (30) in the following form

$$S_a(\omega_e) = \frac{1.25}{4\omega_m^5} H^2 B(\alpha) \frac{(\omega_e/\omega_o)^4}{\left[1 + \left(\frac{\omega_e}{\omega_o} \right)^4 \right]^3} \quad (43)$$

where $S_a(\omega_e)$ the approximate spectrum

$$\alpha = \frac{U}{g} \omega_m \cos \phi \quad (44)$$

$B(\alpha)$, $\gamma(\alpha)$ functions given in table 2.1

Now a transfer function can be derived from (43) such as to provide an output with the spectrum in (40) when driven by white noise. It is easy to see that

$$H_a(s) = \sqrt{S_0} \frac{(s/\omega_0)^2}{\left[1 + 2J \frac{s}{\omega_0} + \left(\frac{s}{\omega_0}\right)^2\right]^3} \quad (45)$$

where

$$S_0 = \frac{1.25}{4\omega_m} H^2 B(\alpha) \quad (46)$$

$$\omega_0 = \gamma(\alpha) \omega_m \quad (47)$$

$$J = 0.707$$

A plot of the spectrum for various wind speeds is given in Figure 2.3, while the spectrum and its rational approximation is plotted in Figure 2.4 for fully developed seas and $H^{1/3} = 3$ m.

Important Remark

It is customary to define the power spectral density as the Fourier transform of the autocorrelation $R(\tau)$

$$S(\omega) = \int_{-\infty}^{\infty} R(\tau) e^{-i\omega\tau} d\tau \quad (48)$$

In wave theory, the spectrum is defined one sided (for positive frequencies only) as follows

$$S_{\beta}(\omega) = \frac{1}{\pi} \int_{-\infty}^{\infty} R(\tau) e^{-i\omega\tau} d\tau \quad \omega > 0 \quad (49)$$

For this reason, the relation between the spectrum $S(\omega)$ as required for the present application and the Bretschneider spectrum $S_{\beta}(\omega)$ is:

$$S(\omega) = \begin{cases} \pi S_{\beta}(\omega) & \omega > 0 \\ \pi S_{\beta}(-\omega) & \omega < 0 \end{cases} \quad (50)$$

Therefore, the intensity of the white noise required for driving the transfer function (33) is π (or equivalently we can multiply the transfer function by $\sqrt{\pi}$).

TABLE 2.1

Sea Spectrum Coefficients

α	$\gamma (\alpha)$	$\beta (\alpha)$
.00	.9538	1.8861
.10	1.0902	1.6110
.20	1.1809	1.3827
.30	1.2717	1.2116
.40	1.3626	1.0785
.50	1.4539	.9718
.60	1.5448	.8845
.70	1.6360	.8116
.80	1.7272	.7498
.90	1.8182	.6968
1.00	1.9095	.6509
1.10	2.0008	.6106
1.20	2.0918	.5750
1.30	2.1833	.5434
1.40	2.2744	.5150
1.50	2.3657	.4895
1.60	2.4567	.4664
1.70	2.5481	.4454
1.80	2.6395	.4262
1.90	2.7306	.4085
2.00	2.8218	.3923

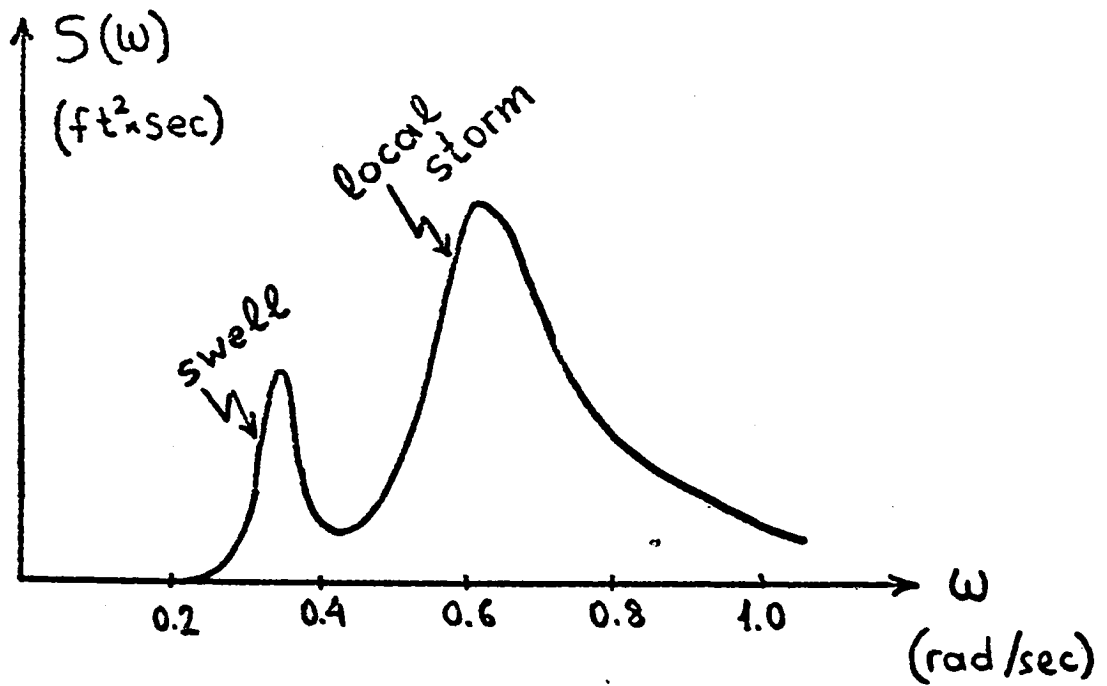


Figure 2.1

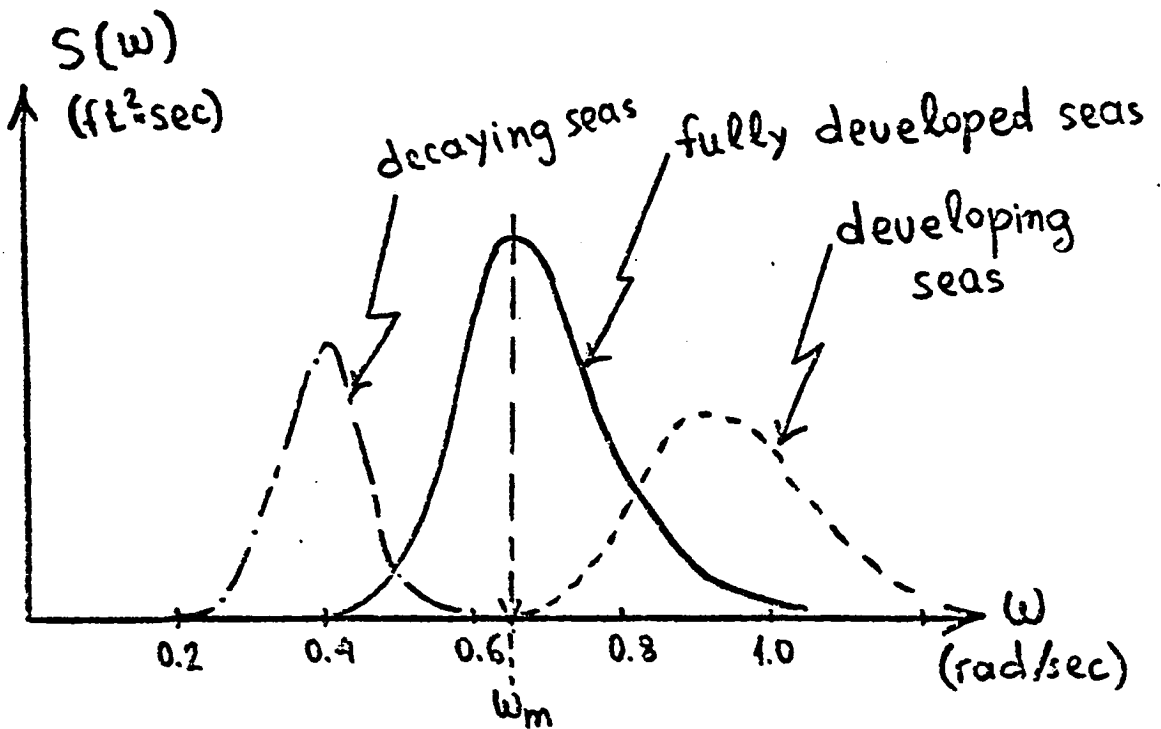


Figure 2.2

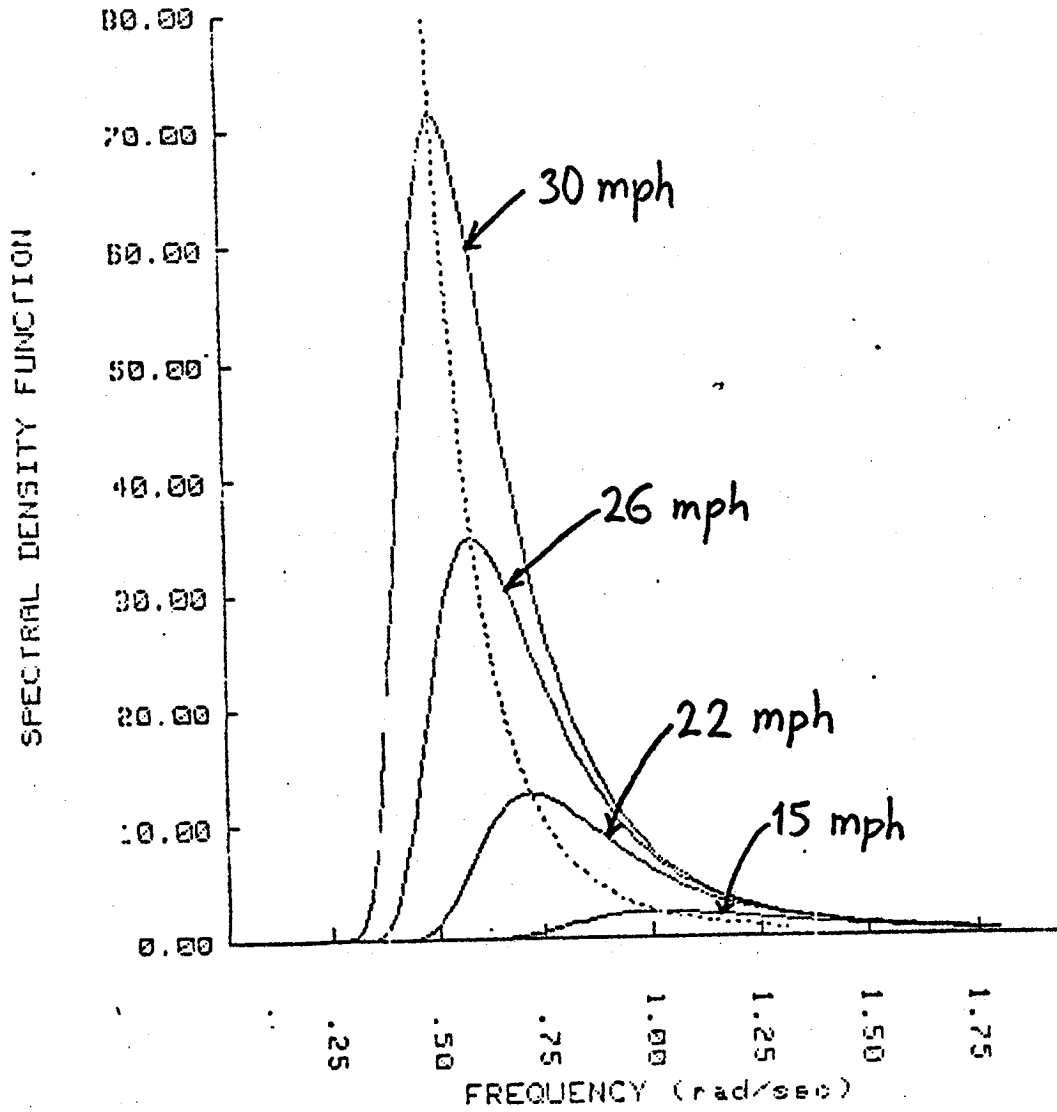


Figure 2.3 Bretschneider spectrum at various wind speeds (fully developed seas).

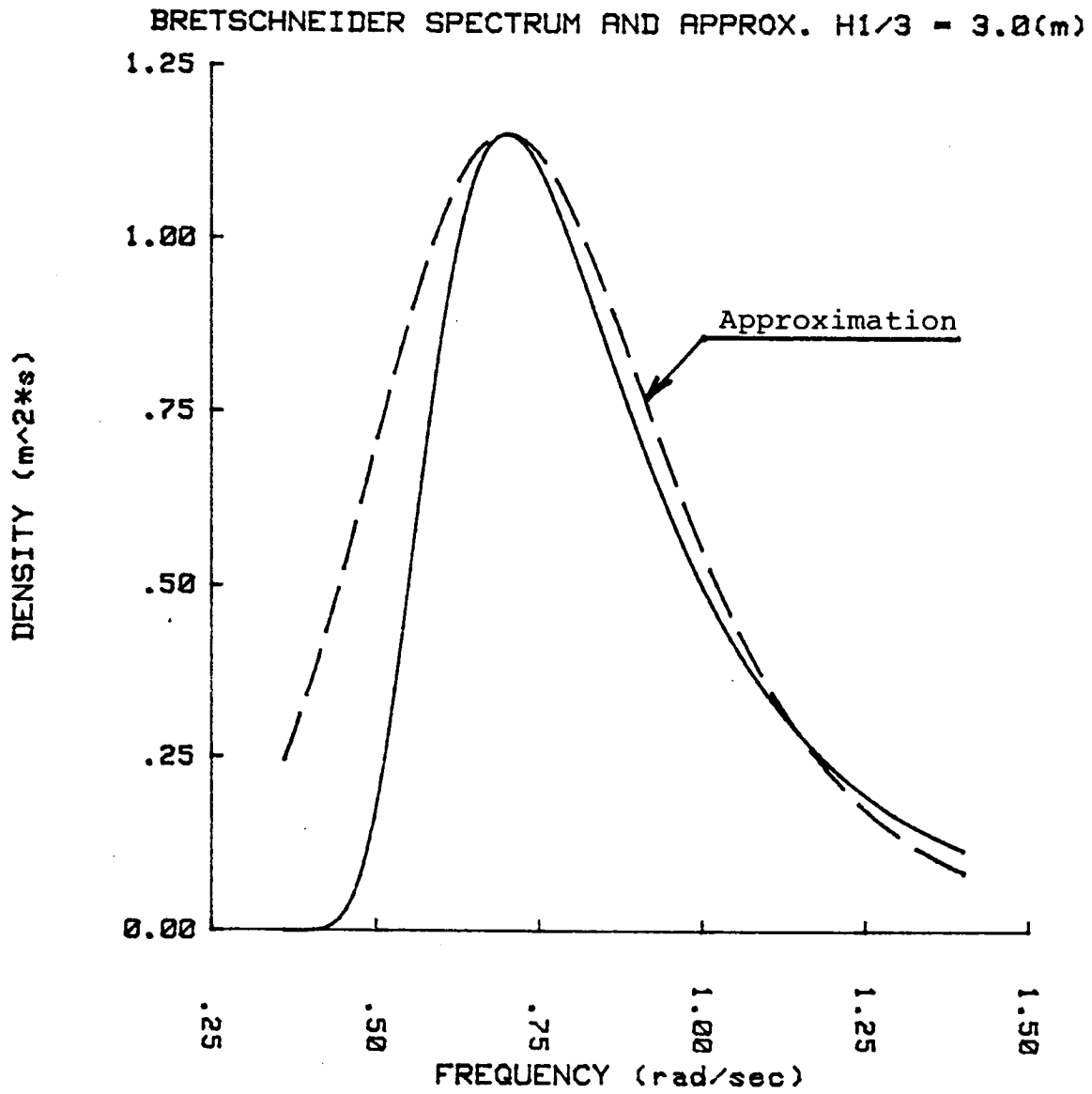


Figure 2.4 Bretschneider Spectrum and Approximation

Chapter 3: DERIVATION OF THE STATE - SPACE EQUATION

We proceed to derive a state-space form of the equations of motion. Starting with the sea, we can construct the following representation (three cascaded second order systems)

$$\frac{\dot{\mathbf{x}}_s}{\omega} = \begin{bmatrix} 0 & 1 & 0 & 0 & 0 & 0 \\ -\omega_o^2 & -2J\omega_o & 0 & \omega_o^2 & 0 & 0 \\ 0 & 0 & 0 & 1 & 0 & 0 \\ 0 & 0 & -\omega_o^2 & -2J\omega_o & 0 & \omega_o^2 \\ 0 & 0 & 0 & 0 & 0 & 1 \\ 0 & 0 & 0 & 0 & -\omega_o^2 & -2J\omega_o \end{bmatrix} \mathbf{x}_s + \begin{bmatrix} 0 \\ 0 \\ 0 \\ 0 \\ 0 \\ 1 \end{bmatrix} \omega \quad (51)$$

$$\eta = [\sqrt{s_o} \ 0 \ 0 \ 0 \ 0 \ 0] \mathbf{x}_s$$

or

$$\dot{\mathbf{x}}_s = \mathbf{A}_s \mathbf{x}_s + \mathbf{B}_s \omega \quad (52)$$

$$\eta = \mathbf{C}_s \mathbf{x}_s$$

Heave-Pitch Model

The following model is derived for the force (some algebra was involved to reduce the dimension of the state).

$$\dot{\underline{x}}_f = \begin{bmatrix} 0 & 1 & 0 & 0 & 0 \\ -\omega_o & -2J\omega_o & \omega_o^2 & 0 & 0 \\ 0 & 0 & 0 & 1 & 0 \\ 0 & 0 & -\omega_o^2 & -2J\omega_o & 0 \\ \theta_1 & \theta_2 & \theta_3 & \theta_4 & 1 \end{bmatrix} \underline{x}_f + \begin{bmatrix} 0 \\ 0 \\ 0 \\ 1 \\ 0 \end{bmatrix} \eta$$

$$\begin{bmatrix} F_3 \\ F_5 \end{bmatrix} = \begin{bmatrix} \alpha_1 \omega_o^2 & 0 & 0 & 0 & 0 \\ 0 & 0 & 0 & 0 & \alpha_2 \cos \phi \end{bmatrix} \underline{x}_f \quad (53)$$

or written in short

$$\dot{\underline{x}}_f = A_f \underline{x}_f + B_f \eta$$

$$\begin{bmatrix} F_3 \\ F_5 \end{bmatrix} = C_f \underline{x}_f \quad (54)$$

The inertia model can be written as follows:

$$\dot{\underline{x}}_m = \begin{bmatrix} 0 & 1 & 0 & 0 \\ \beta_1 & \beta_2 & \beta_3 & \beta_4 \\ 0 & 0 & 0 & 1 \\ \beta_5 & \beta_6 & \beta_7 & \beta_8 \end{bmatrix} \underline{x}_m + \begin{bmatrix} 0 & 0 \\ D_1 & D_2 \\ 0 & 0 \\ D_3 & D_4 \end{bmatrix} \begin{bmatrix} F_3 \\ F_5 \end{bmatrix} \quad (55)$$

$$\begin{bmatrix} x_3 \\ x_5 \end{bmatrix} = \begin{bmatrix} 1 & 0 & 0 & 0 \\ 0 & 0 & 1 & 0 \end{bmatrix} \underline{x}_m$$

where

$$\begin{bmatrix} D_1 & D_2 \\ D_3 & D_4 \end{bmatrix} = \begin{bmatrix} A_{33} & A_{35} \\ A_{53} & A_{55} \end{bmatrix}^{-1} \quad (56)$$

$$\begin{bmatrix} \beta^1 & \beta^2 & \beta^3 & \beta^4 \\ \beta^5 & \beta^6 & \beta^7 & \beta^8 \end{bmatrix} = - \begin{bmatrix} D_1 & D_2 \\ D_3 & D_4 \end{bmatrix} \begin{bmatrix} C_{33} & B_{33} & C_{35} & B_{35} \\ C_{53} & B_{53} & C_{55} & B_{55} \end{bmatrix} \quad (57)$$

and we can write in short

$$\dot{\underline{x}}_m = A_m \underline{x}_m + B_m \begin{bmatrix} F_3 \\ F_5 \end{bmatrix} \quad (58)$$

$$\begin{bmatrix} x_3 \\ x_5 \end{bmatrix} = C_m \underline{x}_m$$

Now the total model can be constructed as follows:

$$\dot{\underline{x}}_t = A_t \underline{x}_t + B_t W \quad (59)$$

$$\begin{bmatrix} x_3 \\ x_5 \end{bmatrix} = C_t \underline{x}_t$$

where

$$A_t = \begin{bmatrix} A_s & O & O \\ O & A_m & B_m C_f \\ B_f C_s & O & A_f \end{bmatrix}$$

$$B_t = \begin{bmatrix} B_s & O & O \end{bmatrix}^T$$

$$C_t = \begin{bmatrix} O & C_m & O \end{bmatrix}$$

(60abc)

Data were obtained for the DD-963 destroyer from the M.I.T. Seakeeping Program and are given in Appendix 2. Appendix 4 lists a computer program that produces the A_t , B_t , C_t matrices once the ship speed, wave heading, significant wave height and modal frequency were specified. The output can be used directly as input to the LIDS control and filter design package.

Table 3.1 provides the numerical values of matrix A for speed 20 knots, angle 0° (head seas), significant wave height 10 ft. and modal frequency 0.72 rad/sec (sea state 5).

Sway-Roll-Yaw Model

The sway, roll, yaw exciting forces and moments are essentially driven by the slope of the sea elevation, which for regular waves equals the wavenumber times the amplitude, or for deep water we can write

$$\text{Slope} = \frac{\omega^2}{g} a$$

i.e. in the time domain:

$$\text{Slope} = -\frac{1}{g} \frac{d^2}{dt^2} \eta \quad (61)$$

As outlined in Chapter 1, the fact that only roll has a spring constant causes zero pole cancellation problems, which can be avoided by introducing the matrices T and U described by equations (36) through (38). The original equation is in the form

$$(M+A) \ddot{\underline{x}}_1 + B\dot{\underline{x}}_1 + C\underline{x}_1 = \underline{F}_1 \quad (62)$$

where \underline{x}_1 is of dimension 3:

$$\underline{x}_1 = \begin{bmatrix} \text{sway} \\ \text{roll} \\ \text{yaw} \end{bmatrix} = \begin{bmatrix} x_2 \\ x_4 \\ x_6 \end{bmatrix}, \quad \underline{F}_1 = \begin{bmatrix} F_2 \\ F_4 \\ F_6 \end{bmatrix} \quad (63)$$

M is the mass matrix, A and B the added mass and damping matrices respectively, C is the hydrostatic matrix and F the vector of exciting force and moments. Then

$$S^2 \underline{x}_1 = -[M+A]^{-1} s \underline{x}_1 - [M+A]^{-1} C \underline{x}_1 + [M+A]^{-1} \underline{F}_1 \quad (64)$$

By letting

$$\begin{aligned}\underline{x}^T &= [x_2, \dot{x}_4, x_4, x_6] \\ \underline{F}^T &= [{}^jF_2, F_2, F_4, {}^jF_4, F_6]\end{aligned}\quad (65ab)$$

and using the T and U matrices of equations (36), (38) we obtain a state space description of (64) without zero-pole cancellation, in the form

$$\dot{\underline{x}} = T \underline{x} + U F \quad (66)$$

The state space representation of equations (27) through (29) is in the form

$$\dot{\underline{x}}_j = \begin{bmatrix} 0 & 1 \\ -\omega_j^2 & -2\zeta_j\omega_j \end{bmatrix} \underline{x}_j + \begin{bmatrix} 0 \\ 1 \end{bmatrix} \dot{\eta} \quad (67)$$

where $j = 2, 4, 6$, while

$$\begin{bmatrix} {}^jF_j \\ F_j \end{bmatrix} = \begin{bmatrix} A_j\omega_j^2 & 0 \\ 0 & A_j\omega_j^2 \end{bmatrix} \underline{x}_j \quad (68)$$

For this reason we build a force matrix A_F :

$$A_F = \begin{bmatrix} A_2 & \emptyset & \emptyset \\ \emptyset & A_4 & \emptyset \\ \emptyset & \emptyset & A_6 \end{bmatrix} \quad (69)$$

and a matrix B_F driving the force dynamics with $\dot{\eta}$, i.e. using the sea model, which is exactly the same as in the case of heave, pitch (6 states), so

$$B_F(i,j) = 0$$

except

$$B_F(2,2) = -A_2 \omega_2^2$$

$$B_F(4,2) = -A_4 \omega_4^2$$

(70abcd)

$$B_F(6,2) = -A_6 \omega_6^2$$

Then using the same sea model described in equations (52ab) we obtain the overall model as

$$\dot{\underline{x}}_t = \begin{matrix} (16 \times 16) \\ A_t \end{matrix} \underline{x}_t + \begin{matrix} (16 \times 1) \\ B_t W \end{matrix}$$

(71ab)

$$\begin{bmatrix} x_2 \\ x_4 \\ x_6 \end{bmatrix} = \begin{matrix} (3 \times 16) \\ C_t \end{matrix} \underline{x}_t$$

where

$$A_t = \begin{bmatrix} A_S & \emptyset & \emptyset \\ B_F & A_F & \emptyset \\ \emptyset & U & T \end{bmatrix}$$

$$B_t^T = [B_S^T \quad \emptyset]$$

(72abc)

$$C_t = \begin{bmatrix} \cdot & 1 & 0 & 0 & 0 \\ \emptyset & \cdot & 0 & 0 & 1 & 0 \\ \cdot & \cdot & 0 & 0 & 0 & 1 \end{bmatrix}$$

Data for all quantities involved are given in Appendix 2, while Appendix 4 lists the computer programs that can produce the matrices A_t , B_t , C_t once the ship speed, wave heading, significant wave height and modal frequency are specified.

Table 3.1 provides the A_t matrix for speed 15.5 knots, heading 45° , significant wave height 10 ft. and modal frequency 0.72 rad/sec (sea state 5).

TABLE 3.1

Matrix A for heave and pitch (15 x 15)

0.	1.	0.	0.	0.	0.	0.	0.	0.	0.	0.	0.	0.	0.	0.
-1.491E+00	-1.726E+00	0.	1.491E+00	0.	0.	0.	0.	0.	0.	0.	0.	0.	0.	0.
0.	0.	0.	1.	0.	0.	0.	0.	0.	0.	0.	0.	0.	0.	0.
0.	0.	-1.491E+00	-1.726E+00	0.	1.491E+00	0.	0.	0.	0.	0.	0.	0.	0.	0.
0.	0.	0.	0.	0.	1.	0.	0.	0.	0.	0.	0.	0.	0.	0.
0.	0.	0.	0.	-1.491E+00	-1.726E+00	0.	0.	0.	0.	0.	0.	0.	0.	0.
0.	0.	0.	0.	0.	0.	0.	1.	0.	0.	0.	0.	0.	0.	0.
0.	0.	0.	0.	0.	0.	-1.213E+00	-5.350E-01	-9.452E+00	-2.190E+01	7.850E-01	0.	0.	0.	-5.027E-01
0.	0.	0.	0.	0.	0.	0.	0.	0.	1.	0.	0.	0.	0.	0.
0.	0.	0.	0.	0.	0.	0.	0.	-1.163E+00	-4.347E-01	-1.529E-03	0.	0.	0.	1.605E-02
0.	0.	0.	0.	0.	0.	0.	0.	0.	0.	0.	1.	0.	0.	0.
0.	0.	0.	0.	0.	0.	0.	0.	0.	0.	-6.635E-01	-1.152E+00	6.635E-01	0.	0.
0.	0.	0.	0.	0.	0.	0.	0.	0.	0.	0.	0.	1.	0.	0.
0.	0.	0.	0.	0.	0.	0.	0.	0.	0.	0.	0.	-6.635E-01	-1.152E+00	0.
6.595E+00	0.	0.	0.	0.	0.	0.	0.	0.	0.	0.	0.	0.	0.	0.
0.	0.	0.	0.	0.	0.	0.	0.	0.	0.	9.720E-01	1.249E+00	-9.720E-01	4.402E-01	-1.050E+00

Matrix A for sway, roll, yaw (16 x 16)

0.	1.	0.	0.	0.	0.	0.	0.	0.	0.	0.	0.	0.	0.	0.	0.
-1.136E+00	-1.507E+00	0.	1.136E+00	0.	0.	0.	0.	0.	0.	0.	0.	0.	0.	0.	0.
0.	0.	0.	1.	0.	0.	0.	0.	0.	0.	0.	0.	0.	0.	0.	0.
0.	0.	-1.136E+00	-1.507E+00	0.	1.136E+00	0.	0.	0.	0.	0.	0.	0.	0.	0.	0.
0.	0.	0.	0.	0.	1.	0.	0.	0.	0.	0.	0.	0.	0.	0.	0.
0.	0.	0.	0.	-1.136E+00	-1.507E+00	0.	0.	0.	0.	0.	0.	0.	0.	0.	0.
0.	0.	0.	0.	0.	0.	0.	1.	0.	0.	0.	0.	0.	0.	0.	0.
0.	5.722E+01	0.	0.	0.	0.	-2.610E-01	-5.202E-01	0.	0.	0.	0.	0.	0.	0.	0.
0.	0.	0.	0.	0.	0.	0.	0.	0.	1.	0.	0.	0.	0.	0.	0.
0.	6.059E+02	0.	0.	0.	0.	0.	0.	-4.575E-01	-6.686E-01	0.	0.	0.	0.	0.	0.
0.	0.	0.	0.	0.	0.	0.	0.	0.	0.	0.	1.	0.	0.	0.	0.
0.	6.481E+03	0.	0.	0.	0.	0.	0.	0.	0.	-0.111E-01	-4.450E-01	0.	0.	0.	0.
0.	0.	0.	0.	0.	0.	0.	0.	0.	0.	-4.468E-08	0.	-0.343E-03	2.740E-01	1.097E-01	0.041E+00
0.	0.	0.	0.	0.	0.	0.	0.	0.	0.	0.	0.	4.343E-05	-1.961E-02	-2.344E-01	1.206E-02
0.	0.	0.	0.	0.	0.	0.	0.	0.	0.	0.	0.	0.	1.	0.	0.
0.	0.	0.	0.	0.	0.	0.	0.	0.	0.	0.	0.	0.	0.	0.	0.
0.	0.	0.	0.	0.	0.	-4.057E-06	0.	0.	0.	1.299E-07	0.	-4.611E-04	-2.319E-02	4.092E-04	-3.242E-02

Chapter 4: KALMAN FILTER AND SIMULATION

The heave-pitch approximation resulted in a 15 state system and the sway-roll-yaw approximation in a 16 state system. Given that 6 states describe the sea, the total system required for 5 degree of freedom motion studies would contain 25 states. If the sea spectrum contains two peaks then a 31 state model is required.

The heave-pitch group is not coupled with the sway-roll-yaw group so that the study of each group can be independent. This is not to indicate that in a total design the two groups must remain independent, since they are excited by the same sea.

Heave-Pitch Motions

It is assumed that the heave and pitch motions are measured.

The gyroscopes can provide accurate measurements of angles, up to about 1/10 degree. The noise therefore is due to structural vibrations, which in the longitudinal direction can be significant due to the beam-like response of the vessel. As a result the measurement noise was estimated based on data from ship vibrations. The same applies to the heave measurement noise.

A Kalman filter was designed for speed $V = 21^{\text{ft}}/\text{sec}$ and waves coming at 0° (head seas) with significant wave height $H = 10$ ft. and modal frequency $\omega_m = 0.73$ rad/sec (sea state 5). The measurement noise intensity matrix was selected from ship vibration

data to be

$$V = \begin{bmatrix} 0.75 & 0 \\ 0 & 0.0003 \end{bmatrix}$$

The model poles are shown in table 4.1, while the filter poles are within a radius of 1.3 rad/sec as seen in table 4.2. Typical simulation results are shown in Figures 4.1 and 4.2. In these figures exact knowledge is assumed for the significant wave height and modal frequency. The accuracy of the filter is very good both for heave and pitch.

Subsequently, the same filter was used combined with a ship and sea model different than the nominal one, to investigate the sensitivity to the following parameters:

The influence of the significant wave height is very small when the modal frequency is accurately known. On the contrary, the influence of the modal frequency is quite critical; particularly for pitch (see Figures 4.6 and 4.7). The same conclusion is reached when a double peak sea spectrum is used [22],[23].

The effect of the forward speed and wave direction was found to be unimportant particularly for heave, while for small changes in wave angle ($\pm 15^\circ$) the pitch prediction error was not affected significantly [22].

Sway-Roll-Yaw Motions

As in the case of heave and pitch, the measurement noise consists primarily of structural vibrations rather than instrument noise. For roll such vibrations are quite small for a destroyer vessel and similarly for sway and yaw the vibrations are smaller than in the case of heave and pitch.

The noise intensity used was nonetheless similar to the heave, pitch noise, so as to bound the filter eigenvalues below 2 rad/sec, which is the typical wave bandwidth.

A specific example has been worked out for a forward ship speed of 15.5 ft/sec and waves at 45° and sea state 5 (significant wave height of 10 ft. and modal frequency of 0.72 rad/sec). The measurement noise intensity matrix was

$$\text{diag } \{0.1 \text{ ft}^2, 2 \times 10^{-4} (\text{rad})^2, 2 \times 10^{-4} (\text{rad})^2\}$$

The simulation shows very good estimation as seen in figures 4.3, 4.4, and 4.5. Yaw is very small and the measurement noise is large relative to the yaw motion, nonetheless the yaw estimation based primarily on the roll, sway measurements is very good.

Table 4.2 presents the results of a sensitivity study of the influence of the various parameters involved. The most critical parameter is again the modal frequency. The ship speed and the wave direction are not critical for the estimation error. This is a very important conclusion as far as the wave direction is concerned, because in reality, seas are directional and very difficult to measure, or even model appropriately.

The influence of systematic measurement errors was studied by using a calibration factor. This factor is defined to be the ratio of the measurement fed to the filter over the actual measurement, thus introducing a systematic error. If C is the calibration factor, then the systematic error as a percentage of the actual measurement is $100 \cdot (1-C)$. In the case of a 10% error, the most significant change was found in the case of the roll motion. In the case of a calibration factor 0 (indicating a disconnected measurement) significant errors resulted, especially for roll in the case of disconnected roll measurements (Table 4.3).

Table 4.4 presents the poles of the model used, while Table 4.5 shows the poles of the Kalman Filter derived for the nominal condition as described above. Figures 4.8 through 4.10 are simulation results and show the significant effect of the modal frequency on the estimation error. Finally, Figure 4.11 shows the simulation of the sway motion estimation when the roll measurement is disconnected.

Ship Speed: $U = 21$ ft/sec		Heading angle: 0°	
SEA: $H=10$ ft, $w_m = 0.72 \frac{\text{rad}}{\text{sec}}$		$H=10$ ft, $w_m = 0.52 \frac{\text{rad}}{\text{sec}}$	
$P_{1,2} = -0.199 \pm 1.111 i$		same	
$P_{3,4} = -0.286 \pm 1.016 i$		same	
$P_5 = -1.058$		$P_5 = -0.696$	
$P_{6,7} = -0.576 \pm 0.576 i$		same	
$P_{8,9} = -0.576 \pm 0.576 i$		same	
$P_{10,11} = -0.863 \pm 0.863 i$		$P_{10,11} = -0.571 \pm 0.571 i$	
$P_{12,13} = -0.863 \pm 0.863 i$		$P_{12,13} = -0.571 \pm 0.571 i$	
$P_{14,15} = -0.863 \pm 0.863 i$		$P_{14,15} = -0.571 \pm 0.571 i$	

TABLE 4.1: Poles of the heave, pitch model

Ship Speed: $U = 21$ ft/sec, Heading angle: 0°	
SEA: $H = 10$ ft	$W_m = 0.72$ rad/sec
$P_{1,2} = -1.289 \pm 0.540 i$ $P_{3,4} = -1.134 \pm 1.033 i$ $P_5 = -1.340$ $P_{6,7} = -0.903 \pm 0.7280 i$ $P_{8,9} = -0.777 \pm 1.376 i$ $P_{10,11} = -0.273 \pm 1.572 i$ $P_{12,13} = -0.248 \pm 0.918 i$ $P_{14,15} = -0.0936 \pm 0.0940 i$	

TABLE 4.2 Poles of the heave, pitch Kalman Filter

TABLE 4.3

Sensitivity of the RMS error of sway, roll, yaw motion, to changes in the parameters of the ship-sea model. C (sway) indicates a calibration coefficient in the sway measurement (and similarly for the other motions), to handle systematic errors in the measurements.

Parameter Changed	Error Sway (ft)	Error Roll (deg)	Error Yaw (deg)
Basic Case	0.241	0.56	0.0776
U=20 ft/sec	0.245	0.568	0.0963
$\omega_m=0.52$ rad/sec	0.314	0.91	0.0858
$\phi=60^\circ$	0.296	0.624	0.112
C (sway)=0.9	0.255	0.586	0.081
C (roll)=0.9	0.247	0.708	0.0808
C (yaw)=0.9	0.242	0.56	0.0777
C (sway)=0.0	0.518	1.21	0.1408
C (roll)=0.0	0.376	4.08	0.158
C (yaw)=0.0	0.242	0.563	0.0785
RMS values of the motions (nominal case)	0.60	4.56	0.227
Measurement noise intensity	$(.316 \text{ ft})^2$	$(.81^\circ)^2$	$(.81^\circ)^2$

Ship speed : $U=15.5\text{ft/s}$		Wave heading angle : $\phi=45^\circ$	
SEA : $H=10\text{ft}$ $\omega_m=0.72\text{rad/s}$		SEA : $H=12\text{ft}$ $\omega_m=0.4807\text{rad/s}$	
Ship model poles :			
$P_{1,2}$	$= -0.754 \pm 0.754 i$	$P_{1;2}$	$= -0.470 \pm 0.470 i$
$P_{3,4}$	$= -0.754 \pm 0.754 i$	$P_{3,4}$	$= -0.470 \pm 0.470 i$
$P_{5,6}$	$= -0.754 \pm 0.754 i$	$P_{5,6}$	$= -0.470 \pm 0.470 i$
$P_{7,8}$	$= -0.223 \pm 0.873 i$		
$P_{9,10}$	$= -0.335 \pm 0.588 i$		
$P_{11,12}$	$= -0.260 \pm 0.440 i$		SAME
$P_{13,14}$	$= -0.00983 \pm 0.484 i$		
$P_{15,16}$	$= -0.0204 \pm 0.0597 i$		

TABLE 4.4 : Poles of the sway, roll, yaw model

SEA H=10ft $\omega_m=0.72\text{rad/s}$		
Kalman filter poles :		
$p_{1,2}$	= -1.067 ±	1.086 i
$p_{3,4}$	= -0.457 ±	1.312 i
$p_{5,6}$	= -1.279 ±	0.477 i
$p_{7,8}$	= -0.210 ±	0.934 i
$p_{9,10}$	= -0.365 ±	0.523 i
$p_{11,12}$	= -0.087 ±	0.446 i
$p_{13,14}$	= -0.159 ±	0.165 i
$p_{15,16}$	= -0.0203 ±	0.0595 i

TABLE 4.5: Poles of the sway, roll, yaw Kalman filter

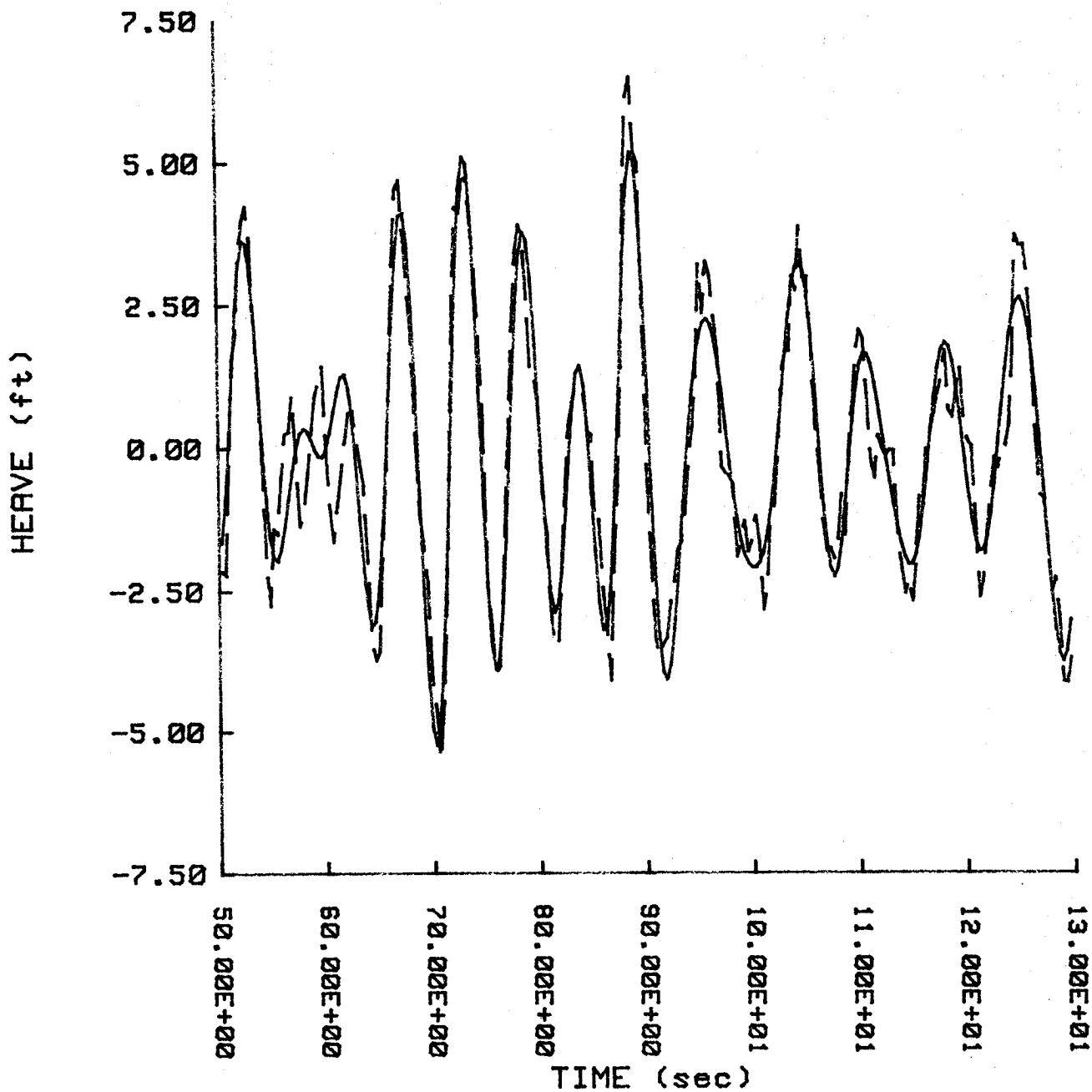


Figure 4.1

Results of Heave Simulation and Its Kalam Filter Estimate (dotted line), Using Accurate Model at $U=21$ ft/sec and 0° Angle of Incidence and in sea state 5.

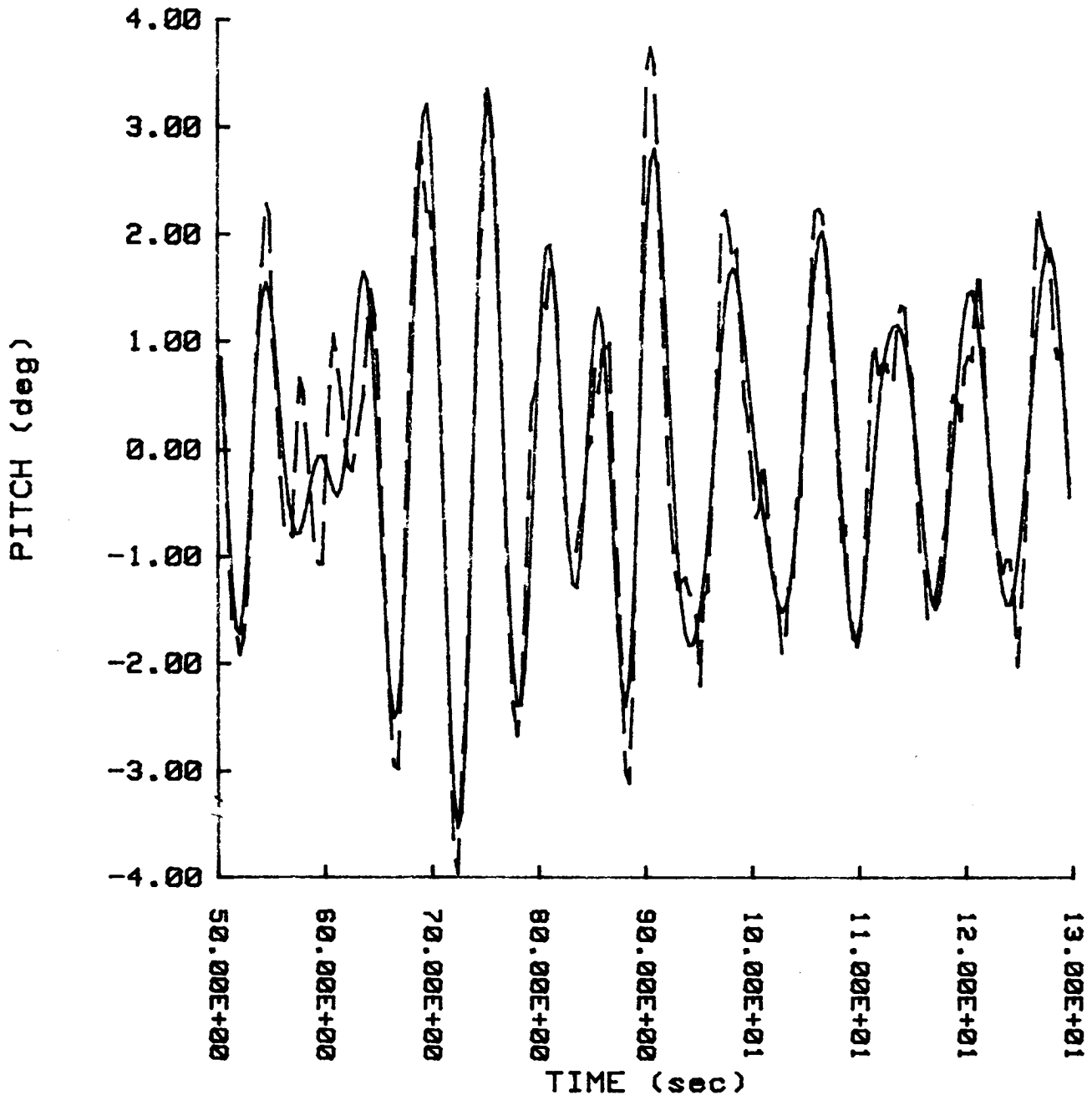


Figure 4.2

Results of Pitch Simulation and Its Kalman Filter Estimate.
Same conditions as in 4.1.

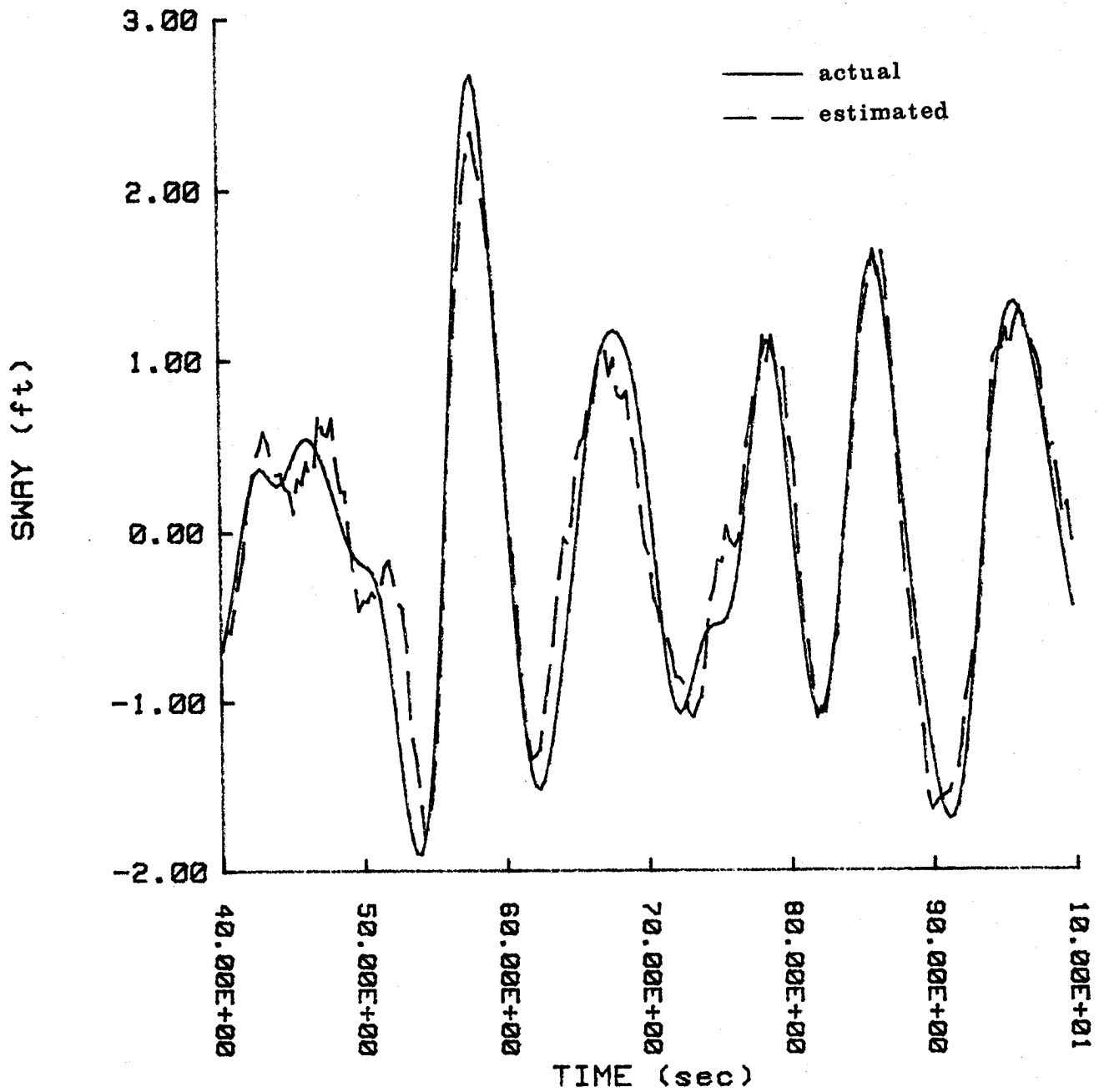


Figure 4.3

Results of Sway Simulation and Its Kalman Filter Estimate (dotted line), Using Accurate Model at $U=15.5$ ft/sec and 45° Angle of Incidence, and in sea state 5.

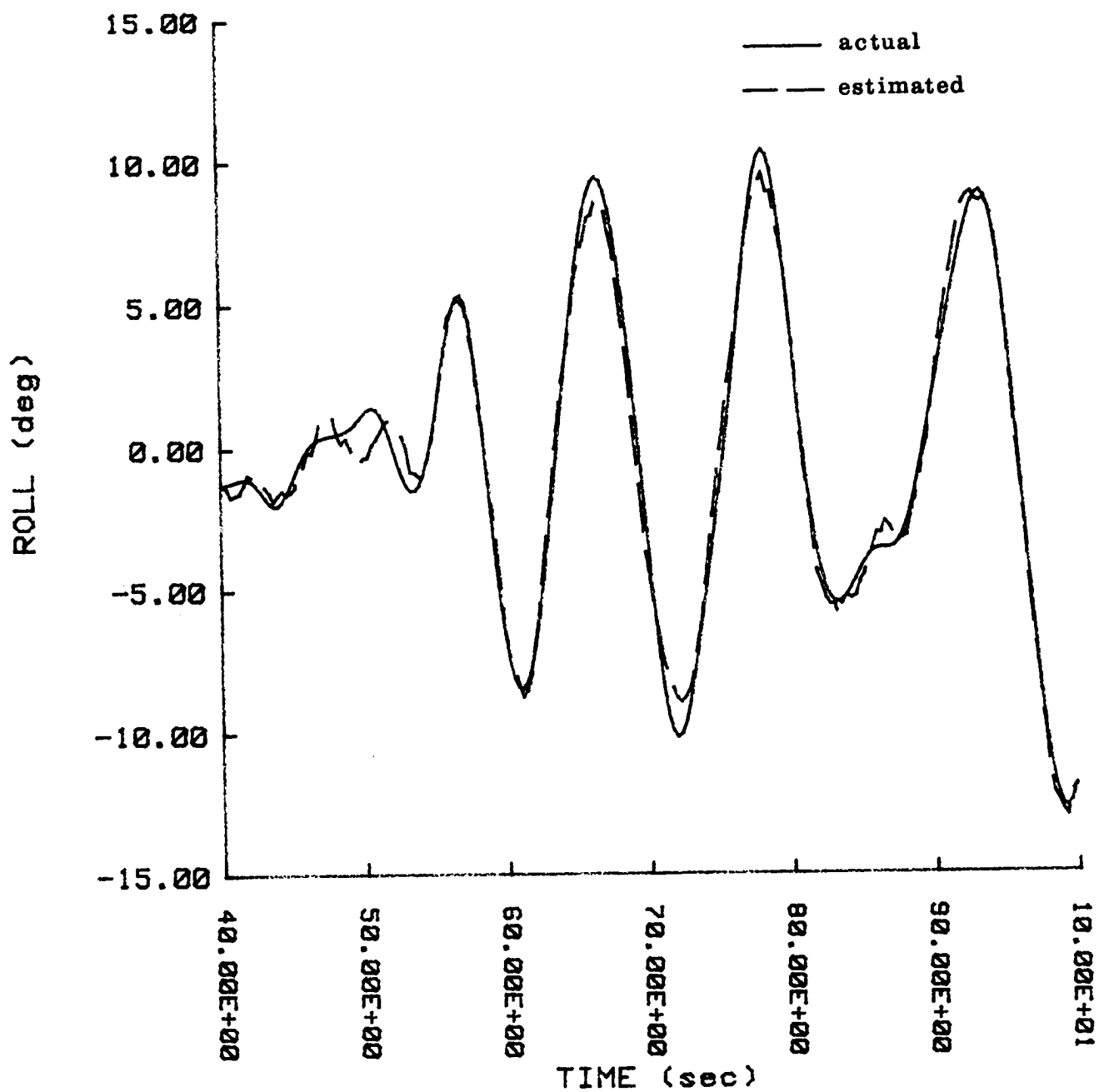


Figure 4.4

Results of Roll Simulation and Its Kalman Filter Estimate.
Same conditions as in 4.3.

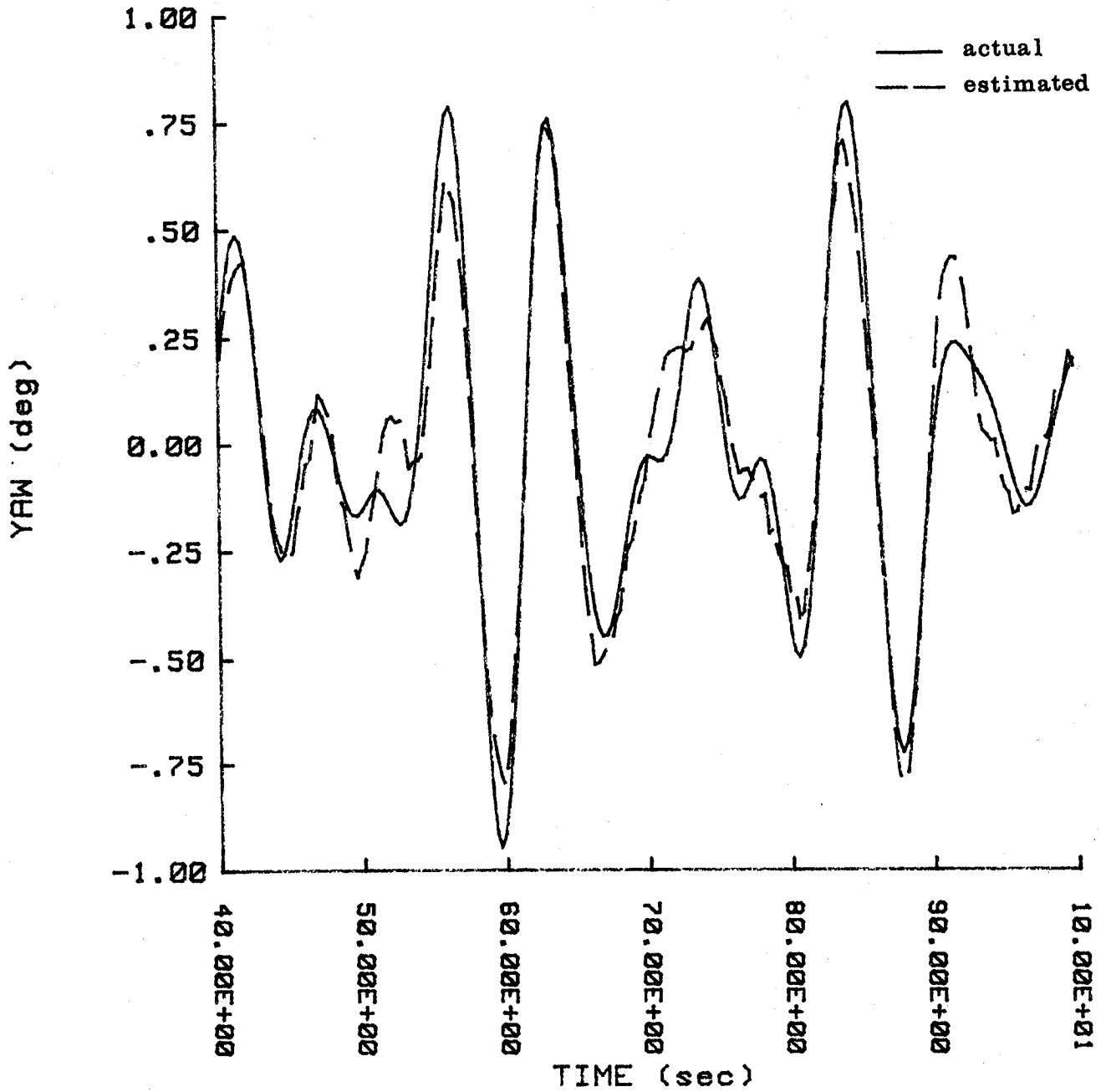


Figure 4.5

Results of Yaw Simulation and Its Kalman Filter Estimate.
Same condition as in 4.3.

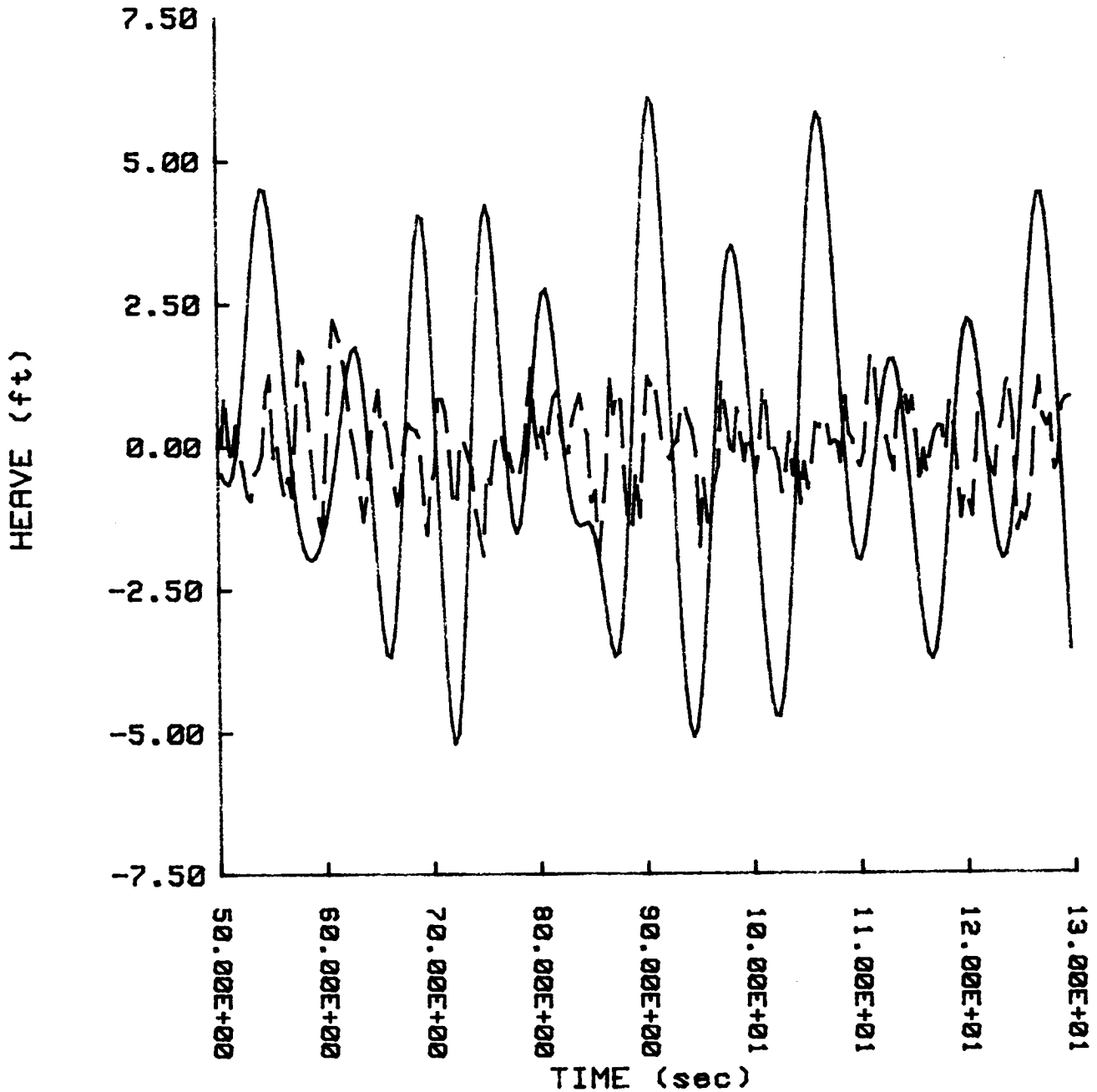


Figure 4.6

Results of Heave Simulation and Its Kalman Filter Estimate (dotted line). The actual wave spectrum model frequency is 0.52 rad/sec, while the value used in the Kalman Filter is 0.72 rad/sec. All other parameters as in 4.1.

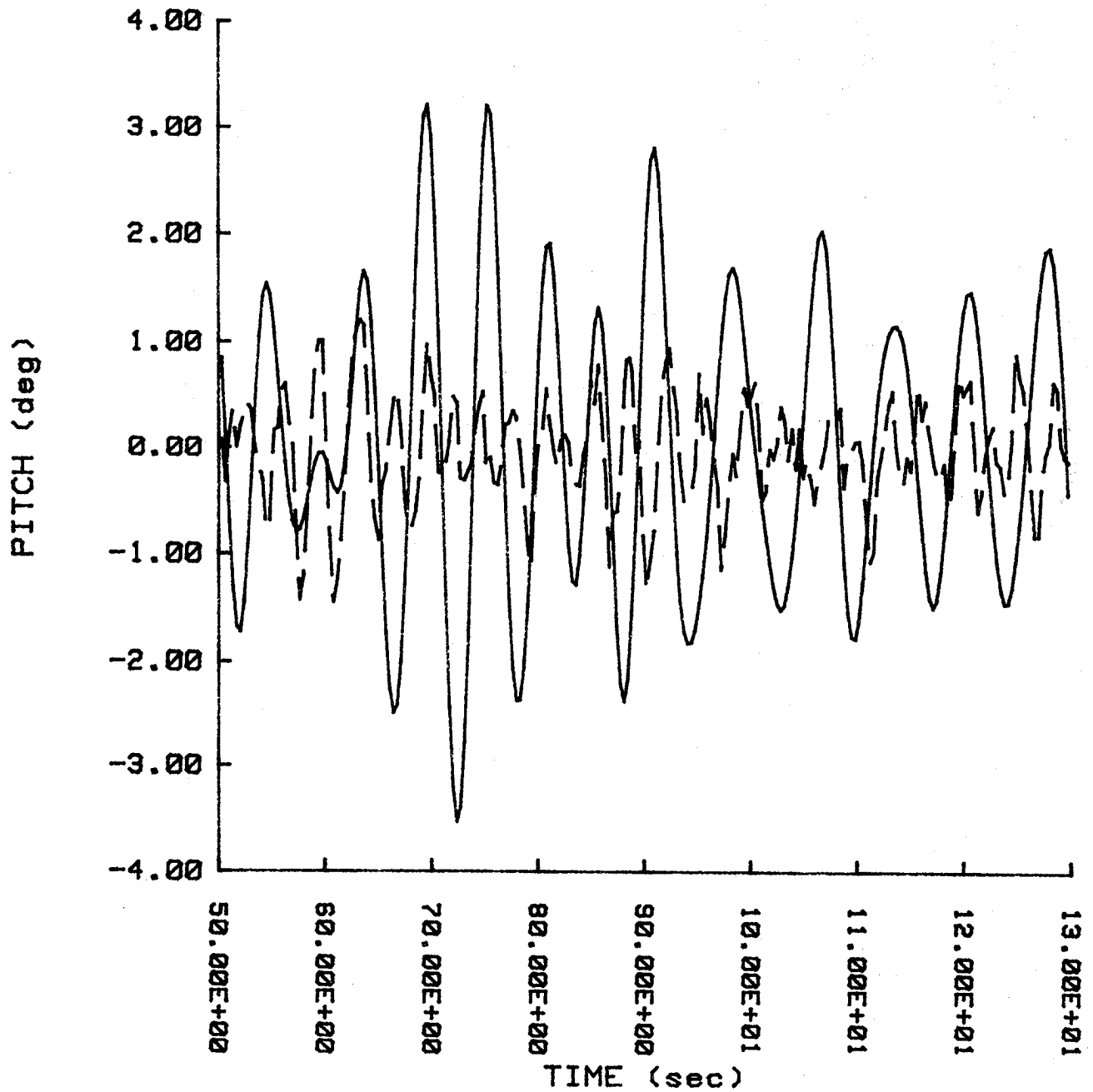


Figure 4.7

Results of Pitch Simulation and Its Kalman Filter Estimate.
Same condition as in 4.6.

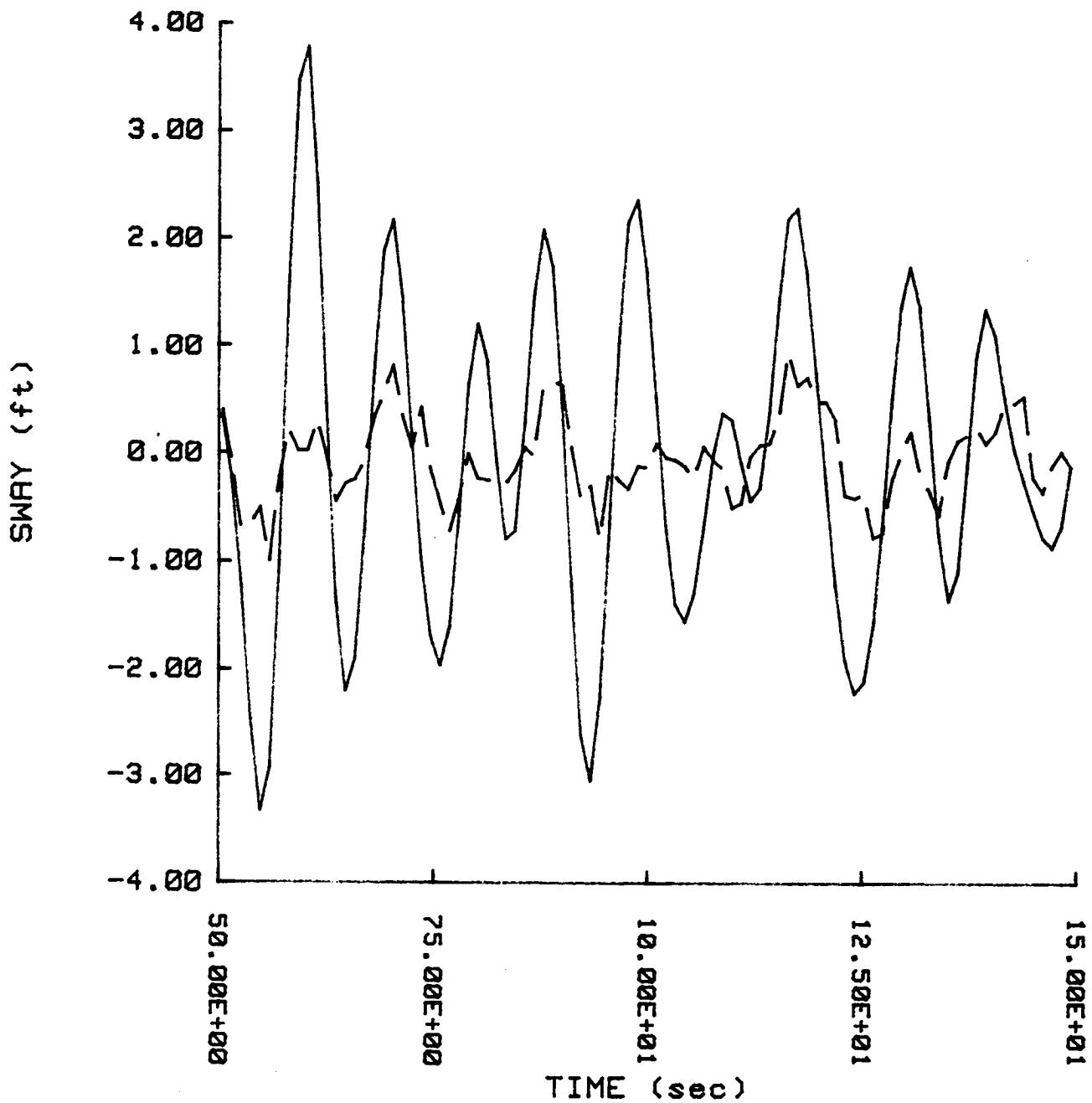


Figure 4.8

Results of Sway Simulation and Its Kalman Filter Estimate (dotted line). Actual $\omega_m = 0.52$ rad/sec, while in Kalman Filter $\omega_m = 0.72$ rad/sec. All other parameters as in 4.3.

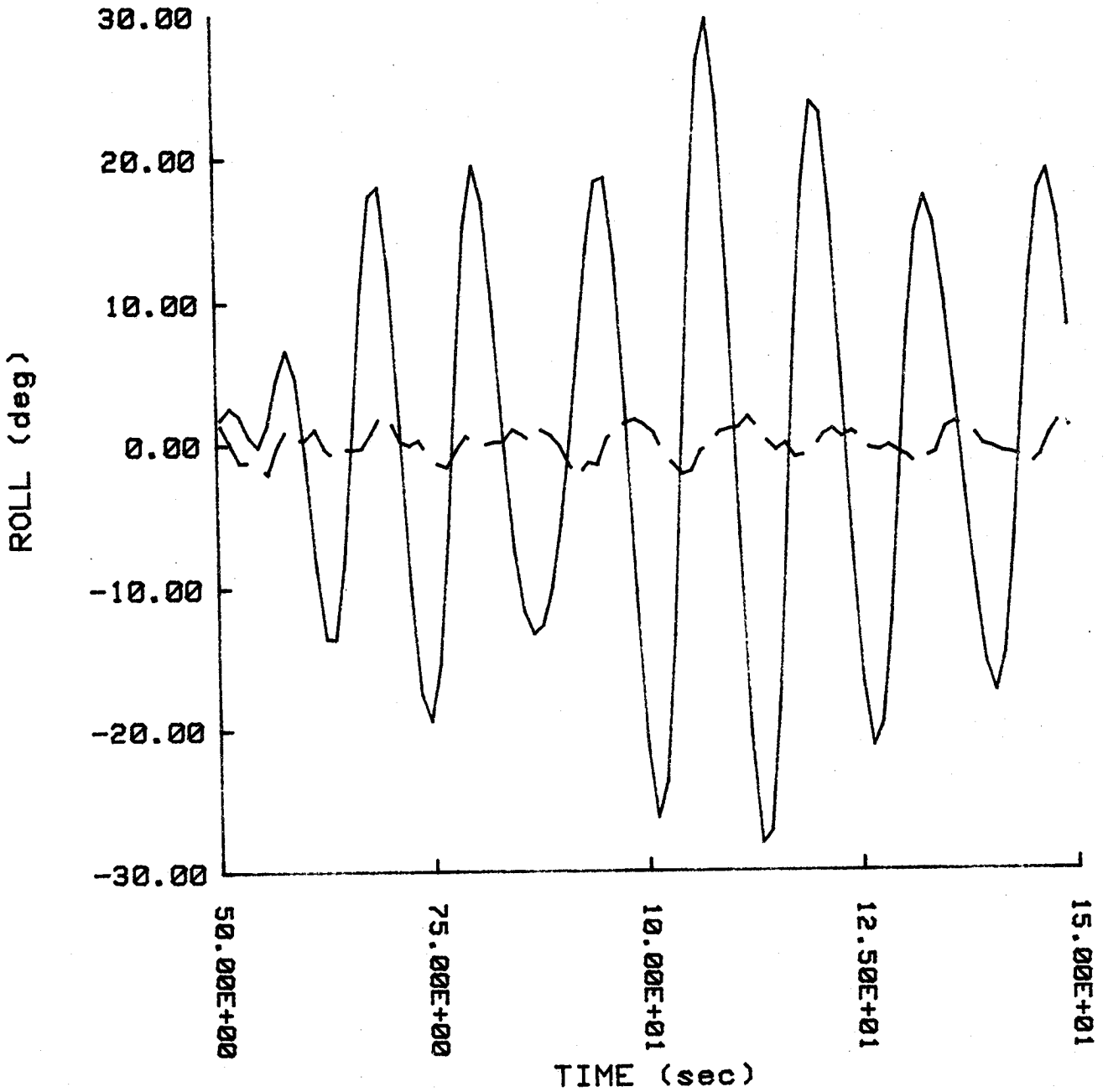


Figure 4.9

Results of Roll Simulation and Its Kalman Filter Estimate.
Same conditions as in 4.8.

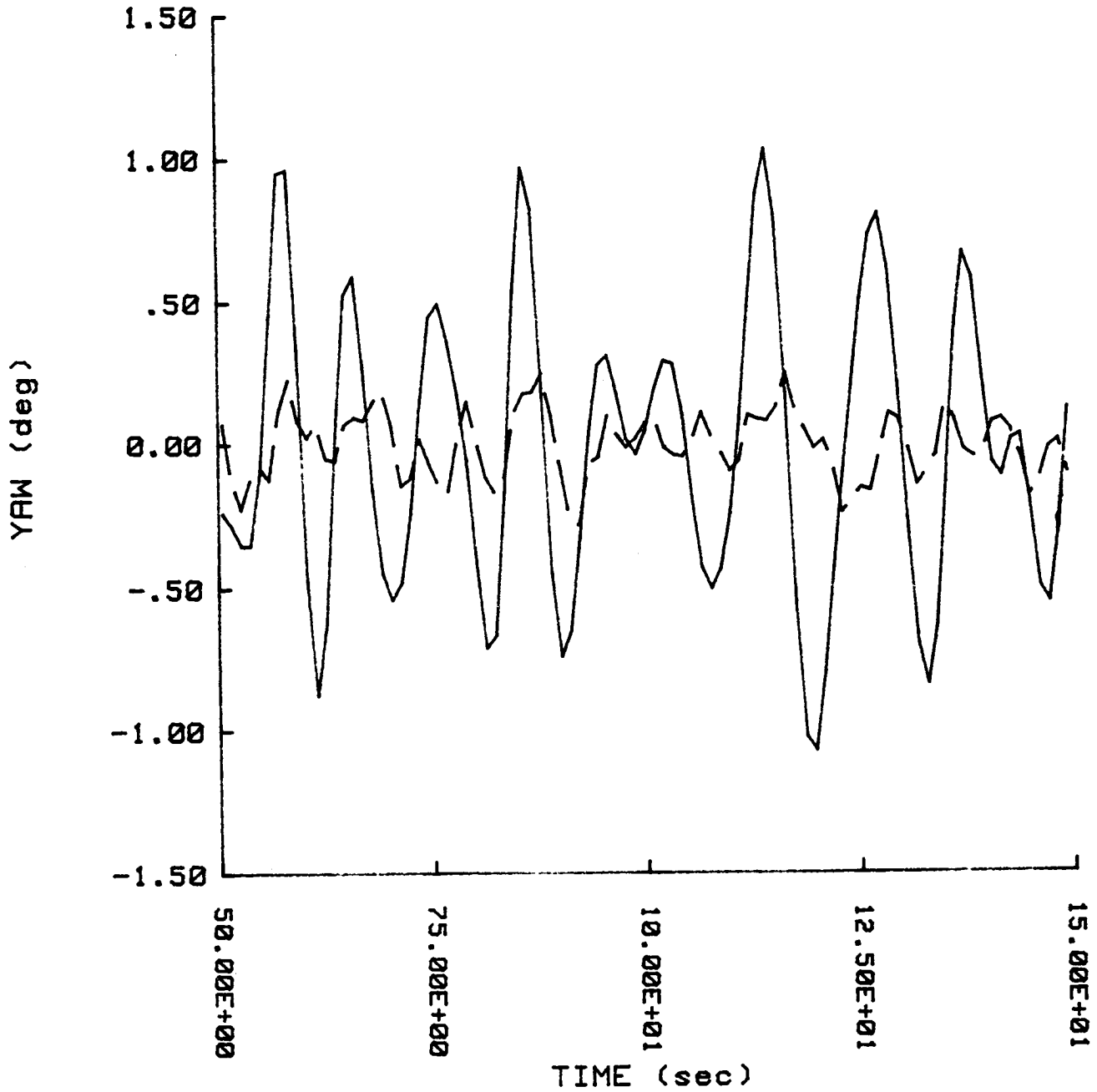


Figure 4.10

Results of Yaw Simulation and Its Kalman Filter Estimate.

Same conditions as in 4.8.

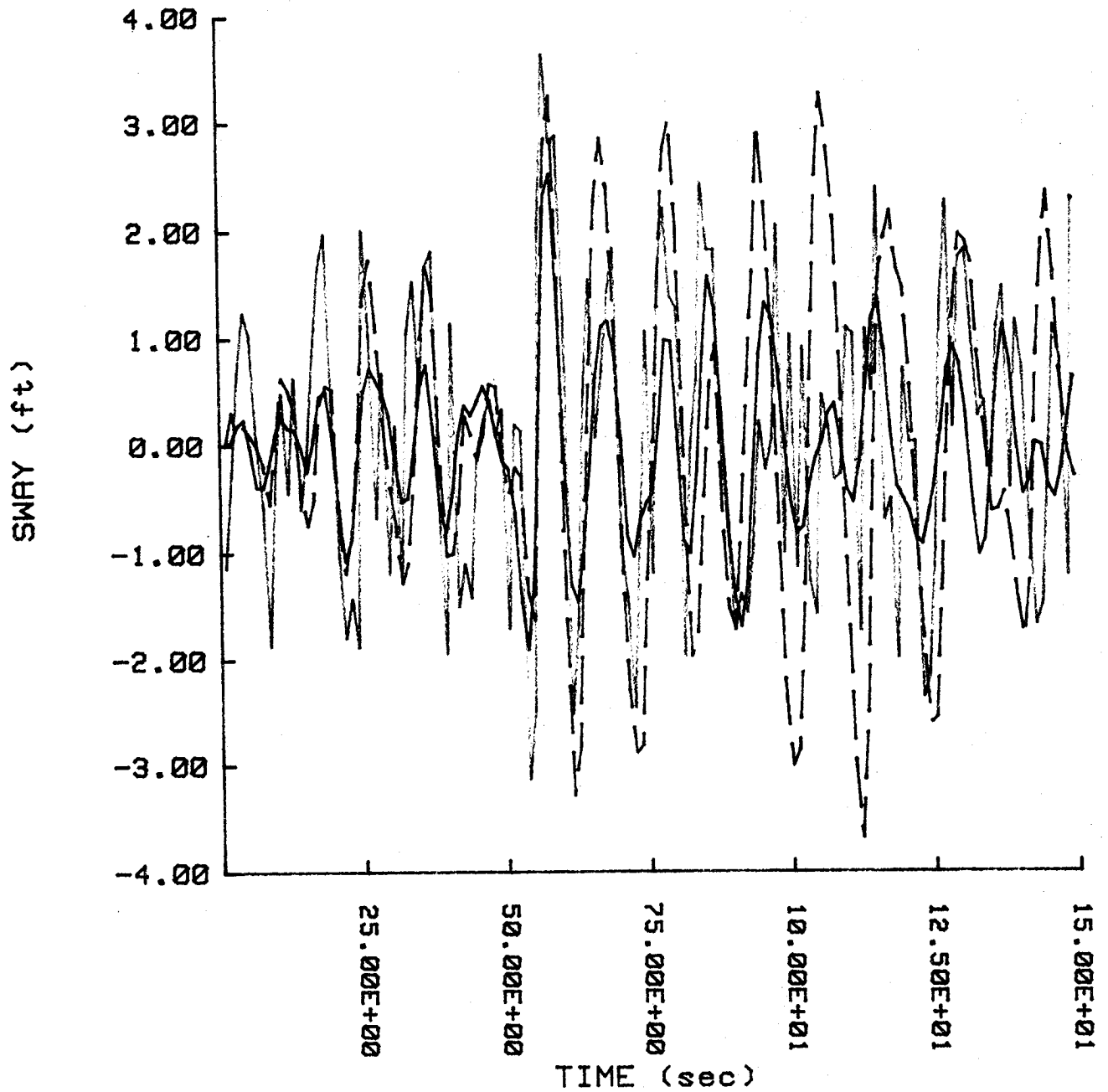


Figure 4.11

Results of Yaw Simulation and Its Kalman Filter Estimate (dotted line), using noisy measurements (light line) when the roll measurement is disconnected. Same other conditions as in 4.3.

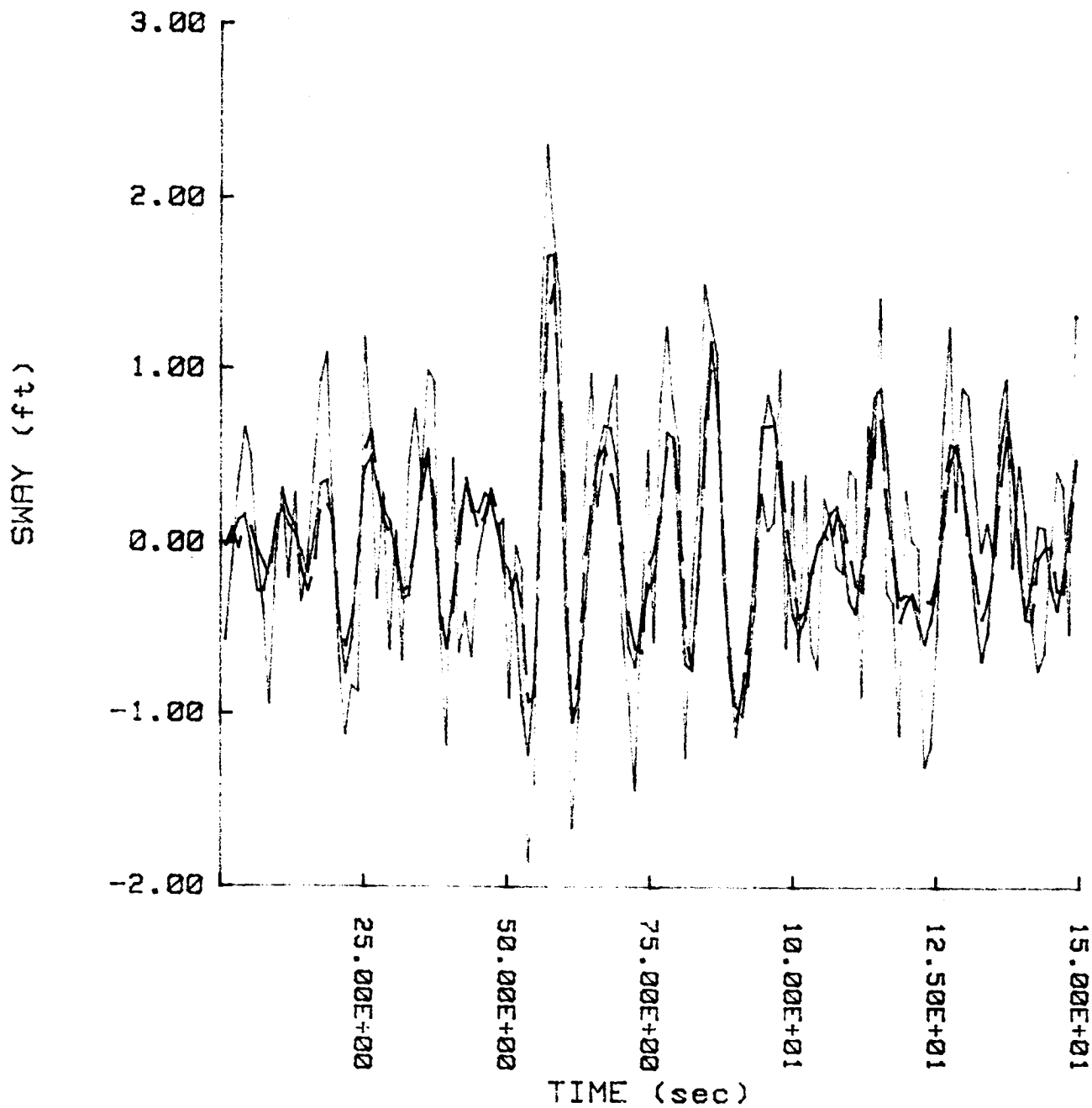


Figure 4.12

Results of Sway Simulation and Its Kalman Filter Estimate (dotted line), using measurements (light line) when the actual angle of incidence is 60° and the value used in the Kalman Filter is 45° . Same other conditions as in 4.3.

Chapter 5: SHIP MOTION PREDICTION

It is of interest to use the models developed in the previous sections to forecast the behavior of the vessel within a few seconds. The feasibility to predict the motions could assist significantly the pilot in committing the aircraft to landing under favorable conditions.

An automatic landing does not require within LOG theory such information since the predictable part of the motions is included in the state and therefore used directly. Nonetheless the prediction is of primary importance for pilot landing or semi-automatic landing.

Similarly for offshore operations a display of a prediction of the most critical vessel motions could reduce the operation risk significantly. The operator could choose a time window of minimal motion or acceleration and then transfer cargo or personnel.

The subject has been considered in the literature [6], [11], [24] using both frequency and time domain techniques.

Theoretical Background

The first to treat the subject of developing a predicting filter was Wiener [29]. If a random process has power spectrum $S(\omega)$ a spectral factorization is first required, i.e.

$$A(\omega) = \psi(\omega) \psi^*(\omega) \quad (73)$$

where $*$ denotes complex conjugation and $\psi(s)$ is an analytic function of s with the exception of a finite number of poles in the left half plane. Then the transfer function of the optimal predictor $K(\omega)$, in the sense of minimizing the expected value of the error, is

given by the expression:

$$K(\omega) = \left(\frac{1}{\psi(\omega)} \right) \int_0^{\infty} Y(t+a) e^{-i\omega t} dt \quad (74)$$

where $Y(t)$ is the inverse Fourier transform of $\psi(\omega)$ and a is the prediction time. The importance of this result is to provide a number of intuitive results, such as the fact that a narrow band process is predictable while at the extreme a wide band process is unpredictable. The disadvantage of this approach is that it may require differentiators in its implementation, depending on the form of the spectrum [29].

The alternative is to use state space models where no such problems appear. In fact the predictive filter has a very simple form. If the system has a state space description

$$\begin{aligned} \dot{\underline{x}} &= A\underline{x} + \underline{W}_1 \\ \underline{y} &= C\underline{x} + \underline{W}_2 \end{aligned} \quad (75ab)$$

where \underline{W}_1 and \underline{W}_2 are white noise signals, it is not hard to see that if the state \underline{x} is perfectly known at t then the predictable part of $\underline{x}(t+\tau)$, denoted by \underline{x}_p , is

$$\underline{x}_p(t+\tau) = e^{A\tau} \underline{x}(t) \quad (76)$$

If the state is not available the Kalman filter estimate is used instead [5],[8]:

$$\underline{x}_p(t+\tau) = e^{A\tau} \hat{\underline{x}}(t) \quad (77)$$

i.e. the propagation of the equation

$$\begin{aligned} \dot{\underline{x}}_p(t+\tau) &= A \underline{x}_p(t+\tau) \\ \underline{x}_p(t) &= \hat{\underline{x}}(t) \end{aligned} \quad (78ab)$$

For a stable matrix A , $\underline{x}_p(t+\tau) \rightarrow 0$ as $\tau \rightarrow \infty$, reflecting the fact that the influence of the driving white noise completely alters the state of the system, once the homogeneous solution has died out.

The covariance of the error

$$\underline{e} = \underline{x}_p - \underline{x}$$

denoted as P_p is governed by the equation

$$\dot{P}_p(\tau) = A P_p(\tau) + P_p(\tau) A^T + V_1 \quad (79)$$

When the state is perfectly known the initial condition is:

$$P_p(0) = 0 \quad (80a)$$

While in the case of using the Kalman filter estimate

$$P_p(0) = P(t) \quad (80b)$$

where $P(t)$ is the error covariance of the Kalman filter at the "present" time t .

The two models developed for the vertical and horizontal motions have been used to study the predictability of the ship motions. Figures 5.1 through 5.5 show simulation results assuming perfect state knowledge. Similarly perfect state knowledge has been assumed and the covariance has been propagated using equations (79), (80). Figure 5.6 is a plot of the heave, pitch motions rms error versus prediction time, while Figure 5.7 depicts the sway, roll,

yaw rms errors versus prediction time. The error has been non-dimensionalized with respect to the corresponding rms motions.

As expected, the error tends to 100% for large prediction times. Roll is a narrow band process and as expected it is the most predictable motion, up to ten seconds ahead. The remaining four motions are predictable up to five seconds ahead.

These results hold in the ideal case. The actual performance will be lower due to the presence of noise in the measurements, fewer measurements than states and modeling errors.

To assess the effect of measurement noise some simulations were made, whose results are shown in Figures 5.8 through 5.10. A rather extreme case was considered: In the case of the vertical motions only two measurements were available, heave and pitch, and in the case of the horizontal motions, only the sway, roll, and yaw motions were available. As seen in the figures, the same noise used to derive the Kalman filter gains was used, which is quite significant. As expected, the performance deteriorated although roll is still predictable up to eight seconds. The other four motions are predictable up to about two seconds.

In the case of modeling errors, let the correct model be

$$\dot{\underline{x}} = A\underline{x} + \underline{W} \quad (81)$$

while the prediction model is

$$\dot{\underline{x}}_p = A^* \underline{x}_p \quad (82)$$

with $A^* = A + \delta A$. Then the error $\underline{e} = \underline{x}_p - \underline{x}$ is governed by the equation

$$\dot{\underline{e}} = A^*\underline{e} + \delta A \underline{x} - \underline{W} \quad (83)$$

or by letting $\underline{x}_1 = \begin{bmatrix} \underline{e} \\ \underline{x} \end{bmatrix}^T$

$$\dot{\underline{x}}_1 = \begin{bmatrix} A^* & \delta A \\ 0 & A \end{bmatrix} \underline{x}_1 + \begin{bmatrix} -\underline{W} \\ \underline{W} \end{bmatrix} \quad (84)$$

so by denoting:

$$P = E\{\underline{e} \underline{e}^T\}, \quad V = E\{\underline{x} \underline{e}^T\}, \quad V = E\{\underline{x} \underline{x}^T\} \quad (85)$$

the following equations are obtained

$$\dot{P} = A^* P + P A^{*T} + \delta A \cdot V + V^T \cdot \delta A^T + V_1$$

$$\dot{V} = A V + V A^{*T} + U \cdot \delta A^T - V_1$$

$$\dot{U} = A \cdot U + U A^T + V_1 \quad (86abc)$$

U, the covariance of the vessel model, can be assumed to be in steady state so the first two equations can be used to propagate V and P. Figures 5.12, 5.13, and 5.14 depict the error covariance of the vessel motions when the model used is different than the actual one. Since one of the most critical parameters is the modal frequency, its effect has been studied: The nominal value is 0.52 rad/sec, while the value used in the prediction filter is 0.72 rad/sec. The covariance at the initial time is assumed to be zero (perfect state knowledge).

As can be seen from these figures, the effect of modeling error is important in the case of the modal frequency, providing a reduction of about 30-50% in the prediction time within prescribed confidence limits.

The sinusoidal behavior of the covariance propagation at about twice the motion natural frequency (as seen in the case of roll, for example) can be explained by the form of the covariance equation

$$\dot{P} = A P + P A^T - V \quad (87)$$

For example the unforced equation

$$\begin{aligned} \dot{P} &= A P + P A^T \\ P(0) &= Q \end{aligned} \quad (88ab)$$

has the solution

$$P(t) = e^{At} Q e^{A^T t} \quad (89)$$

which is composed of exponentials in the form

$$e^{(\lambda_i + \lambda_j)t}$$

where λ_i are the eigenvalues of A . As a result $2\lambda_i$ will appear and in the case of roll it is obvious that twice the roll natural frequency dominates the response.

Reduced Number of States

Another aspect of interest is omitting states. In such a case we denote by \underline{x} the nominal state of dimension n and by \underline{x}^* the implemented state of dimension m , $n \geq m$. We assume that \underline{x}^* is obtained by simply omitting some states, so that

$$\underline{x}^* = W\underline{x} \quad (90)$$

where

$$W = [I_m \quad \emptyset] \quad (91)$$

with I_m the unit ($m \times m$) matrix. The nominal system equation is

$$\begin{aligned} \dot{\underline{x}} &= A \underline{x} + B\underline{W}_1 \\ \underline{z} &= C\underline{x} + \underline{W}_2 \end{aligned} \quad (92ab)$$

while the prediction filter is

$$\begin{aligned} \dot{\underline{x}}_p &= A^* \underline{x}_p \\ \underline{z}_p &= C^* \underline{x}_p \end{aligned} \quad (93ab)$$

where \underline{x}_p has dimension m , A^* is the $m \times m$ reduced system matrix and C^* the reduced observation matrix. Then we define:

$$\delta A = W^T A^* W - A \quad (94)$$

and we obtain the covariance equations [8]:

$$\begin{aligned} \dot{P} &= W^T \cdot A^* \cdot W \cdot P + P \cdot W^T \cdot A^{*T} \cdot W + \delta A \cdot V + V^T \cdot \delta A^T + V_1 \\ \dot{V} &= A \cdot V + V \cdot W^T \cdot A^{*T} \cdot W + U \cdot \delta A^T - V_1 \\ \dot{U} &= AU + UA^T + V_1 \end{aligned} \quad (95abc)$$

Then we proceed to determine the error covariance as explained above using A_p , B_p , and C_p as the system matrices.

The inclusion of non-minimum phase zeros was considered to be an important part of the overall modeling. This was confirmed by studying the effect of omitting these zeros on the prediction error covariance. This is seen in Figure 5.15, where the heave and pitch rms error, non-dimensionalized over the corresponding rms motion, is plotted versus prediction time. As expected, pitch error increases substantially, since pitch lags heave at low frequencies by 90° . Because heave and pitch are coupled, the error in heave is also affected, resulting in poor prediction of both heave and pitch.

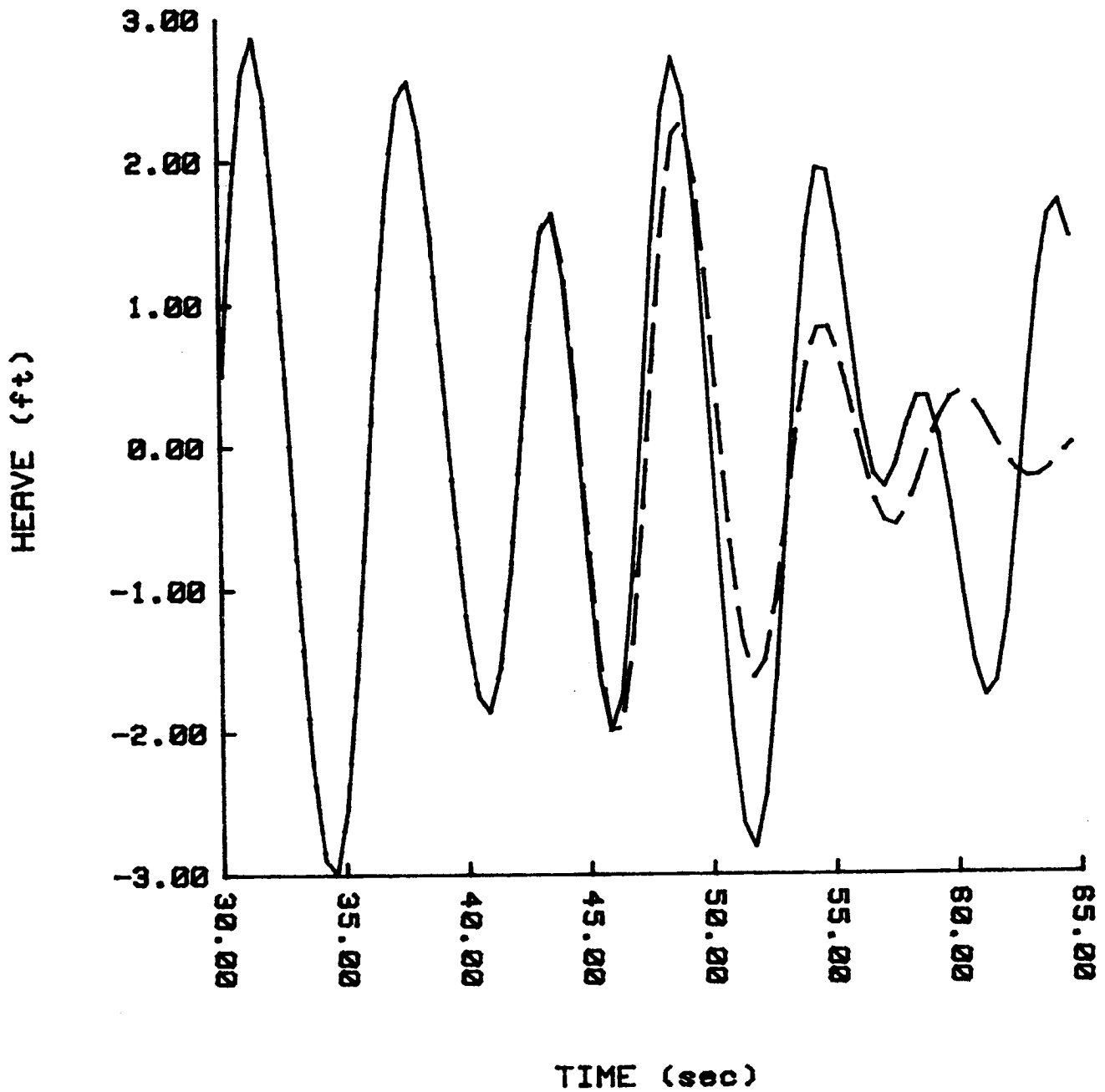


Figure 5.1

Heave Simulation Results and Its Prediction (dotted line starting at $t=40$ sec) for $U=21$ ft/sec and $\phi=0^\circ$, and in sea state 5. Perfect state knowledge is assumed.

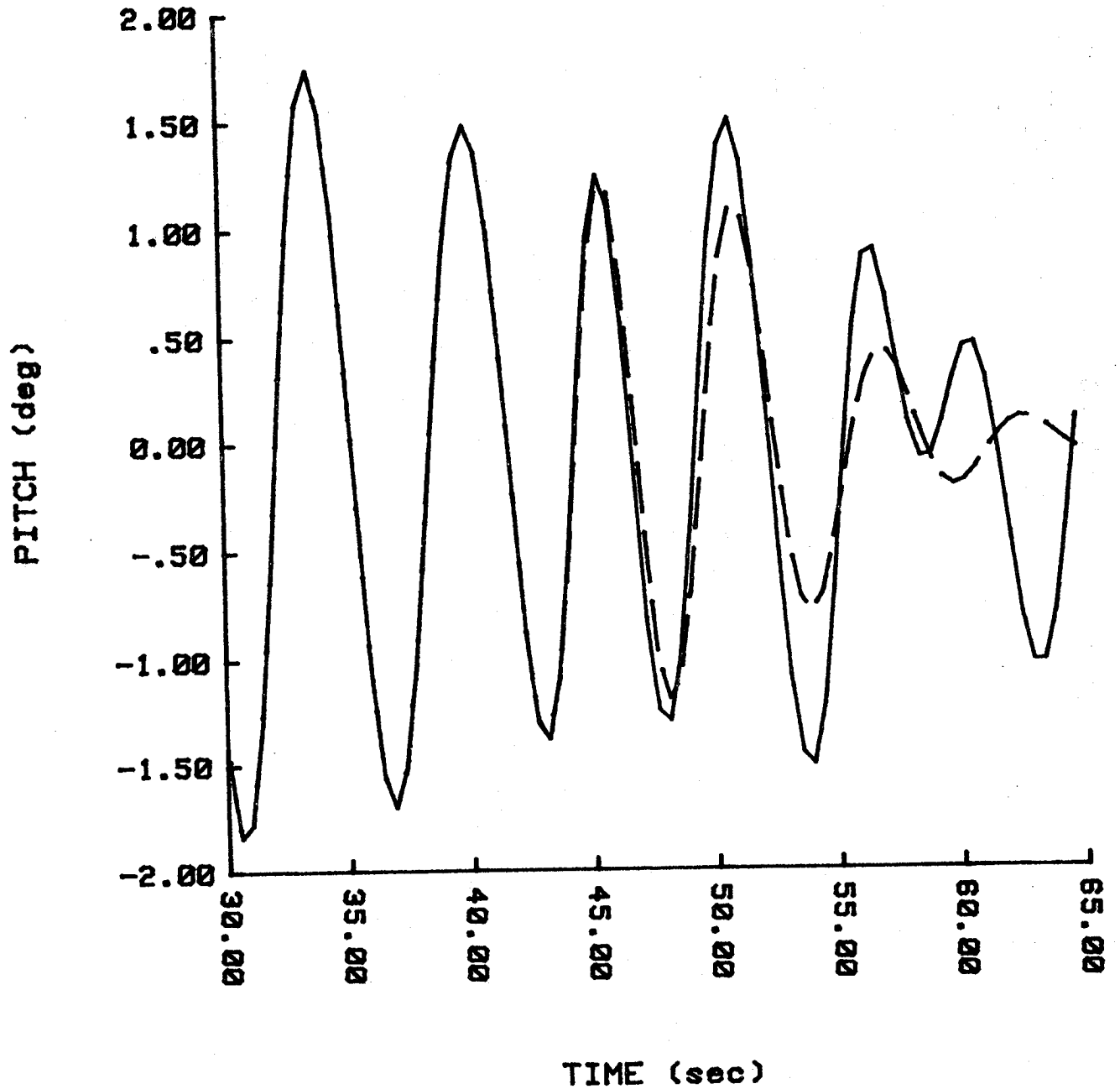


Figure 5.2

Pitch Simulation Results and Its Prediction. Same conditions as in 5.1.

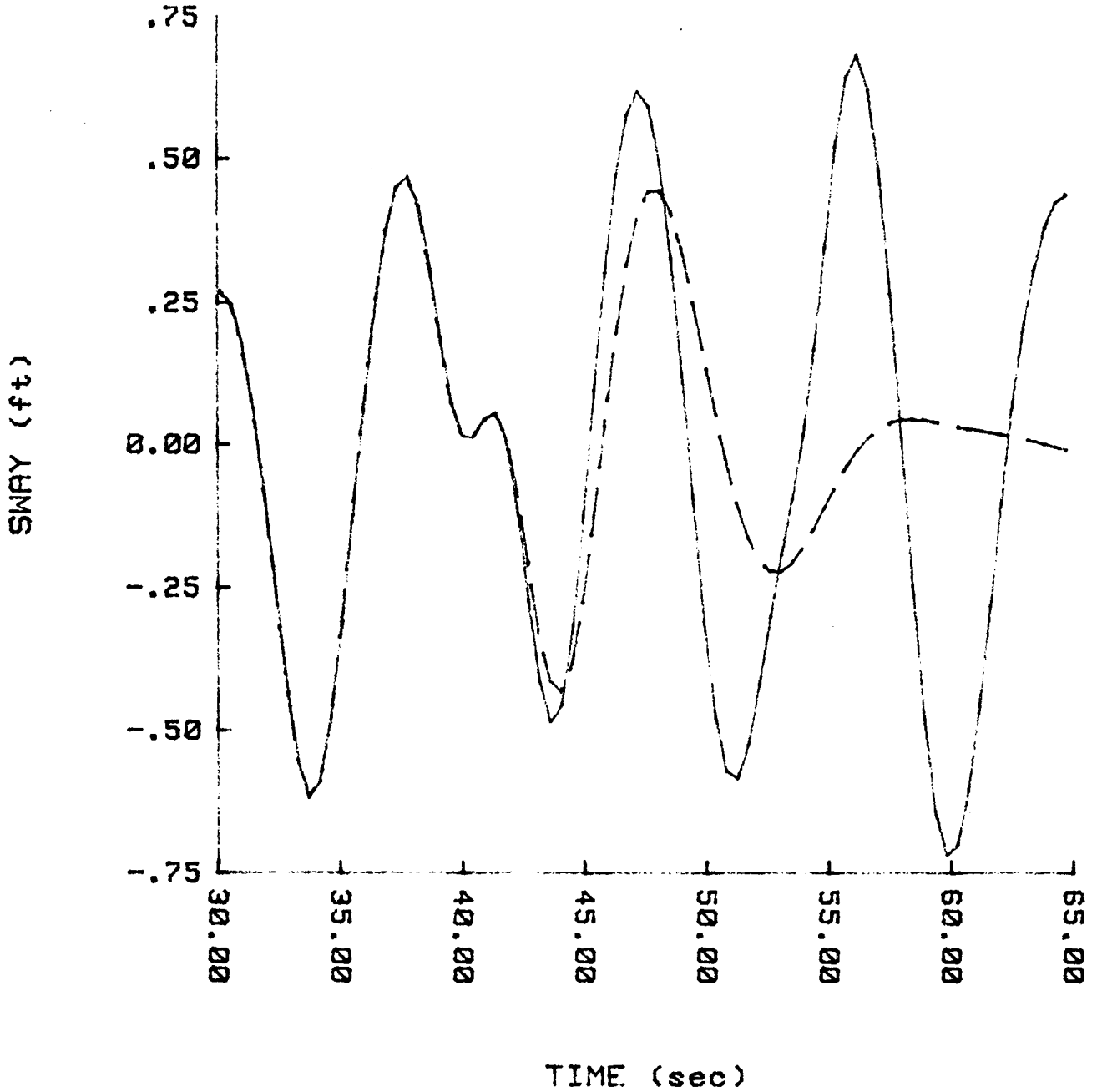


Figure 5.3

Sway Simulation Results and Its Prediction (dotted line starting at $t=40$ sec) for $U=15.5$ ft/sec and $\phi=45^\circ$, and in sea state 5. Perfect state knowledge is assumed.

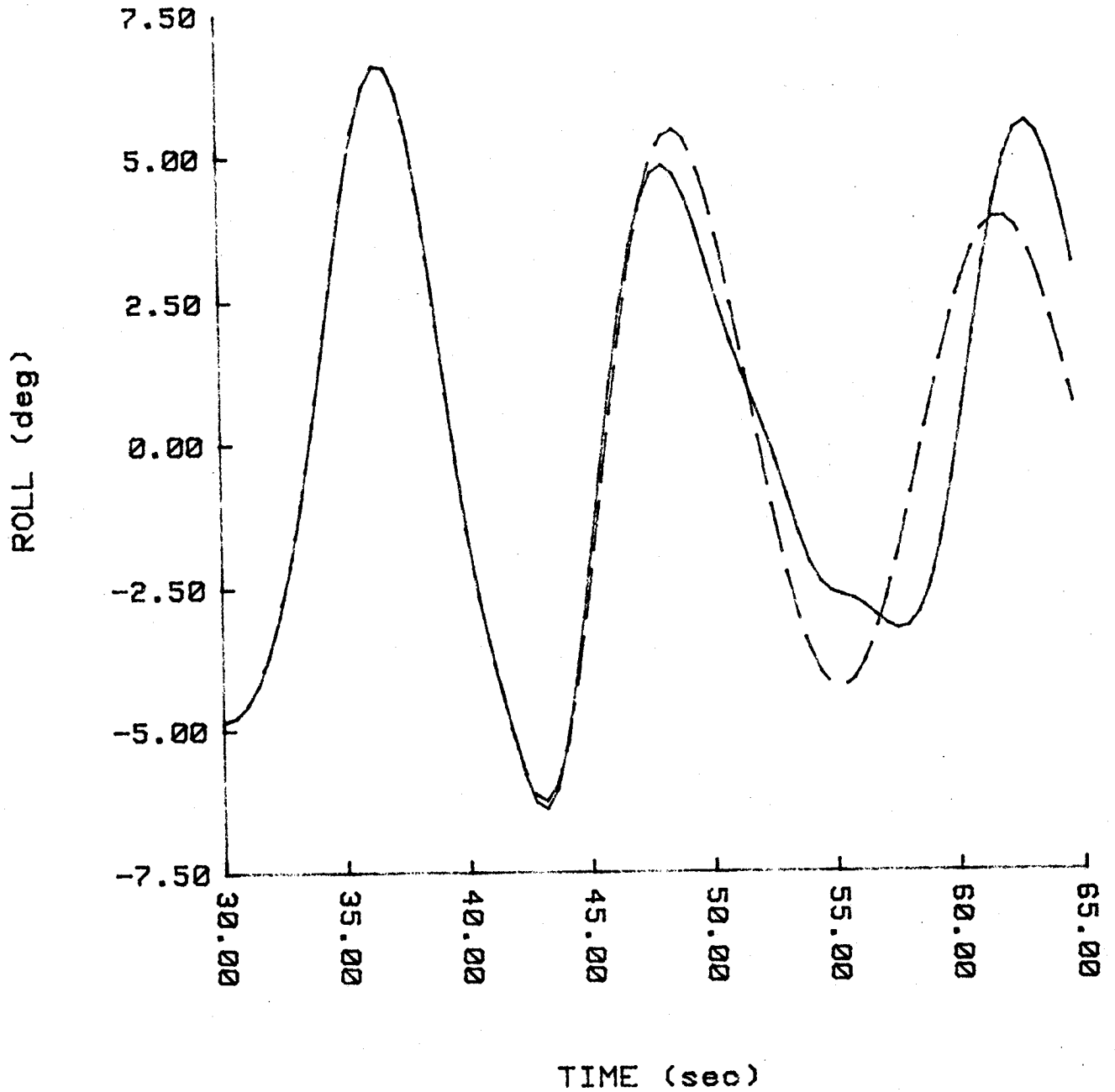


Figure 5.4

Roll Simulation Results and Its Prediction. Same conditions as in 5.3.

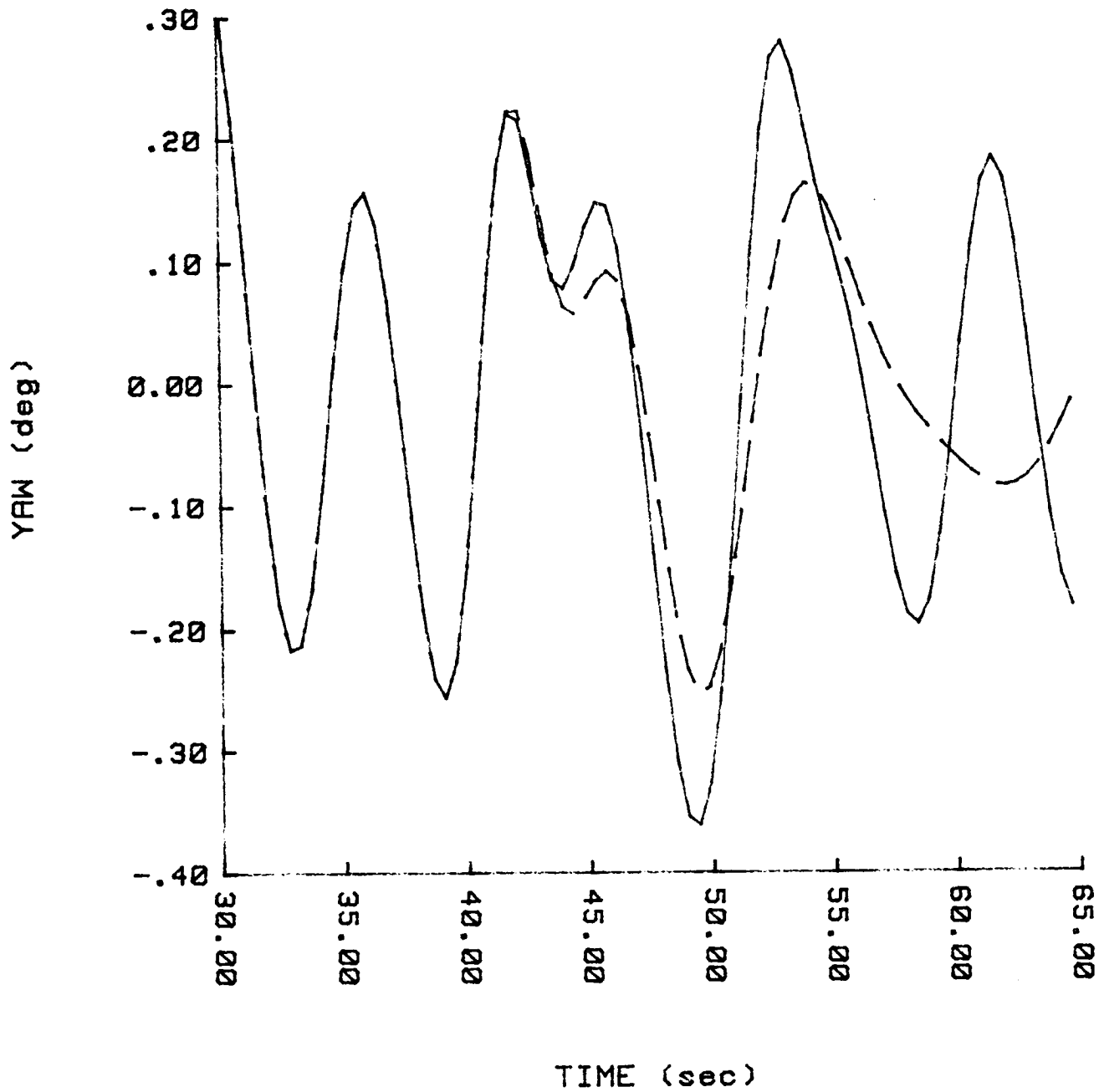


Figure 5.5

Yaw Simulation Results and Its Prediction. Same conditions as in 5.3.

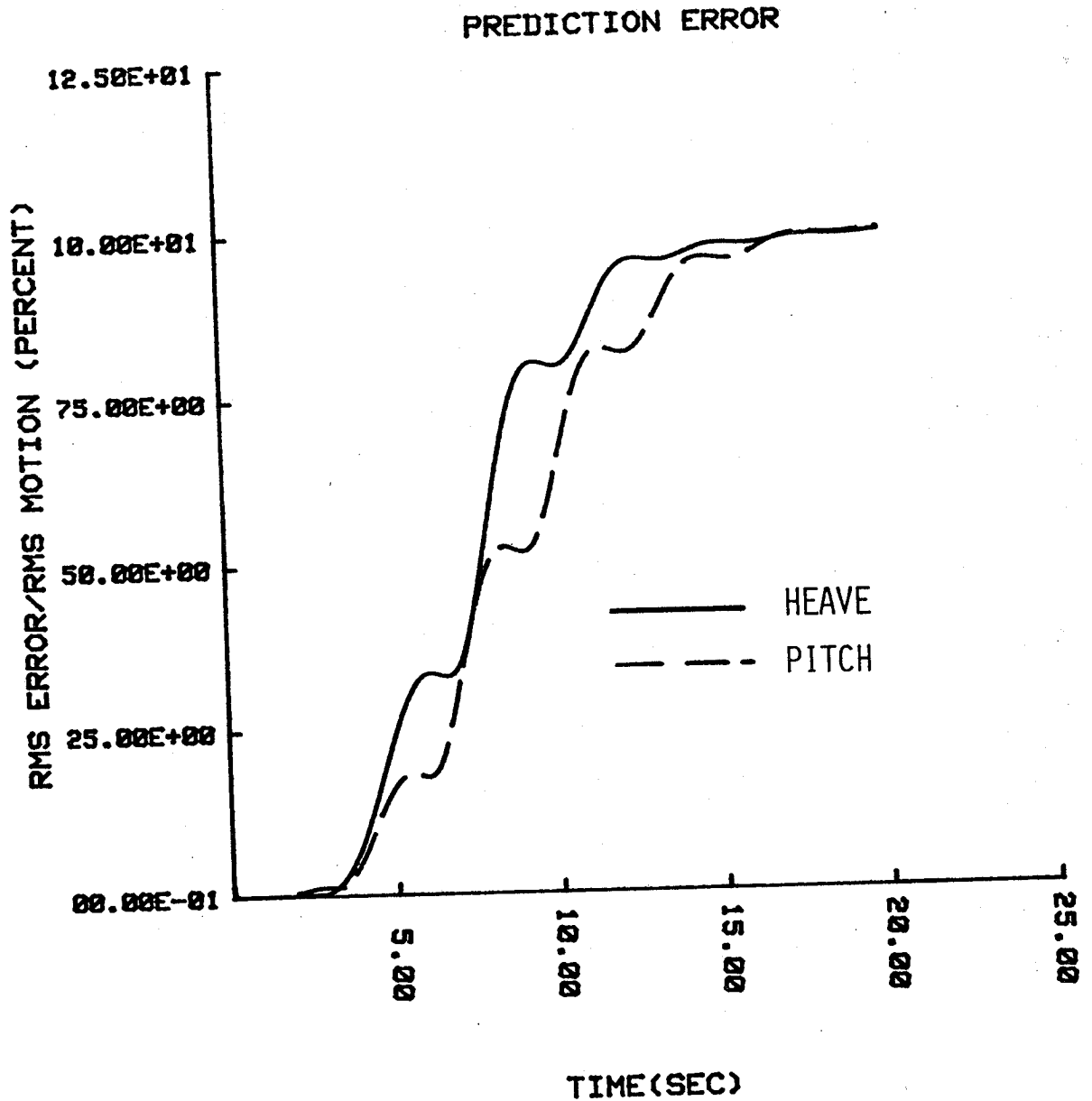


Figure 5.6

RMS Prediction Error Over RMS Motion Versus Prediction Time for Heave and Pitch, $U=21$ ft/sec, $W_m=0.72$ rad/sec, sea state 5.

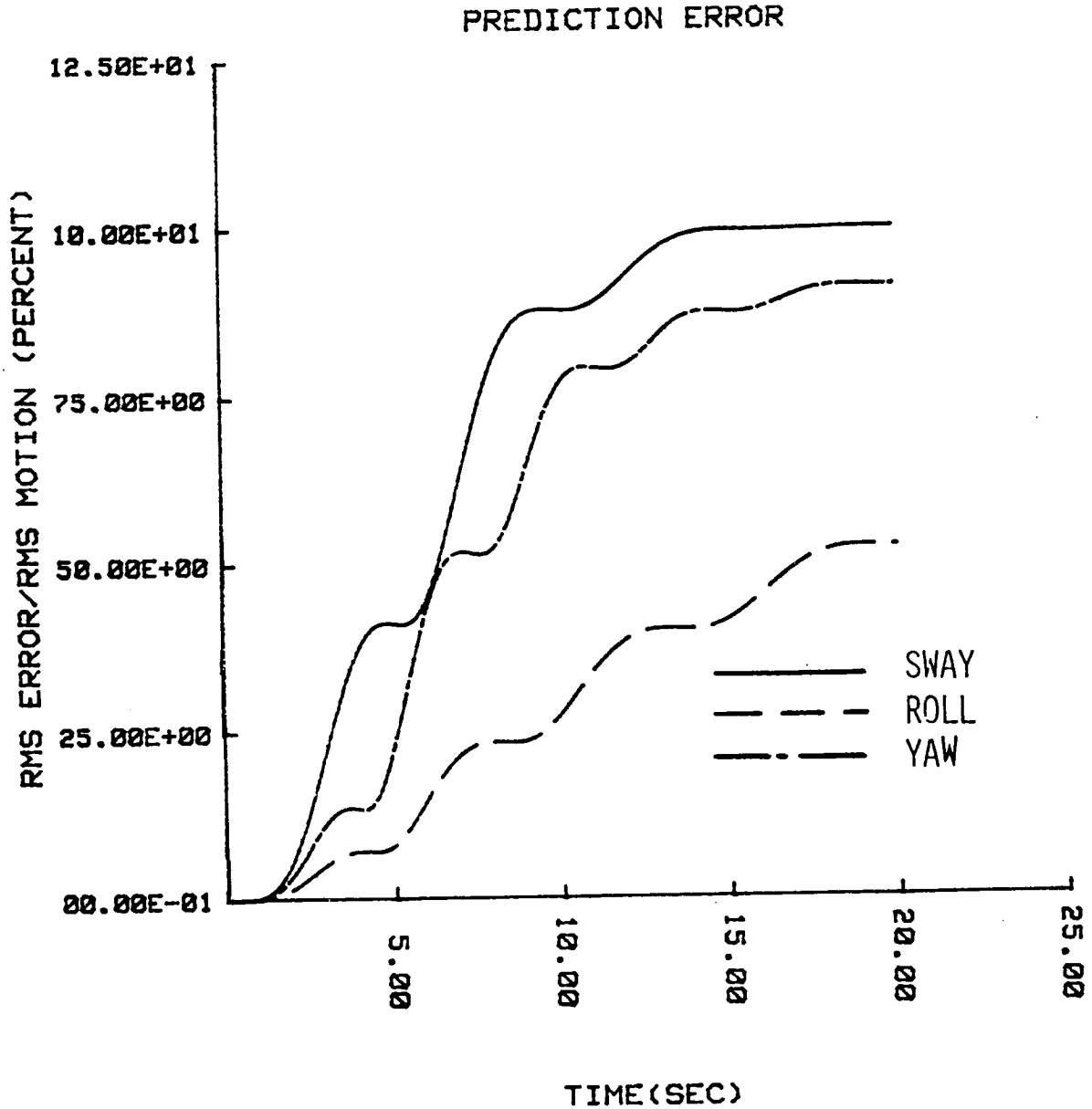


Figure 5.7

RMS Prediction Error Over RMS Motion Versus Prediction Time for Sway, Roll, Yaw. $U=15.1$ ft/sec, $\phi=45^\circ$, sea state 5.

HEAVE SIMULATION, PREDICTION

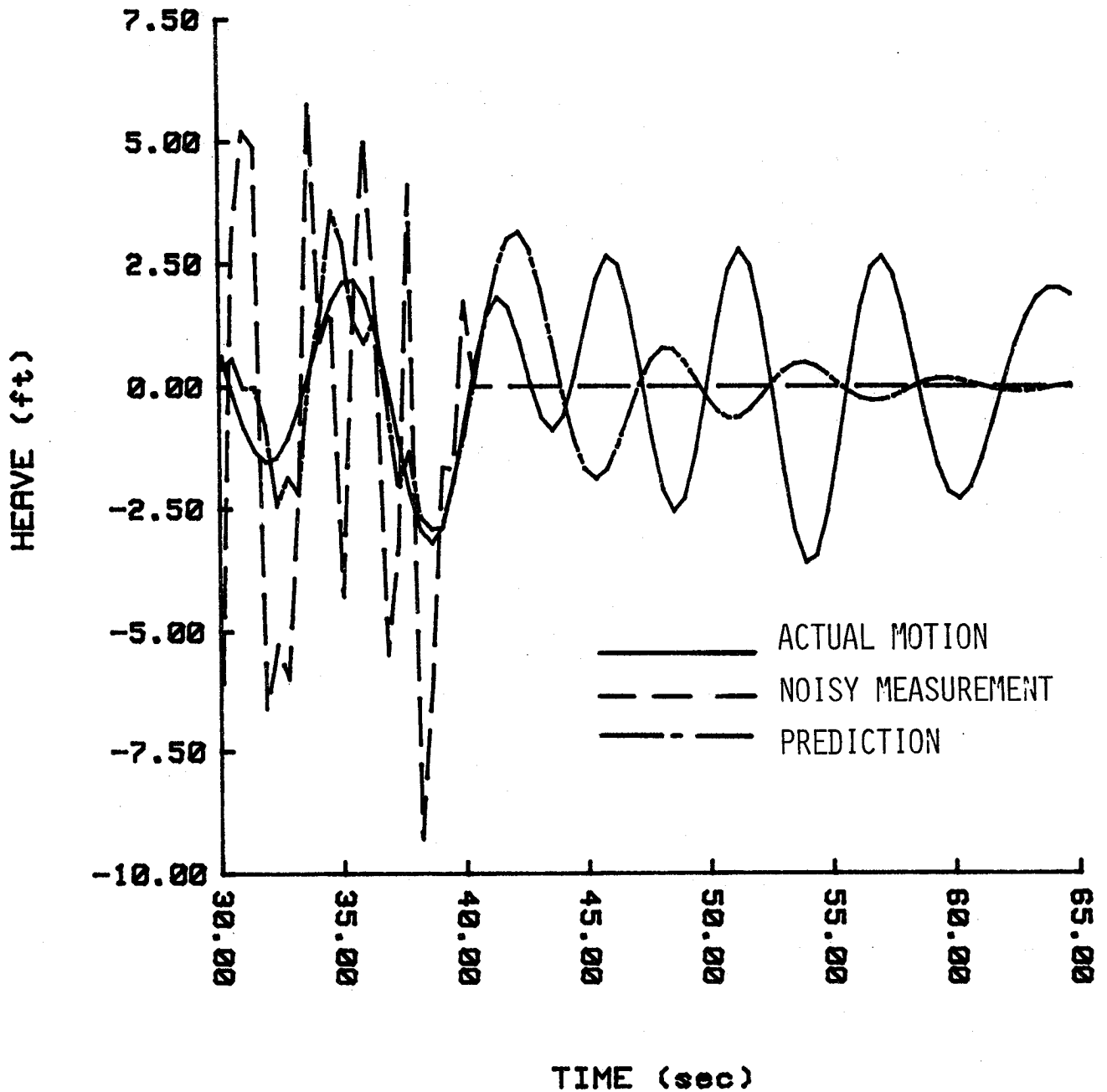


Figure 5.8

Heave Simulation Results, Its Kalman Filter Estimate (up to 40 sec) and Its Prediction Using the Kalman Filter Estimate (after $t=40$ sec). Same conditions as in 5.1.

SWAY SIMULATION, PREDICTION

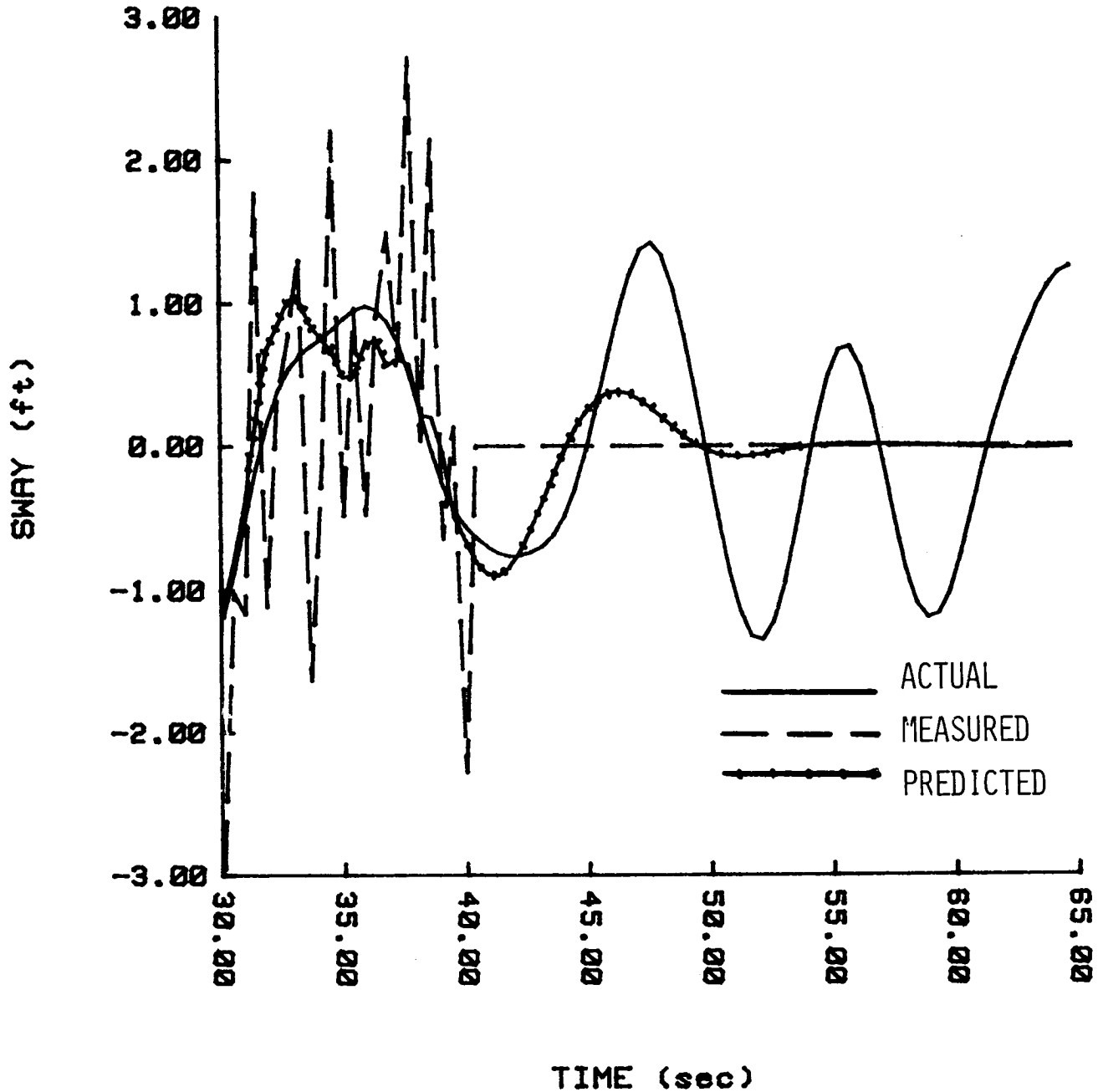


Figure 5.9

Sway Simulation Results, Its Kalman Filter Estimate (up to 40 sec) and Its Prediction Using the Kalman Filter Estimate (after $t=40$ sec). Same conditions as in 5.3.

ROLL SIMULATION, PREDICTION

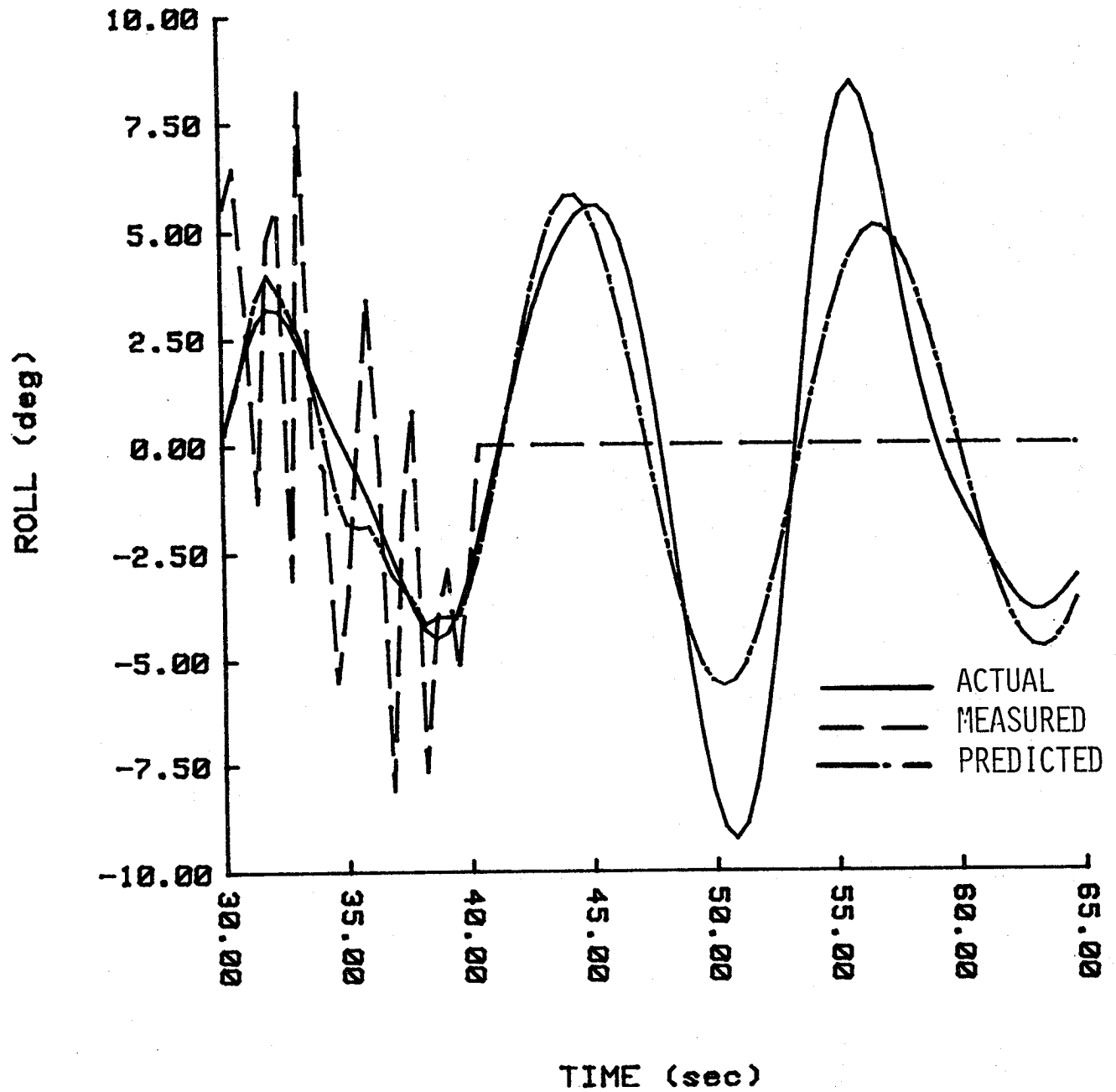


Figure 5.10

Roll Simulation and Prediction. Same conditions as in 5.9.

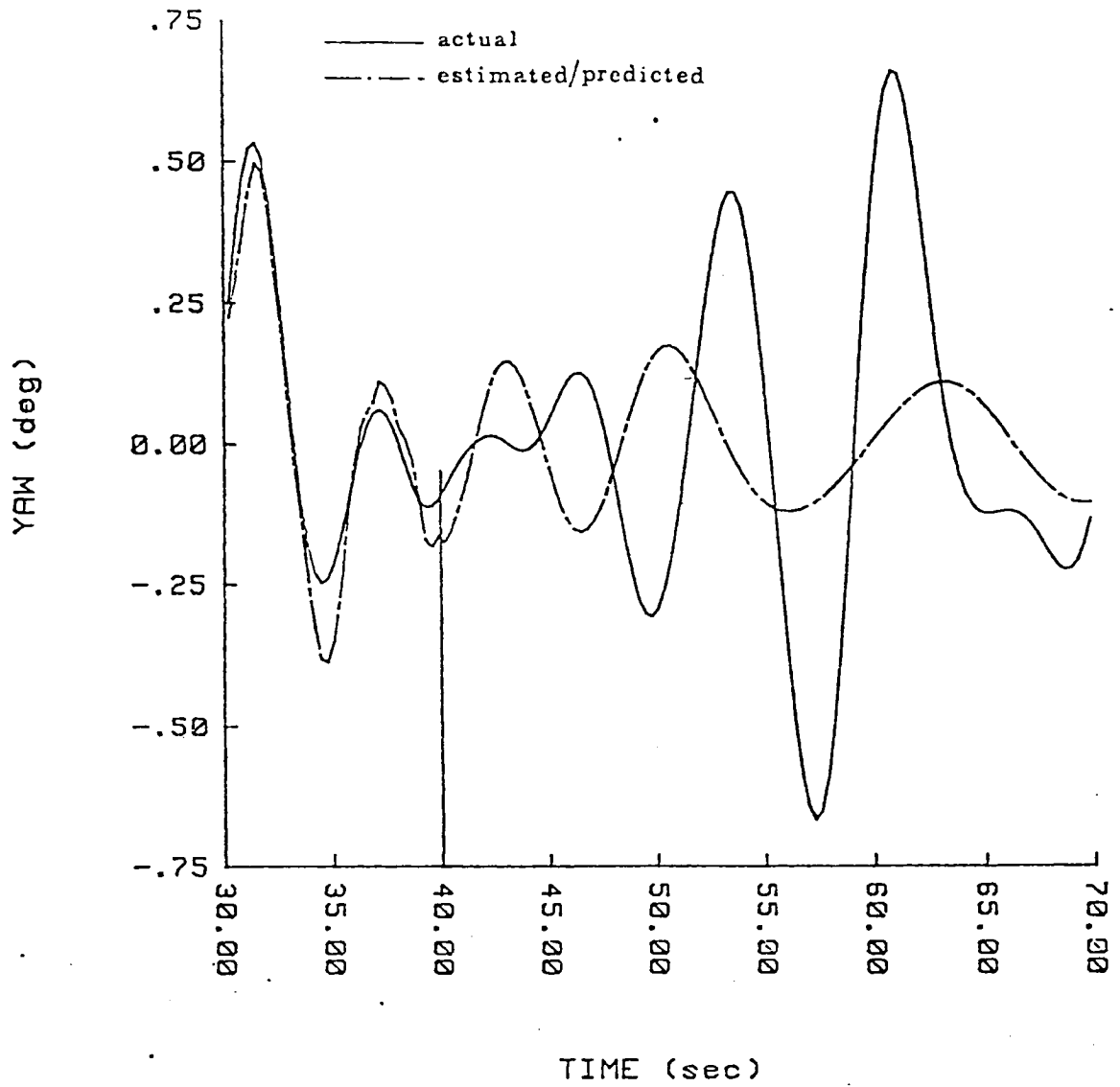


Figure 5.11
Yaw Simulation and Prediction. Same conditions as 5.9.

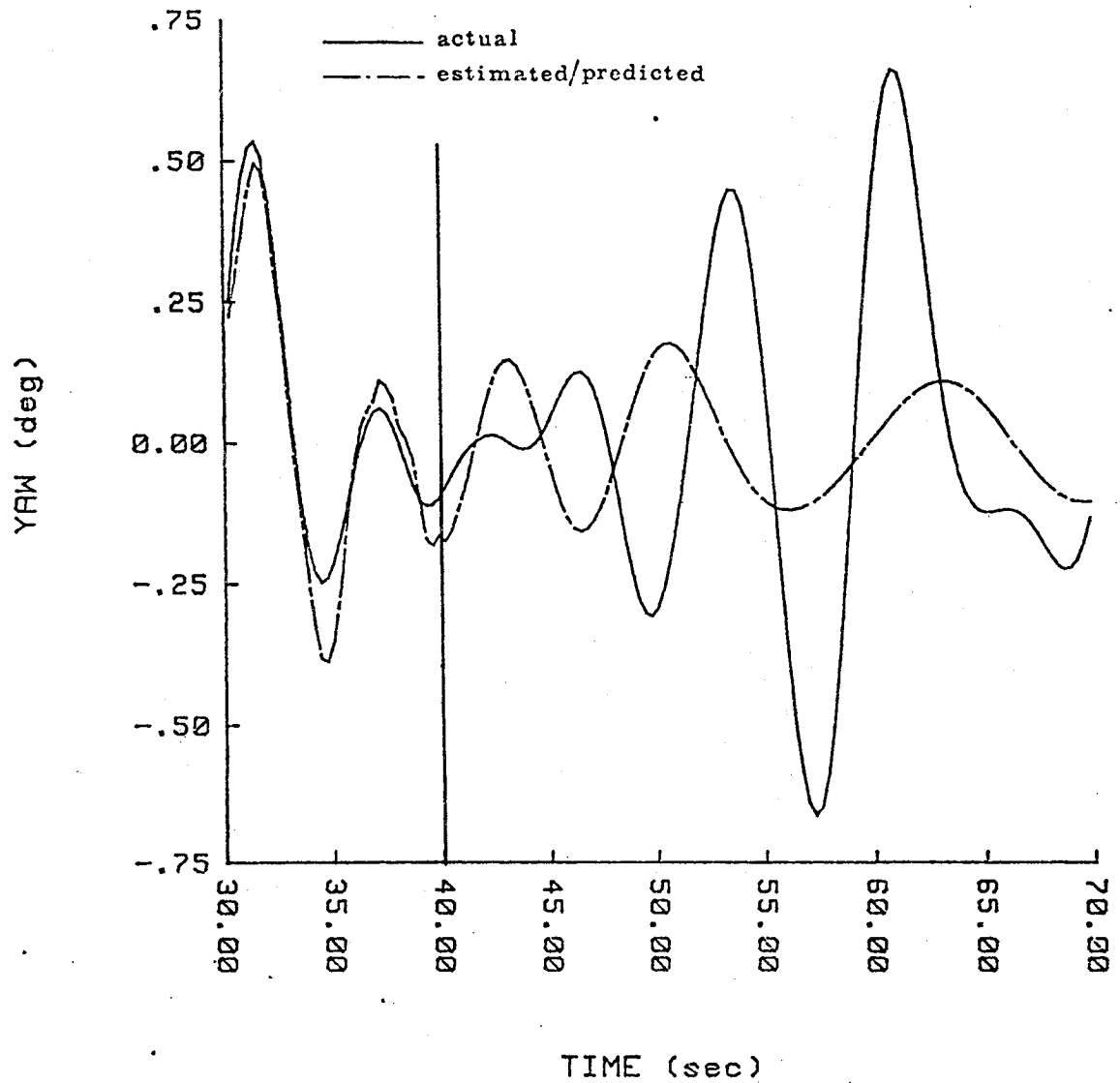


Figure 5.11:

Yaw Simulation and Prediction. Same conditions as 5.9.

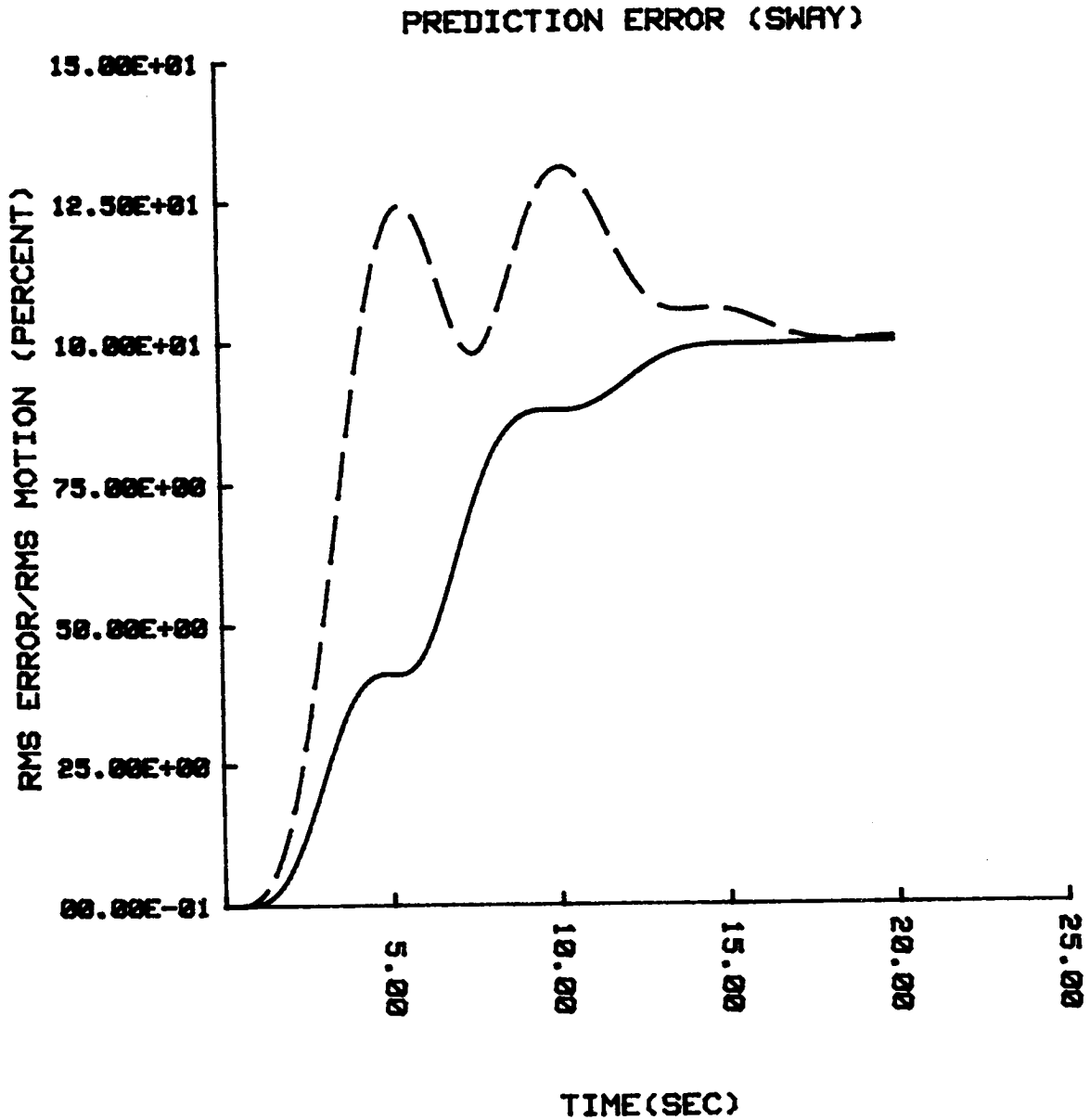


Figure 5.12

RMS Prediction Error Versus RMS Motion Versus Prediction Time for Sway. Actual $W_m = 0.52$ rad/sec, used $W_m = 0.72$ rad/sec. All other conditions as in 5.3.

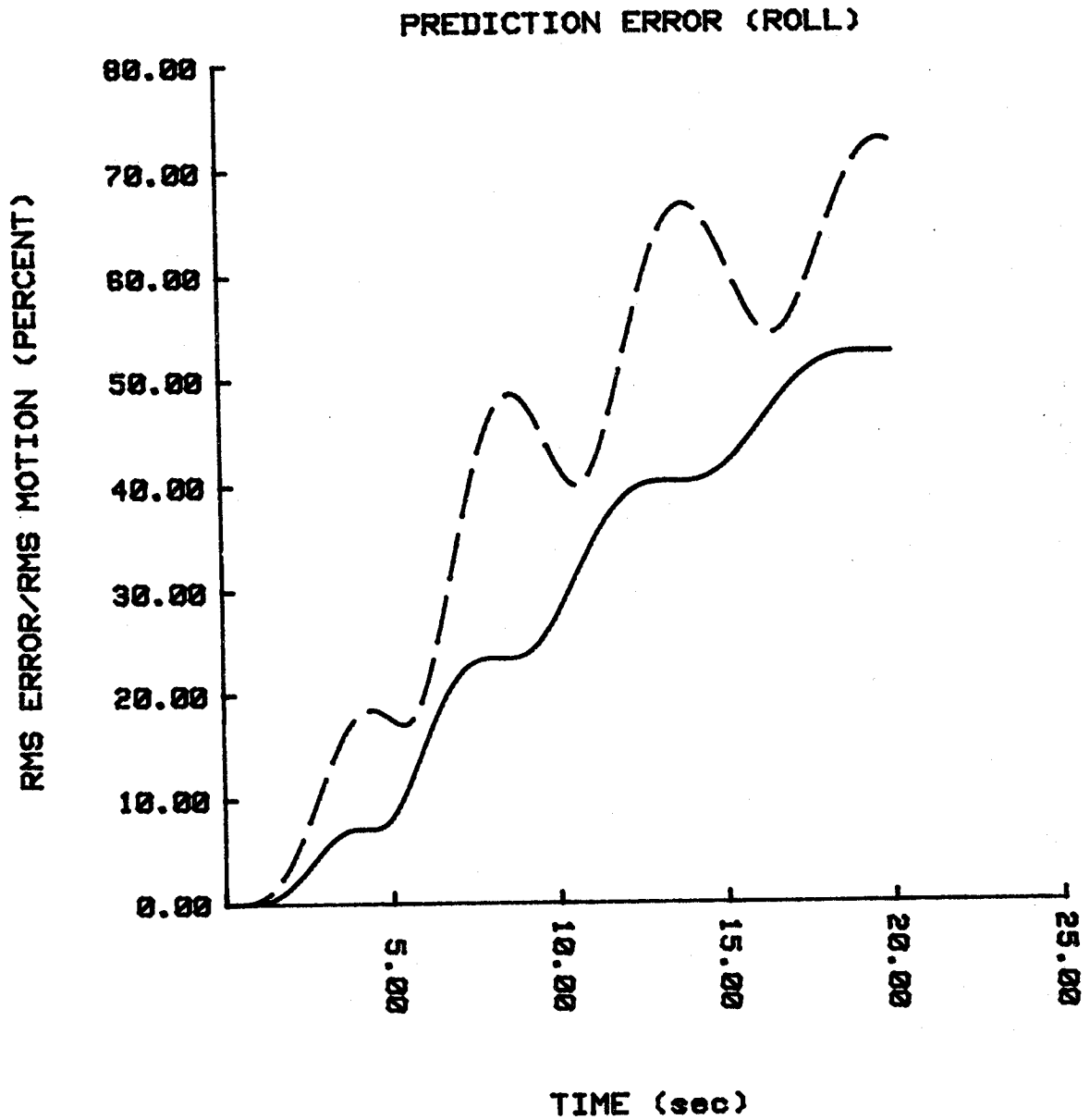


Figure 5.13

RMS Error Versus Prediction Time Roll. Same condition as in 5.12.

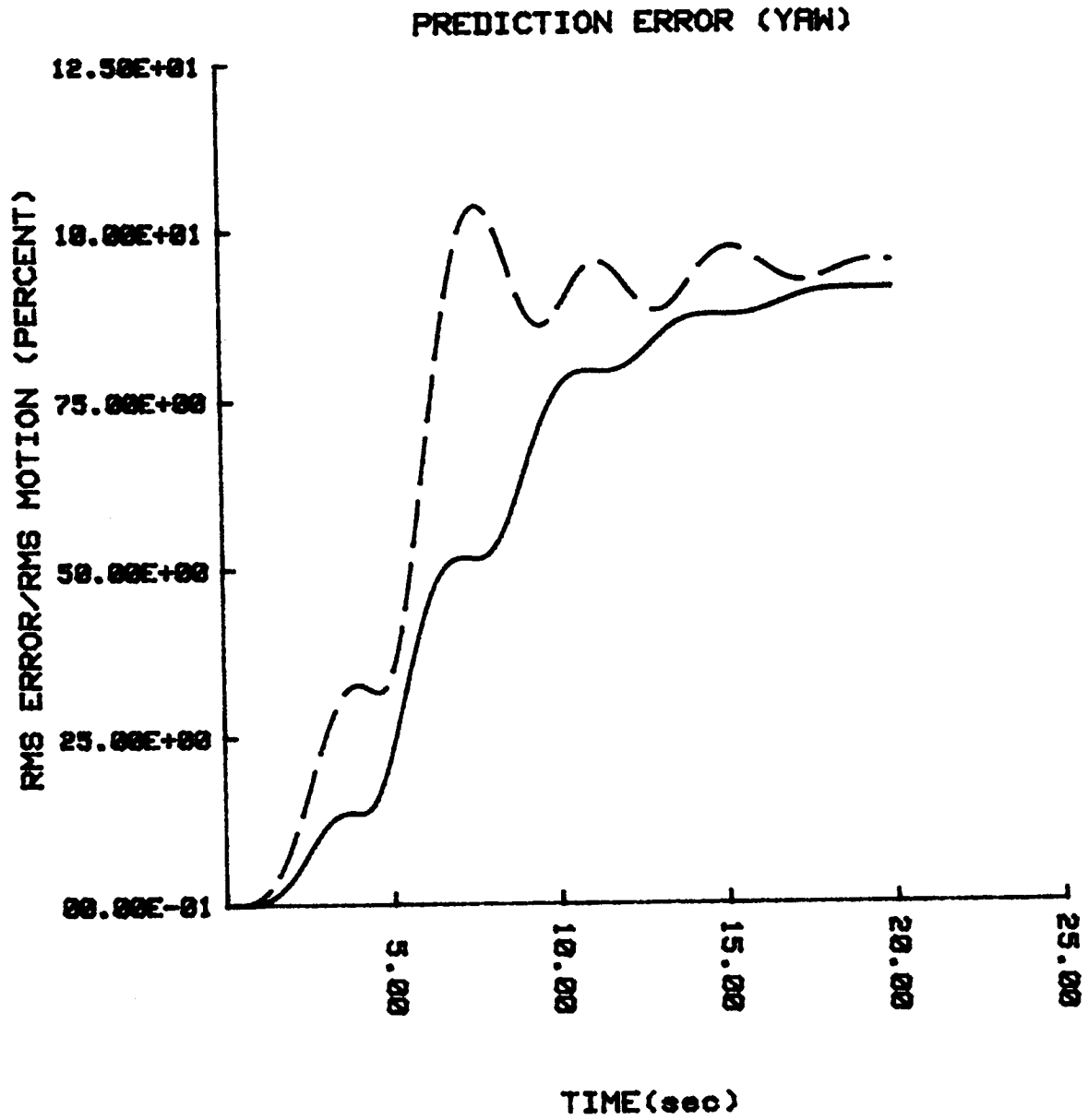


Figure 5.14

RMS Error Versus Prediction Time for Yaw. Same conditions as in 5.12.

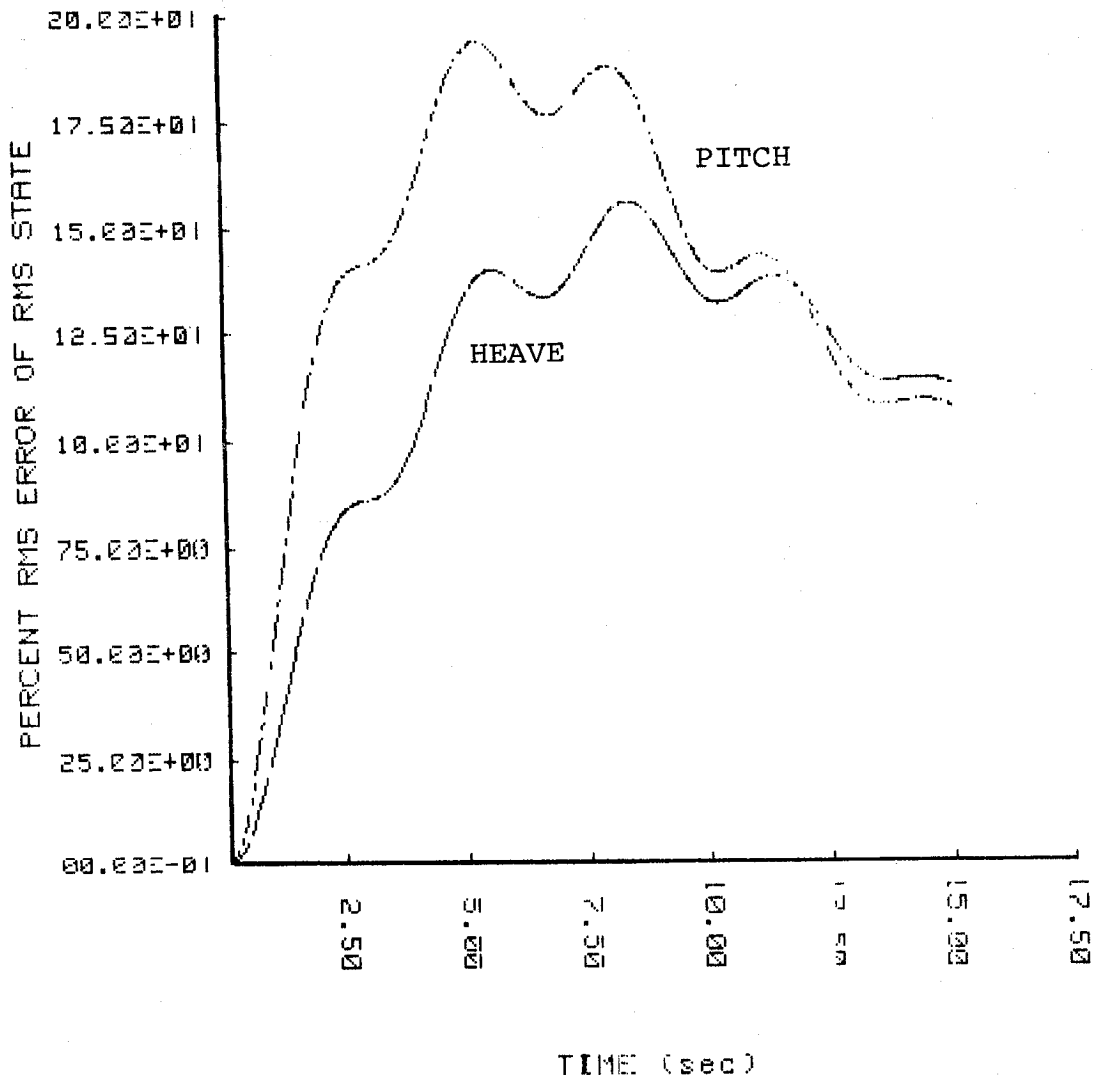


Figure 5.15

RMS Prediction Error Over RMS Motion for Heave and Pitch.
 $U=21$ ft/sec, $\phi=0^\circ$, sea state 5. In the prediction model the nonminimum phase zero have been omitted.

CONCLUSIONS

A satisfactory approximation of the ship motion equations as provided by hydrodynamic theory has been achieved. The approximation is valid within the wave frequency range and for seas described by the Bretschneider spectrum, whose major limitations are

- (a) uni-directional seas
- (b) unlimited fetch, deep water

The resulting two groups of motions, i.e., heave-pitch and sway-roll-yaw can be approximated separately requiring 15 and 16 states respectively. If both must be used a 25 state system is required.

The model depends parametrically on the ship speed, the wave angle and the significant wave height and modal frequency.

The Kalman filter is designed using as measurement noise intensity, values from ship vibration amplitudes. For sway-roll-yaw the vibration levels are small, nonetheless, to bound the filter eigenvalues below 2.0 rad/sec similar values were used, as for heave-pitch.

It should be remembered that heave and pitch are related by a non-minimum phase transfer function, resulting in reduced filter accuracy. Actually, heave is 90° out of phase for low frequencies with respect to all the other motions.

A sensitivity analysis of the filter performance indicates that the most critical parameter is the spectrum modal frequency. It should be remembered that a sea spectrum may contain more than one peak, in which case it is essential to obtain an accurate estimate of both peak frequencies.

Of particular interest is the fact that the wave direction does not have a significant influence on the estimation error. This means that although our modeling used a uni-directional Bretschneider spectrum, it can be applied in its present form for directional seas.

The models derived herein can be used to predict the ship's motions up to 5 seconds ahead in time for all motions and 10 seconds for roll. When modeling errors and noise are taken into account, a more realistic estimate of 2-3 seconds for all motions and 6-8 seconds for roll is obtained.

Again, the modal frequency of the sea spectrum is the most critical parameter. Also, the nonminimum phase zeros can deteriorate the performance of the predictor significantly if omitted.

ACKNOWLEDGEMENTS

Erik Tiemroth, graduate student in the Ocean Engineering Department, has prepared some of the programs presented in this study and assisted in the debugging and running of several others.

Material and information was provided by Prof. Gunter Stein of the EECS Department and Chris McMuldloch, a graduate student in the EECS Department.

The work was carried out at the Laboratory for Information and Decision Systems with support from the National Aeronautics and Space Administration Ames Research Center under Grant NGL - 22 - 009 - 124.

REFERENCES

- (1) Athans, M., "The Role and Use of the Stochastic Linear-Quadratic - Gaussian Problem in Control System Design", IEEE Trans. on Automatic Control, Vol. AC-16, Dec. 1971.
- (2) Balchen, J.G., Jenssen, N.A., Saelid, S., "Dynamic Positioning Using Kalman Filtering and Optimal Control Theory," Automation in Offshore Oil Field Operations, 1976, pp. 183-188.
- (3) Barr, R.A., Ankudinov, V., "Ship Rolling, Its Prediction and Reduction Using Roll Stabilization," Marine Technology, Jan. 1977.
- (4) Bodson, M., "Lateral Control System Design for VTOL Landing on a DD963 in High Sea States," S.M. Thesis, Dept. of Electrical Engineering and Computer Science, MIT, Cambridge, Mass. 1982.
- (5) Bryson, A., Ho, Y.C., "Applied Optimal Control," Hemisphere Publishing, Co., New York, 1975.
- (6) Dalzell, J.F., "A Note on Short-Time Prediction of Ship Motions," Journal of Ship Research, Vol. 9, No. 2, 1965.
- (7) Doyle, J.C., Stein, G., "Robustness with Observers," IEEE Trans. on Automatic Control, Vol. AC-24, August 1979.
- (8) Gelb, A., editor, "Applied Optimal Estimation," MIT Press, Cambridge, MA. 1974.
- (9) Grimble, M.J., Patton, R.J., Wise, D.A., "The Design of a Dynamic Ship Positioning Control System Using Extended Kalman Filtering Technique," Oceans '79, San Diego, CA, Sept. 1979.
- (10) Kallstrom, C.G., "Simulation of Ship Steering," Dept. of Automatic Control, Lund Institute of Technology, Lund, Sweden, Coden: LUTFD2/(TFRT-7109)/1-353/1976.
- (11) Kaplan, P., Kaff, A.I., "Evaluation and Verification of Computer Calculations of Wave-Induced Ship Structural Loads," Ship Structure Committee, Report No. SSC-229, 1972.
- (12) Kaplan, P., "A Study of Prediction Techniques for Aircraft Carrier Motion at Sea," AIAA Sixth Aerospace Science Meeting, Paper No. 68-123, 1968.
- (13) Kim, C.H., Chou, F.S., Tien, D., "Motions and Hydrodynamic Loads of a Ship Advancing in Oblique Waves," Trans. SNAME, Vol. 88, 1980.

- (14) Kwakernaak, H., Sivan, R., "Linear Optimal Control Systems," Wiley, 1972.
- (15) McMuldloch, C.G., "VTOL Controls for Shipboard Landing," Laboratory for Information and Decision Systems, Report LIDS-TH-928, 1979, MIT, Cambridge, MA.
- (16) Newman, J.N., "Marine Hydrodynamics," MIT Press, 1978, Cambridge, MA.
- (17) Ogilvie, T.F., "Recent Progress Toward the Understanding and Prediction of Ship Motions," Fifth Symposium on Naval Hydrodynamics, Bergen, Norway, 1964.
- (18) Salvesen, N., Tuck, E.O., Faltinsen, O., "Ship Motions and Sea Loads," Trans. SNAME, Vol. 78, 1970.
- (19) Sidar, M., Doolin, B.F., "On the Feasibility of Real Time Prediction of Aircraft Carrier Motion at Sea," NASA Techn. Memo X-6245, 1975.
- (20) Smith, O.J.M., "Feedback Control Systems," McGraw Hill, New York 1958.
- (21) St. Denis, M., Pierson, W.J., "On the Motions of Ships in Confused Seas," Trans. SNAME, 1953.
- (22) Tick, L.J., "Differential Equations with Frequency Dependent Coefficients," J. of Ship Research, Vol. 3, No. 2., 1959.
- (23) Triantafyllou, M., Athans, M., "Real Time Estimation of the Motions of a Destroyer Using Kalman Filtering Techniques," Laboratory for Information and Decision Systems Report, MIT, Cambridge, MA 1981.
- (24) Triantafyllou, M., Athans, M., "Real Time Estimation of the Heaving and Pitching Motions of a Ship Using a Kalman Filter," Proc. Oceans '81, Boston, MA, Sept. 1981.
- (25) Triantafyllou, M., Bodson, M., "Real Time Prediction of Marine Vessel Motion Using Kalman Filtering Techniques," Proc. OTC, Houston, Texas, 1982.
- (26) Vugt, J.H., "The Hydrodynamic Forces and Ship Motions in Oblique Waves," Netherlands Ship Research Center TNO Report No. 150S, Dec., 1971.

- (27) Yumori, I.R., "Real Time Prediction of Ship Response to Ocean Waves Using Time Series Analysis," Oceans '81, Boston, MA., Sept. 1981.
- (28) "5-Degree of Freedom Seakeeping Program Manual," Design Laboratory, Ocean Engineering Dept., MIT, Cambridge, MA, 1979.
- (29) "Dynamic Control Systems Software - User's Manual," Laboratory for Information and Decision Systems, MIT, Cambridge, MA. 1980.
- (30) Wiener, N., "Time Series," MIT Press, Cambridge, MA. 1949.

APPENDIX 1

Hydrodynamic Theory

In the text, the simple one dimensional equation of heave motion was derived to demonstrate the principles involved. Here we will proceed to write the overall equations of motion.

We will avoid extensive hydrodynamic theory developments since [15] and [17] provide an in depth coverage. Within linear theory, we intend to write the added mass, damping and exciting force terms.

The equations of motion can be written as

$$\{-\omega^2 [M + A] + i\omega B + C\} \underline{x} = \underline{F}\eta \quad (1)$$

where

$$M = \{M_{ij}\}, A = \{A_{ij}\}, B = \{B_{ij}\}, C = \{C_{ij}\} \quad (2)$$

We can find the various matrices from hydrodynamic theory [15], [17] and dynamics. We omit surge as a second order quantity so that \underline{x} is a vector of dimension five:

$$M = \begin{bmatrix} m & 0 & -mz_c & 0 & 0 \\ 0 & m & 0 & 0 & 0 \\ -mz_c & 0 & I_{xx} & 0 & I_{xz} \\ 0 & 0 & 0 & I_{yy} & 0 \\ 0 & 0 & I_{zx} & 0 & I_{zz} \end{bmatrix} \quad (3)$$

with m the mass of the ship, z_c the distance of the center of

gravity, vertically, from the origin.

$$A = \begin{bmatrix} A_{22} & 0 & A_{24} & 0 & A_{26} \\ 0 & A_{33} & 0 & A_{35} & 0 \\ A_{42} & 0 & A_{44} & 0 & A_{46} \\ 0 & A_{53} & 0 & A_{55} & 0 \\ A_{62} & 0 & A_{64} & 0 & A_{66} \end{bmatrix} \quad (4)$$

$$B = \begin{bmatrix} B_{22} & 0 & B_{24} & 0 & B_{26} \\ 0 & B_{33} & 0 & B_{35} & 0 \\ B_{42} & 0 & B_{44} & 0 & B_{46} \\ 0 & B_{53} & 0 & B_{55} & 0 \\ B_{62} & 0 & B_{64} & 0 & B_{66} \end{bmatrix} \quad (5)$$

$$C = \begin{bmatrix} 0 & 0 & 0 & 0 & 0 \\ 0 & \rho g A_{wp} & 0 & C_{35} & 0 \\ 0 & 0 & \Delta (GM)_T & 0 & 0 \\ 0 & C_{53} & 0 & \Delta (GM)_L & 0 \\ 0 & 0 & 0 & 0 & 0 \end{bmatrix} \quad (6)$$

With A_{wp} the waterplane area of the ship, Δ the displacement, $(GM)_T$ the transverse metacentric height and $(GM)_L$ the longitudinal metacentric height.

The following relations hold true within strip theory [17]

$$A_{33} = A_{33}^{\circ} - \frac{U}{\omega^2} b_{33}^A$$

$$B_{33} = B_{33}^{\circ} + U \alpha_{33}^A$$

$$A_{35} = A_{35}^{\circ} - \frac{U}{\omega^2} + \frac{U}{\omega^2} x_A b_{33}^A - \frac{U^2}{\omega^2} \alpha_{33}^A$$

$$B_{35} = B_{35}^{\circ} + UA_{33}^{\circ} - Ux_A \alpha_{33}^A - \frac{U^2}{\omega^2} b_{33}^A$$

$$A_{53} = A_{53}^{\circ} + \frac{U}{\omega^2} B_{33}^{\circ} + \frac{U}{\omega^2} x_A b_{33}^A$$

$$B_{53} = B_{53}^{\circ} - UA_{33}^{\circ} - Ux_A \alpha_{33}^A$$

$$A_{55} = A_{55}^{\circ} + \frac{U^2}{\omega^2} A_{33}^{\circ} - \frac{U}{\omega^2} x_A^2 b_{33}^A + \frac{U^2}{\omega^2} x_A \alpha_{33}^A$$

$$B_{55} = B_{55}^{\circ} + \frac{U^2}{\omega^2} B_{33}^{\circ} + Ux_A^2 \alpha_{33}^A + \frac{U^2}{\omega^2} x_A b_{33}^A$$

The superscript 0 denotes quantities at zero speed. x_A is the distance to the aftermost cross-section of the ship and a_{ij}^A , b_{ij}^A are its sectional added mass characteristics. These last two quantities are important only for cruiser stern ships. The A_{ij}° , B_{ij}° can be found using the M.I.T. Seakeeping Program [27]. Similarly, we can find:

$$A_{22} = A_{22}^{\circ} - \frac{U}{\omega^2} b_{22}^A$$

$$B_{22} = B_{22}^{\circ} + U \alpha_{22}^A$$

$$A_{24} = A_{42} = A_{24}^{\circ} - \frac{U}{\omega^2} b_{24}^A$$

$$B_{24} = B_{42} = B_{24}^{\circ} + U \alpha_{24}^A$$

$$A_{26} = A_{26}^{\circ} + \frac{U}{\omega^2} B_{22}^{\circ} - \frac{U}{\omega^2} x_A b_{22}^A + \frac{U^2}{\omega^2} \alpha_{22}^A$$

$$B_{26} = B_{26}^{\circ} - U A_{22}^{\circ} + U x_A \alpha_{22}^A + \frac{U^2}{\omega^2} b_{22}^A$$

$$A_{44} = A_{44}^{\circ} - \frac{U}{\omega^2} b_{24}^A$$

$$B_{44} = B_{44}^{\circ} + U \alpha_{44}^A + B_{44}^*$$

with B_{44}^* the equivalent nonlinear damping

$$A_{46} = A_{46}^{\circ} + \frac{U}{\omega^2} B_{24}^{\circ} - \frac{U}{\omega^2} x_A b_{24}^A + \frac{U^2}{\omega^2} \alpha_{24}^A$$

$$B_{46} = B_{46}^{\circ} - U A_{24}^{\circ} + U x_A \alpha_{24}^A + \frac{U^2}{\omega^2} b_{24}^A$$

$$A_{62} = A_{26}^{\circ} - \frac{U}{\omega^2} B_{22}^{\circ} - \frac{U}{\omega^2} x_A b_{22}^A$$

$$B_{62} = B_{26}^{\circ} + U A_{22}^{\circ} + U x_A \alpha_{22}^A$$

$$A_{64} = A_{46}^{\circ} - \frac{U}{\omega^2} B_{24}^{\circ} - \frac{U}{\omega^2} x_A b_{24}^A$$

$$B_{64} = B_{46}^{\circ} + U A_{24}^{\circ} + U x_A \alpha_{24}^A$$

$$A_{66} = A_{66}^{\circ} + \frac{U^2}{\omega^2} A_{22}^{\circ} - \frac{U}{\omega^2} x_A^2 b_{22}^A + \frac{U^2}{\omega^2} x_A \alpha_{22}^A$$

$$B_{66} = B_{66}^{\circ} + \frac{U^2}{\omega^2} B_{22}^{\circ} + U x_A^2 \alpha_{22}^A + \frac{U^2}{\omega^2} x_A b_{22}^A$$

$$F_2 = \alpha_0 \rho \int (f_2 + h_2) d\xi + \alpha_0 \rho \frac{U}{i\omega} h_2^A$$

$$F_6 = \alpha_0 \rho \int \left[\xi (f_2 + h_2) + \frac{U}{i\omega} h_2 \right] d\xi + \alpha_0 \rho \frac{U}{i\omega} x_A h_2^A$$

$$F_4 = \alpha_0 \rho \int (f_4 + h_4) d\xi + \alpha_0 \rho \frac{U}{i\omega} h_4^A$$

$$F_3 = \rho \alpha_0 \int (f_3 + h_3) d\xi + \rho \alpha_0 \frac{U}{i\omega} h_3^A$$

$$F_5 = -\rho \alpha_0 \int \left[\xi (f_3 + h_3) + \frac{U}{i\omega} h_3 \right] d\xi - \rho \alpha_0 \frac{U}{i\omega} x_A h_3^A$$

where f_j is the sectional Froude-Kryloff force and h_j the sectional diffraction force.

VCG = Vertical Center of Gravity = - 4.6 ft.
(from waterplane)

GM = Metacentric Height = 4.16 ft.

XCG = Longitudinal Center of Gravity = 1.07 ft. AFT
(from admidships)

Δ = Displacement = 6,800 ton

C_b = Block Coefficient = 0.461

APPENDIX 2

The M.I.T. Sea-keeping Program [27] was used to derive the hydrodynamic data. The values used to develop the simple models for heave-pitch and sway-roll-yaw (as already mentioned, to first order heave and pitch are uncoupled from sway, roll and yaw).

All units are consistent such that the forces are obtained in tons, the moments in ton·ft., the linear motions in ft. and the angular motions in radians. The programs change the angular motions and express them in degrees only in the final (output) stage.

Heave-Pitch Characteristics

M	=	214	C ₃₃	=	587
A ⁰ ₃₃	=	281	B ⁰ ₃₃	=	260
A ⁰ ₃₅	=	15500	B ⁰ ₃₅	=	15500
C ₃₅	=	260			
I ₅₅	=	3.76*10 ⁶	A ₅₅	=	4.20*10 ⁶
B ₅₅	=	3.8*10 ⁶	C ₅₅	=	9.53*10 ⁶
A ₁	=	550			
A ₂	=	120000			

The principal ship characteristics have as follows

L _{BP}	=	Length between perpendiculars	=	529 ft.
B	=	Beam	=	55 ft.
T	=	Draft	=	18 ft.

Sway - Roll - Yaw Characteristics

$$A_{44} = 22,800$$

$$I_{44} = 104,000$$

$$B_{44} = 800 + B_{44}^*$$

$$C_{44} = 28,800$$

$$A_{24} = -760$$

$$B_{24} = -50$$

$$A_{46} = 181,000$$

$$B_{46} = 5,600$$

$$A_{22} = 220$$

$$B_{22} = 10$$

$$A_{66} = 4.16 \times 10^6$$

$$I_{66} = 3.8 \times 10^6$$

$$B_{66} = 130,000$$

$$A_{26} = 14,500$$

$$B_{26} = 370$$

$$A_2 = 380$$

$$A_4 = 2,400$$

$$A_6 = 23,000$$

APPENDIX 3

Simulation

The simulation of a continuous system

$$\dot{x} = Ax + BW_1$$

$$y = Cx + W_2$$

where the white noise signals W_1 , W_2 have intensity V_1 , V_2 respectively, is performed by constructing the equivalent discrete system

$$x(t+\delta t) = A_k x(t) + B_k W_{k1}$$

$$y(t) = C x(t) + W_{k2}$$

where $A_k = e^{A\delta t} = I + A\delta t + A^2\delta t^2/2! + \dots$

$$B_k W_{k1} = \int_t^{t+\delta t} e^{A(t-\tau)} B W_1(\tau) d\tau$$

An approximation would be

$$x(t+\delta t) = (I+A\delta t)x(t) + (B\delta t)W_{k1}$$

$$y(t) = Cx(t) + W_{k2}$$

where W_{k1} , W_{k2} discrete white noise of intensity V_{k1} , V_{k2} respectively, given by:

$$V_{k1} = V_1 / \delta t$$

$$V_{k2} = V_2 / \delta t$$

If a random number generator is provided with a range between 0 and 1, the following relation provides W_{k1} (and similarly W_{k2})

$$W_{k1} = (\text{RND} - 0.5) \cdot \sqrt{12 \cdot V_{k1}}$$

where RND is a random number between 0 and 1.

Higher order approximations to A_k may be necessary in some cases. Problems appear in particular with lightly damped systems, i.e., when the matrix A possesses eigenvalues $-a \pm ib$ where $0 < a \ll b$. Such for example, is the case of roll whose damping is typically around 10% of the critical value.

The approximation:

$$e^{(-a \pm ib)\delta t} \approx (1 - a \cdot \delta t) \pm ib \cdot \delta t$$

is valid provided

$$a \cdot \delta t \ll 1$$

$$b \cdot \delta t \ll 1$$

The next order term is:

$$(-a \pm ib)^2 \frac{\delta t^2}{2}$$

so for accuracy we require,

$$\left| (a^2 - b^2) \frac{\delta t^2}{2} \right| \ll a \delta t$$

$$ab \delta t^2 \ll b \delta t$$

which results in a single additional condition

$$\delta t \ll \left| \frac{2a}{a^2 - b^2} \right|$$

It is easy to see that when $a \ll b$ then

$$\delta t \ll \min \left[\frac{1}{2a}, \frac{2}{b} \cdot \left(\frac{a}{b}\right) \right]$$

This requirement may be very demanding for simulation by imposing an extremely small time step. If an appropriate step is not chosen then the real part of the (neglected) second order term reduces the first order real part, thus resulting in a reduction of the already small damping. By using a higher order approximation, in the form

$$e^{A \cdot \delta t} \simeq I + A \cdot \delta t + \dots + \frac{A^m \delta t^m}{m!}$$

such problems are resolved. In the present case, the sway-roll-yaw model requires such treatment for efficient simulation.

Appendix 4

Computer Program Listing

```

DIMENSION A(15,15),C(2,15),SIGMA(15,15),XI(2,2)
FX(X)=5.*(-X**4+1.)*(1.+2.*X*ALFA)-2.*ALFA*X**5
WRITE(6,2000)
2000 FORMAT(3X,'INPUT THE SPEED (FT/SEC) AND WAVE ANGLE (DEGREES)')
READ(5,*)U,T1
T=T1*3.14159/180.
G=32.2
WRITE(6,2010)
2010 FORMAT(3X,'INPUT THE SIGN. WAVE HEIGHT (FT) AND MODAL FREQ. (RAD/SEC)')
READ(5,*)Z2,OMM
ALFA=U/G*OMM*COS(T)
U1=.2
U2=5.
AA=FX(U1)
903 UM=(U1+U2)*.5
IF(ABS(U1-U2).LT..0001*UM) GO TO 901
CC=FX(UM)
IF(AA*CC.GT.0.) GO TO 902
U2=UM
GO TO 903
902 U1=UM
AA=CC
GO TO 903
901 ZS=UM+UM**2*ALFA
GAM=ZS*2.**.25
ZS1=(1.+(ZS/GAM)**4)**3/ZS**4
ZS2=EXP(-1.25/UM**4)/UM**5/(1.+2.*ALFA*UM)
BE1=ZS1*ZS2
A33=495.
B33=260.
C33=537.
A35=15500.
B35=11700.+280.*U
C35=260.*U+17250.
A53=15500.
B53=11700.-280.*U
C53=-260*U+17250.
A55=7.95*10.**6
B55=3.8*10**6
C55=-280.*U**2+9.53*10.**6
D=A33*A55-A35*A53
D1=A55/D
D2=-A35/D
D3=-A53/D
D4=A33/D
Z1=-(D1*B33+D2*B53)
Z2=-(D1*C33+D2*C53)
Z3=-(D1*B35+D2*B55)
Z4=-(D1*C35+D2*C55)
Z5=-(D3*B33+D4*B53)
Z6=-(D3*C33+D4*C53)
Z7=-(D3*B35+D4*B55)
Z8=-(D3*C35+D4*C55)
RL=529.

```

```

MOD00010
MOD00020
MOD00030
MOD00040
MOD00050
MOD00060
MOD00070
MOD00080
MOD00090
MOD00100
MOD00110
MOD00120
MOD00130
MOD00140
MOD00150
MOD00160
MOD00170
MOD00180
MOD00190
MOD00200
MOD00210
MOD00220
MOD00230
MOD00240
MOD00250
MOD00260
MOD00270
MOD00280
MOD00290
MOD00300
MOD00310
MOD00320
MOD00330
MOD00340
MOD00350
MOD00360
MOD00370
MOD00380
MOD00390
MOD00400
MOD00410
MOD00420
MOD00430
MOD00440
MOD00450
MOD00460
MOD00470
MOD00480
MOD00490
MOD00500
MOD00510
MOD00520
MOD00530
MOD00540
MOD00550

```

Program to prepare
matrices for the heave-
pitch motions.

```

B=55.
FO=SQRT(2.*3.14159*G/(RL*COS(T)+B))+2.*3.14159/(RL*COS(T)+B)*U*COS
MOD00560
MOD00570
MOD00580
MOD00590
MOD00600
MOD00610
MOD00620
MOD00630
MOD00640
MOD00650
MOD00660
MOD00670
MOD00680
MOD00690
MOD00700
MOD00710
MOD00720
MOD00730
MOD00740
MOD00750
MOD00760
MOD00770
MOD00780
MOD00790
MOD00800
MOD00810
MOD00820
MOD00830
MOD00840
MOD00850
MOD00860
MOD00870
MOD00880
MOD00890
MOD00900
MOD00910
MOD00920
MOD00930
MOD00940
MOD00950
MOD00960
MOD00970
MOD00980
MOD00990
MOD01000
MOD01010
MOD01020
MOD01030
MOD01040
MOD01050
MOD01060
MOD01070
MOD01080
MOD01090
MOD01100
1(T)
ZT=.7071
OMNE=OMM+OMM**2*U/32.2*COS(T)
TH1=(2.*ZT*FO**5+FO**4*OMNE)
TH2=(FO**4*(4.*ZT**2-1.))+2.*ZT*FO**3*OMNE)
TH3=-(OMNE*FO**4+2.*ZT*FO**5)
TH4=FO**4
A1=550.
A2=120000.
TH5=D1*A1*FO**2
TH6=D2*A2*COS(T)
TH7=D3*A1*FO**2
TH8=D4*A2*COS(T)
OMN=OMM*GAM
S0=1.25/4.*ZZ**2/OMM**5*BET
VP1=OMN**2
VP2=OMN*2.*ZT
VP3=VP1*SQRT(S0)
DO 800 I=1,15
DO 800 J=1,15
800 A(I,J)=0.
A(1,2)=1.
A(3,4)=1.
A(5,6)=1.
A(7,8)=1.
A(9,10)=1.
A(11,12)=1.
A(13,14)=1.
A(15,15)=-OMNE
A(8,7)=Z2
A(8,8)=Z1
A(8,9)=Z4
A(8,10)=Z3
A(10,7)=Z6
A(10,8)=Z5
A(10,9)=Z8
A(10,10)=Z7
A(15,11)=TH1
A(15,12)=TH2
A(15,13)=TH3
A(15,14)=TH4
A(8,11)=TH5
A(8,15)=TH6
A(10,11)=TH7
A(10,15)=TH8
A(2,1)=-VP1
A(2,2)=-VP2
A(2,4)=VP1
A(4,3)=-VP1
A(4,4)=-VP2
A(4,6)=VP1
A(6,5)=-VP1
A(6,6)=-VP2

```



```
A(12,11)=-FO**2
A(12,12)=-2*ZT*FO
A(12,13)=FJ**2
A(14,13)=-FO**2
A(14,14)=-2*FO*ZT
A(14,1)=VP3
WRITE(6,2200)
2200 FORMAT('** A MATRIX')
DO 890 I=1,15
- WRITE(9,2400) (A(I,J),J=1,15)
2400 FORMAT(8E10.4)
890 CONTINUE
END
```

MOD01110
MOD01120
MOD01130
MOD01140
MOD01150
MOD01160
MOD01170
MOD01180
MOD01190
MOD01200
MOD01210
MOD01220
MOD01230

```

C
C MODEL FOR THE SWAY ROLL YAW MOTIONS OF A DD-963 DESTROYER
C REVISED VERSION
C LAST CORRECTED SEPTEMBER 11 1981
C
  DOUBLE PRECISION A(16,16),XI(16,16),C(3,16),CV(3,16),CA(3,16)
  DOUBLE PRECISION THETA(3,3)
  DOUBLE PRECISION AH(3,3),BH(3,3)
  DOUBLE PRECISION P(3,3),R(3,3),T(4,4),U(4,6)
  DOUBLE PRECISION ZET(16,16),WR(16),WI(16),APS(16,16)
C
C SPEED, ANGLE AND SEA STATE INPUT
C
  WRITE(6,100)
100 FORMAT(2X,'INPUT THE SPEED (FT/SEC) AND ANGLE (DEGREES)')
  READ(5,*)V,T1
  T1=T1/57.29578
  WRITE(6,101)
101 FORMAT(2X,'INPUT THE SIGNIFICANT WAVE HEIGHT (FT) ',
1'AND MODAL FREQUENCY (RAD/SEC)')
  READ(5,*)ZZ,OMM
C
C SEA MODEL
C
  ALFA=V/32.2*OMM*COS(T1)
  ZETTA=0.707
  DELTA=SQRT(1.-2.*ZETTA**2+SQRT(9.-4.*ZETTA**2+4.*ZETTA**4))/2.
  OMN=ABS(OMM*(1.+ALFA)/DELTA)
  BET=((1.-DELTA**2)**2+4.*ZETTA**2*DELTA**2)**3/DELTA**4
  BET=ABS(BET*EXP(-1.25)/(1.+2.*ALFA))
  SO=0.3125*ZZ**2/OMM*BET
  VP1=OMN**2
  VP2=OMN*ZETTA*2
C
C HYDRODYNAMIC DATA
C FORCES
C
  A2=310.*SIN(T1)
  A4=2120.*SIN(T1)
  A6=11300.*SIN(T1)
  ZET2=0.72*SIN(T1)
  ZET4=0.7*SIN(T1)
  ZET6=0.35*SIN(T1)
  OM2=(0.6+V*COS(T1)/89.444)*SIN(T1)
  OM4=(0.76+V*COS(T1)/55.748)*SIN(T1)
  OM6=(0.96+V*COS(T1)/34.939)*SIN(T1)
C
C ADDED MASS - DAMPING
C
  OMES=(0.425+V*COS(T1)/178.27)**2
  AH(1,1)=223.
  AH(1,2)=-759.
  AH(2,1)=-759.
  AH(2,2)=22900.
  BH(1,1)=10.6

```

```

SRY00010
SRY00020
SRY00030
SRY00040
SRY00050
SRY00060
SRY00070
SRY00080
SRY00090
SRY00100
SRY00110
SRY00120
SRY00130
SRY00140
SRY00150
SRY00160
SRY00170
SRY00180
SRY00190
SRY00200
SRY00210
SRY00220
SRY00230
SRY00240
SRY00250
SRY00260
SRY00270
SRY00280
SRY00290
SRY00300
SRY00310
SRY00320
SRY00330
SRY00340
SRY00350
SRY00360
SRY00370
SRY00380
SRY00390
SRY00400
SRY00410
SRY00420
SRY00430
SRY00440
SRY00450
SRY00460
SRY00470
SRY00480
SRY00490
SRY00500
SRY00510
SRY00520
SRY00530
SRY00540
SRY00550

```

Program to prepare matrices
for the sway-roll-yaw motions

	BH(1,2)=-55.4	SRY00560
	BH(2,1)=-55.4	SRY00570
	BH(2,2)=887.	SRY00580
	AH(1,3)=14600.+V*BH(1,1)/OMES	SRY00590
	AH(3,1)=14600.-V*BH(1,1)/OMES	SRY00600
	AH(2,3)=182000.+V*BH(1,2)/OMES	SRY00610
	AH(3,2)=182000.-V*BH(2,1)/OMES	SRY00620
	AH(3,3)=4.18E6+V**2*AH(1,1)/OMES	SRY00630
	BH(1,3)=423.-V*AH(1,1)	SRY00640
	BH(3,1)=423.+V*AH(1,1)	SRY00650
	BH(2,3)=6270.-V*AH(1,2)	SRY00660
	BH(3,2)=6270.+V*AH(1,2)	SRY00670
	BH(3,3)=144000.+V**2*BH(1,1)/OMES	SRY00680
C	NONLINEAR ROLL FACTOR	SRY00690
	FBV=3.	SRY00700
	BH(2,2)=BH(2,2)*FBV	SRY00710
C		SRY00720
C	MASS AND SPRING CONSTANT	SRY00730
C		SRY00740
	AH(1,1)=AH(1,1)+215.	SRY00750
	AH(1,2)=AH(1,2)+988.	SRY00760
	AH(1,3)=AH(1,3)-230.	SRY00770
	AH(2,1)=AH(2,1)+988.	SRY00780
	AH(2,2)=AH(2,2)+104000.	SRY00790
	AH(3,1)=AH(3,1)-230.	SRY00800
	AH(3,3)=AH(3,3)+3.76E6	SRY00810
	C44=28800.	SRY00820
C		SRY00830
C	CONSTRUCTION OF THE MATRICES T AND U	SRY00840
C		SRY00850
	CALL RINV(AH,R)	SRY00860
	CALL RMUL(R,BH,P)	SRY00870
	DO 400 I=1,4	SRY00880
	DO 401 J=1,4	SRY00890
401	T(I,J)=0.	SRY00900
	DO 400 J=1,6	SRY00910
400	U(I,J)=0.	SRY00920
	T(1,1)=R(1,2)*P(2,1)/R(2,2)-P(1,1)	SRY00930
	T(1,2)=R(1,2)/R(2,2)	SRY00940
	T(1,3)=R(1,2)*P(2,2)/R(2,2)-P(1,2)	SRY00950
	T(1,4)=R(1,2)*P(2,3)/R(2,2)-P(1,3)	SRY00960
	U(1,1)=R(1,1)-R(1,2)*R(2,1)/R(2,2)	SRY00970
	U(1,5)=R(1,3)-R(1,2)*R(2,3)/R(2,2)	SRY00980
	T(4,1)=R(3,2)*P(2,1)/R(2,2)-P(3,1)	SRY00990
	T(4,2)=R(3,2)/R(2,2)	SRY01000
	T(4,3)=R(3,2)*P(2,2)/R(2,2)-P(3,2)	SRY01010
	T(4,4)=R(3,2)*P(2,3)/R(2,2)-P(3,3)	SRY01020
	U(4,1)=R(3,1)-R(3,2)*R(2,1)/R(2,2)	SRY01030
	U(4,5)=R(3,3)-R(3,2)*R(2,3)/R(2,2)	SRY01040
	T(3,2)=1	SRY01050
	T(2,1)=-P(2,1)*T(1,1)-P(2,3)*T(4,1)	SRY01060
	T(2,2)=-P(2,1)*T(1,2)-P(2,3)*T(4,2)-P(2,2)	SRY01070
	T(2,3)=-P(2,1)*T(1,3)-P(2,3)*T(4,3)-R(2,2)*C44	SRY01080
	T(2,4)=-P(2,1)*T(1,4)-P(2,3)*T(4,4)	SRY01090
	U(2,1)=-P(2,1)*U(1,1)-P(2,3)*U(4,1)	SRY01100

```

U(2,2)=R(2,1)
U(2,4)=R(2,2)
U(2,5)=-P(2,1)*U(1,5)-P(2,3)*U(4,5)
U(2,6)=R(2,3)

```

```

C
C CONSTRUCTION OF THE MODEL MATRICES
C

```

```

DO 402 I=1,16
DO 402 J=1,16
A(I,J)=0.
402 XI(I,J)=0.
XI(6,6)=S0*3.1415926
A(1,2)=1.
A(2,1)=-VP1
A(2,2)=-VP2
A(2,4)=VP1
A(3,4)=1.
A(4,3)=-VP1
A(4,4)=-VP2
A(4,6)=VP1
A(5,6)=1.
A(6,5)=-VP1
A(6,6)=-VP2
A(7,8)=1.
A(8,2)=A2*OM2**2
A(8,7)=-OM2**2
A(8,8)=-2.*ZET2*OM2
A(9,10)=1.
A(10,2)=A4*OM4**2
A(10,9)=-OM4**2
A(10,10)=-2.*ZET4*OM4
A(11,12)=1.
A(12,2)=A6*OM6**2
A(12,11)=-OM6**2
A(12,12)=-2.*ZET6*OM6
DO 404 I=1,4
IP=I+12
DO 405 J=1,6
JP=J+6
405 A(IP,JP)=U(I,J)
DO 406 J=1,4
JP=J+12
406 A(IP,JP)=T(I,J)
404 CONTINUE
C OUTPUT MATRICES
DO 403 I=1,3
DO 403 J=1,16
C(I,J)=0.
CV(I,J)=0.
403 CA(I,J)=0.
C(1,13)=1.
C(2,15)=1.
C(3,16)=1.
CV(2,14)=1.
DO 407 I=1,6

```

```

SRY01110
SRY01120
SRY01130
SRY01140
SRY01150
SRY01160
SRY01170
SRY01180
SRY01190
SRY01200
SRY01210
SRY01220
SRY01230
SRY01240
SRY01250
SRY01260
SRY01270
SRY01280
SRY01290
SRY01300
SRY01310
SRY01320
SRY01330
SRY01340
SRY01350
SRY01360
SRY01370
SRY01380
SRY01390
SRY01400
SRY01410
SRY01420
SRY01430
SRY01440
SRY01450
SRY01460
SRY01470
SRY01480
SRY01490
SRY01500
SRY01510
SRY01520
SRY01530
SRY01540
SRY01550
SRY01560
SRY01570
SRY01580
SRY01590
SRY01600
SRY01610
SRY01620
SRY01630
SRY01640
SRY01650

```

```

IP=I+6
CV(1,IP)=U(1,I)
CV(3,IP)=U(4,I)
CA(1,IP)=-P(1,1)*U(1,I)-P(1,3)*U(4,I)
CA(2,IP)=U(2,I)
CA(3,IP)=-P(3,1)*U(1,I)-P(3,3)*U(4,I)
407 CONTINUE
CA(1,8)=R(1,1)
CA(1,10)=R(1,2)
CA(1,12)=R(1,3)
CA(3,8)=R(3,1)
CA(3,10)=R(3,2)
CA(3,12)=R(3,3)
DO 408 I=1,4
IP=I+12
CV(1,IP)=T(1,I)
CV(3,IP)=T(4,I)
CA(1,IP)=-P(1,1)*T(1,I)-P(1,3)*T(4,I)
CA(2,IP)=T(2,I)
CA(3,IP)=-P(3,1)*T(1,I)-P(3,3)*T(4,I)
408 CONTINUE
CA(1,14)=CA(1,14)-P(1,2)
CA(1,15)=CA(1,15)-R(1,2)*C44
CA(3,14)=CA(3,14)-P(3,2)
CA(3,15)=CA(3,15)-R(3,2)*C44
C
C OUTPUT
C
GO TO 399
IER1=0
IER2=0
CALL TRNATB(16,16,16,16,A,APS)
CALL LYPCND(16,16,16,APS,XI,ZET,WR,WI,IER1,IER2)
DO 174 I=1,16
XI(I,I)=-XI(I,I)
174 WRITE(9,175)XI(I,I)
175 FORMAT(D11.5)
399 CONTINUE
WRITE(9,310)
310 FORMAT(10X,'----- MATRIX A -----')
WRITE(9,320)((A(I,J),J=1,16),I=1,16)
320 FORMAT(8E14.4)
WRITE(9,330)
330 FORMAT(10X,'----- MATRIX C -----')
WRITE(9,320)((C(I,J),J=1,16),I=1,3)
WRITE(9,340)
340 FORMAT(10X,'----- MATRIX XI -----')
WRITE(9,320)((XI(I,J),J=1,16),I=1,16)
DO 350 I=1,3
DO 350 J=1,3
350 THETA(I,J)=0.
WRITE(6,360)
360 FORMAT(2X,'INPUT THE SWAY-ROLL-YAW NOISE INTENSITIES (3 NUMBERS)')
READ(5,*)THETA(1,1),THETA(2,2),THETA(3,3)
WRITE(9,370)

```

```

SRY01660
SRY01670
SRY01680
SRY01690
SRY01700
SRY01710
SRY01720
SRY01730
SRY01740
SRY01750
SRY01760
SRY01770
SRY01780
SRY01790
SRY01800
SRY01810
SRY01820
SRY01830
SRY01840
SRY01850
SRY01860
SRY01870
SRY01880
SRY01890
SRY01900
SRY01910
SRY01920
SRY01930
SRY01940
SRY01950
SRY01960
SRY01970
SRY01980
SRY01990
SRY02000
SRY02010
SRY02020
SRY02030
SRY02040
SRY02050
SRY02060
SRY02070
SRY02080
SRY02090
SRY02100
SRY02110
SRY02120
SRY02130
SRY02140
SRY02150
SRY02160
SRY02170
SRY02180
SRY02190
SRY02200

```

```

370 FORMAT(10X,'----- MATRIX THETA -----')
WRITE(9,320)((THETA(I,J),J=1,3),I=1,3)
END
SUBROUTINE RINV(A,B)
C 3X3 MATRIX INVERSION
DOUBLE PRECISION A(3,3),B(3,3),C(3,3)
C(1,1)=A(2,2)*A(3,3)-A(3,2)*A(2,3)
C(1,2)=A(2,1)*A(3,3)-A(3,1)*A(2,3)
C(1,3)=A(2,1)*A(3,2)-A(3,1)*A(2,2)
C(2,1)=A(1,2)*A(3,3)-A(3,2)*A(1,3)
C(2,2)=A(1,1)*A(3,3)-A(3,1)*A(1,3)
C(2,3)=A(1,1)*A(3,2)-A(3,1)*A(1,2)
C(3,1)=A(1,2)*A(2,3)-A(2,2)*A(1,3)
C(3,2)=A(1,1)*A(2,3)-A(2,1)*A(1,3)
C(3,3)=A(1,1)*A(2,2)-A(2,1)*A(1,2)
DET=A(1,1)*C(1,1)-A(1,2)*C(1,2)+A(1,3)*C(1,3)
B(1,1)=C(1,1)/DET
B(1,2)=-C(2,1)/DET
B(1,3)=C(3,1)/DET
B(2,1)=-C(1,2)/DET
B(2,2)=C(2,2)/DET
B(2,3)=-C(3,2)/DET
B(3,1)=C(1,3)/DET
B(3,2)=-C(2,3)/DET
B(3,3)=C(3,3)/DET
RETURN
END
SUBROUTINE RMUL(A,B,C)
C 3X3 MATRIX MULTIPLICATION
DOUBLE PRECISION A(3,3),B(3,3),C(3,3)
DO 100 I=1,3
DO 100 J=1,3
C(I,J)=0
DO 100 K=1,3
100 C(I,J)=C(I,J)+A(I,K)*B(K,J)
RETURN
END

```

```

SRYO2210
SRYO2220
SRYO2230
SRYO2240
SRYO2250
SRYO2260
SRYO2270
SRYO2280
SRYO2290
SRYO2300
SRYO2310
SRYO2320
SRYO2330
SRYO2340
SRYO2350
SRYO2360
SRYO2370
SRYO2380
SRYO2390
SRYO2400
SRYO2410
SRYO2420
SRYO2430
SRYO2440
SRYO2450
SRYO2460
SRYO2470
SRYO2480
SRYO2490
SRYO2500
SRYO2510
SRYO2520
SRYO2530
SRYO2540
SRYO2550
SRYO2560
SRYO2570

```